I BEGIN IN THE NAME OF GOD THE MOST BENEFICENT,

THE MOST MERCIFUL.

To my dearest wife,

Rugayah

STUDIES OF COLLECTIVE STATES IN ^{160}Dy AND ^{188}Os NUCLEI.

Noorddin Ibrahim

B.Sc. (Hons.) Malaya, M.Sc. (London)

A Thesis Submitted for the Degree of

Doctor of Philosophy

in the

University of London

Physics Department

Bedford College

London

December 1983.

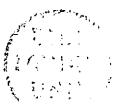

Abstract

Gamma rays following the decay of ^{160}Tb and ^{188}W were detected in both singles and coincidence in order to establish the energy level scheme of the two medium mass nuclei ^{160}Dy and ^{188}Os.

Two large volume Ge(Li) detectors together with a plastic scintillation counter were incorporated in a Dual Parameter Energy-Time Spectrometer to measure the gamma-gamma coincidence spectra: the half-life of the first excited state of ^{160}Dy was measured. An intrinsic Germanium detector was used to measure low energy transitions. New levels and transitions are proposed, relative intensities, log ft values, multipolarities, spins/parities and transition probabilities are deduced.

The nuclear properties of ^{160}Dy and ^{188}Os are analysed in terms of current nuclear models. The deviations from the predictions of the symmetric rotor model for the states in ^{160}Dy are explained in terms of band-mixing. The Coriolis coupling is applied to the negative states which gives good account to the electric dipole transition probabilities. The possible effect of the recently discovered subshell closure at Z=64 is investigated for ^{160}Dy, a nucleus with proton number (Z=66) exactly midway between the closures at 50 and 82, and the number of neutrons (N=94) above the limit of 90. Energy levels, B(E2) absolute values and ratios are compared with IBM-1 calculations assuming either a single Z=50-82 shell or a subshell closure at Z=64. The latter calculation improves agreement with experiment. The O(6) limit description is applied to the ^{188}Os nucleus. Particular attention is made to the 0^+ states and M1 transitions, the presence of which form the basic test for an O(6) type nucleus. The calculations in the context of IBM-1 were undertaken with the aid of the computer codes PHINT and FBEM.

CONTENTS Page

CONTENTS Page

List of Figures

List of Tables

CHAPTER I

INTRODUCTION

1.1 General

Gamma-ray spectroscopy has been a useful tool in probing the structure of a nucleus. The studies of various poperties, such as excited states, quadrupole moments and branching ratios allow different nuclear models to be tested and verified.

Undoubtedly, the advancement of this spectroscopy was attributed to the development of high efficiency detectors. In recent years, large volume Ge(Li) detectors have begun to replace the low efficiency NaI(Tl) counter. These new solid state detectors coupled with sophisticated computer package program codes enable precise measurements of energies and relative intensities of gamma-rays to be made.

Furthermore, the introduction of integrated circuits and microprocessors have led to a more reliable system to be introduced in the γ-γ coincidence measurements. The conventional fast-slow system has been replaced by a Dual Parameter Energy-Time Spectrometer (DPETS); offering enormous advantages in data collection rates within short period which enables the decay scheme of an isotope to rapidly build up.

The present work employs the Dual Parameter System to establish the decay schemes of two even-even medium mass nuclei, ^{160}Dy and ^{188}Os. The former is populated by β^-decay of ^{160}Tb while the latter arises from β^-decay of ^{188}Re. The detailed discussion of these two nuclei will be given in chapters 4 and 5 respectively.

The remaining part of chapter 1 focuses on the general phenomena occuring within a nucleus. Chapter 2 deals with nuclear theory where emphasis is placed on the Interacting Boson Model (IBM). The description of the experimental arrangements is given in chapter 3, and in chapter 6 an overall summary of the present work is presented.

1.2 Source preparation

A nucleus undergoing radioactive decay spontaneously emits α-particles, β-particles or γ-rays, thereby either ridding itself of nuclear excitation energy or achieving a configuration that is or will lead to one of greater stability.

The activity A of a nucleus, at any time t is given by an expression:

$$A = A_0 \, e^{-0.693 t/T} \qquad (1.1)$$

where A_0 is the activity at time zero and T is the half-life of the radioactive material.

The fact that radioactive decay follows the exponential law is a strong evidence that this phenomenon is statistical in nature: every nucleus in a sample of radioactive material has a certain probability of decaying but there is no way of knowing in advance which nuclei will actually decay in a particular time span.

The radioactive material can occur either naturally like Uranium or it can be produced from specific reactions using a non-radioactive target. There exists several possible reactions to produce these radioactive materials but so far the most common and feasible method is the thermal neutron capture. This reaction involves the capturing of one neutron by the target nucleus. Such reaction is normally written as;

$$^{A}_{Z}X_{N} + {}^{1}_{0}n \longrightarrow {}^{A+1}_{Z}X_{N+1} + \gamma \qquad (1.2)$$

or in simplified form by

$$^{A}_{Z}X_{N}\,(n,\gamma)\,{}^{A+1}_{Z}X_{N+1} \qquad (1.3)$$

The notation $^{A}_{Z}X_{N}$ refers to the target nucleus with mass number A and proton (neutron) number Z(N). The product nucleus

is $^{A+1}_{Z}X_{N+1}$ where now the mass has increased by one unit due to the increase in the number of neutron by one.

An example of such a reaction is the production of ^{160}Tb from non-radioactive ^{159}Tb. The reaction is written as:

$$^{159}Tb(n,\gamma)\ ^{160}Tb$$

The radioactive product ^{160}Tb, having a half-life of 70 days, decay through the emission of β^- particles to a more stable ^{160}Dy nucleus.

To achieve this mode of reaction the target element has to be exposed to a neutron beam. The most ideal source of neutrons would be a nuclear reactor. When a material is irradiated in a reactor the rate of build-up of the product radioisotope depends on several factors. These include neutron flux, irradiation time, neutron-capture cross-sections and etc.. The activity in transformations per second A is given by [1]:

$$A = \frac{N_0\ \sigma_1\phi\lambda_1}{\lambda_1+\sigma_2\phi-\sigma_1\phi}\left(e^{-\sigma_1\phi t}-e^{-(\lambda_1+\sigma_2\phi)t}\right) \qquad (1.4)$$

where

N_0 is the number of target nuclei orginally present,

σ_1, σ_2 are the neutron capture cross-sections of the target (in barns) and product nuclei respectively,

ϕ is the effective neutron flux (n $cm^{-2}sec^{-1}$)

λ_1 is the decay constant of the product radioisotope and

t is the irradiation time.

For a short irradiation time, low fluxes ($\sim 10^{10} \rightarrow 10^{12}$n $cm^{-2}sec^{-1}$) and a small σ_2 the specific activity S (in unit Ci/gm) becomes:

$$S = \frac{0.6\ \sigma\phi(1-e^{-0.693t/\tau})}{3.7 \times 10^{10}\ W} \qquad (1.5)$$

where W is the target atomic weight and

τ is the half-life of the product isotope.

This relation is very useful in computing the activity of the product radioisotope and also enables one to determine the length of irradiation time needed.

When a high neutron flux ($\simeq 10^{14}$n cm^{-2}sec^{-1}) is used and the product radioisotope has a high capture cross-section, a second order reaction takes place. By ignoring the possible decay of the product radioisotope, the second reaction can be represented as:

$$ {}^{A}_{Z}X_{N} \; (n,\gamma) \; {}^{A+1}_{Z}X_{N+1} \; (n,\gamma) \; {}^{A+2}_{Z}X_{N+2} $$

The final product is ${}^{A+2}_{Z}X_{N+2}$ which has an extra mass of two compared to the target element.

The rates of nuclide transformation are rather complicated and were described in detail by Bateman [2] and Rubinson [3].

This particular reaction was used in the present work to produce the radioisotope ^{188}W. The target element used was ^{186}W and the reaction,

$$ {}^{186}W(n,\gamma) \; {}^{187}W(n,\gamma) \; {}^{188}W $$

The thermal neutron cross-section for ^{186}W is ~40 barns while that of ^{187}W is ~90 barns [4]. The radioactive ^{188}W decays through β^- emission to ^{188}Re which in turn decays to stable ^{188}Os.

1.3 Electromagnetic radiation.

All excited states of nuclei are subjected to decay to lower states with simultaneous emission of electromagnetic radiation (γ-rays). This radiation is thought to arise from the change in the charge and current distributions in the nuclei.

The classical representation of an electromagnetic radiation source in terms of an oscillating distribution of electric or magnetic charges was taken over into the quantum-mechanical formalism by Heitler [5] to describe nuclear moments and to classify radiative transitions in nuclei. The radiation modes are quantized and are represented in terms of spherical harmonics $Y_{LM}(\theta,\phi)$ of rank L=0, 1, 2, 3.... The multipole order is expressed through the rank L, e.g., radiation represented by the rank L has multipolarity 2^L.

The transverse nature of electromagnetic radiation absolutely rules out monopole (L=0) γ-radiation and precludes single γ-rays from effecting $0 \nrightarrow 0$ transitions. The only way in which γ-rays can participate in $0 \nrightarrow 0$ transitions is through second-order processes, whose probability is low, such as a double-γ emission [6] or the concurrent emission of a γ-ray and a conversion electron [7].

Consequently, in a γ-transition the multipolarity L can assume nonzero values only. As Heitler [5] has shown, L represents the total angular momentum (of absolute magnitude $\hbar[L(L+1)^{\frac{1}{2}}]$) carried by 2^L-pole γ-radiation with respect to the source of the radiation field. Since angular momentum is a conserved quantity in electromagnetic interactions, it follows that in the nuclear transition $\underset{\sim}{J}_i \longrightarrow \underset{\sim}{J}_f$ a vector triangle relation applies to the triad $(\underset{\sim}{J}_i, \underset{\sim}{J}_f, \underset{\sim}{L})$ so that

$$\underset{\sim}{J}_i - \underset{\sim}{J}_f = \underset{\sim}{L} \qquad (1.6)$$

Written in nonvectorial form,

$$\Delta J \equiv |J_i - J_f| \leqslant L \leqslant |J_i + J_f| \qquad (1.7)$$

This constitutes a momentum selection rule which curbs the permitted range of multipolarities L for transitions connecting levels with initial spin J_i and final spin J_f.

For each multipole order, there are two possible classes of radiation: electric 2^L pole (EL) and magnetic 2^L pole (ML). A distinction is made between electric and magnetic

multipoles according to the parity associated with the electromagnetic radiation. This in turn is directly determined by whether or not there is a difference in the parities of the nuclear states between which the transition occurs. Electric multipole radiation of order L has opposite parity to that of magnetic radiation of the same multipolarity L in accordance with the parity rule: electric multipole radiation of order L has parity

$$\Pi_E = (-1)^L \qquad (1.8)$$

and magnetic multipole radiation of order L has parity

$$\Pi_M = (-1)^{L+1} \qquad (1.9)$$

so that radiation EL or ML of even parity is

M1, E2, M3, E4, ...

and the radiation EL or ML of odd parity is

E1, M2, E3, M4, ...

Spin and parity selection rules prescribe the multipole character of γ-transitions and frequently permit multipole mixing in the γ-radiation. Thus, unless J_i or J_f is zero, the rule $|\Delta J| \leq L \leq \Sigma J$ in principle permits the occurrence of several multipolarities L. In practice however, the marked differences in partial lifetimes of different orders L, and of E or M character, reduce the possibilities to mixtures of at most two components, viz:

ML + E(L+1) e.g. M1 + E2

One does not encounter such mixtures as E1+M2 outside exceptional circumstances because the relative emission probability of M2 is so much smaller than that of E1 unless E1 is strongly inhibited.

The admixtures of $L'=L+1$ electric multipolarity in a mixed ML+EL′ transition is expressed by the mixing ratio (δ).

This is defined as the ratio of (reduced) matrix elements:

$$\delta \equiv \frac{< J_f|E(L')|J_i >}{< J_f|M(L)|J_i >} \qquad (1.10)$$

Hence, a value of δ below unity betokens that L is predominantly present, whereas when δ exceeds unity, there is an excess of L′. The value $\delta=0$ characterizes pure L radiation, and $\delta=\infty$ implies pure L′ radiation. The percentage admixture of ML intensity is, accordingly $(1+\delta^2)^{-1}$, and of EL′ is $\delta^2(1+\delta^2)^{-1}$.

The probability of emission of radiation with multipolarity L decreases with increasing L roughly as $(R/\lambda)^{2L}$ where R is the radius of the nucleus and λ is γ wavelength. Since $R << \lambda$ the probability becomes vanishing small for higher-order multipoles. Thus, most transition will proceed primarily with emission of γ-rays of the lowest multipole order permitted by the selection rules or perhaps with a mixture of the lowest two multipole orders of opposite class. The relative probability of emission of EL radiation is appreciably higher than that of the corresponding ML radiation.

The transition probability for the gamma ray is given by [8]:

$$P(XL;\ J_i \to J_f) = \frac{8\pi(L+1)}{L[(2L+1)!!]^2}\ \frac{1}{\hbar}\left(\frac{\omega}{c}\right)^{2L+1} B(XL;\ J_i \to J_f) \qquad (1.11)$$

where

ω is the transition frequency and

$B(XL;\ J_i \to J_f)$ is the reduced transition probability.

The partial gamma ray transition probability $P_\gamma(XL)$ may be obtained from the total transition probability P(XL) by [9]

$$P_\gamma(XL) = P(XL)\ \frac{N_\gamma(XL)}{\Sigma N_d} \qquad (1.12)$$

where ΣN_d is the sum of the intensities of all transitions depopulating the level of interest in the same relative units as the intensity $N_\gamma(XL)$ of the gamma ray transition with multipolarity XL for which $P_\gamma(XL)$ is to be calculated.

The value of P(XL) may be obtained experimentally from the half-life ($T_{\frac{1}{2}}$) of the level using a relationship given by:

$$P(XL) = \frac{\ln 2}{T_{\frac{1}{2}}\ (\text{level})} \qquad (1.13)$$

Some useful relations between the reduced transition probabilities B(XL) and the partial transition probability $P_\gamma(XL)$ are [8]:

$$B(E1) = 6.288 \times 10^{-16}\ E_\gamma^{-3}\ P_\gamma(E1)$$

$$B(E2) = 8.161 \times 10^{-10}\ E_\gamma^{-5}\ P_\gamma(E2) \qquad (1.14)$$

$$B(M1) = 5.687 \times 10^{-14}\ E_\gamma^{-3}\ P_\gamma(M1)$$

where

P_γ is given in sec^{-1} and E_γ, the transition energy given in MeV.

The units of B(EL) and B(ML) will then be $e^2(fm)^{2L}$ and $U_N{}^2 fm^{2L-2}$ respectively.

These relations will be used later, (chapter IV and chapter V), to calculate the absolute transition probabilities and ratios.

1.4 Internal conversion.

As a competing process to γ decay, internal conversion is one of the ways which serves to dissipate the excitation energy of a nucleus. By interacting directly with one or more of the orbital electrons that venture within the nuclear

region, the nucleus can impart its excess energy to the electron in a one step process and cause it to be ejected from the atom. The energy carried is equal to the difference between the transition energy and the electronic binding energy in its respective atomic shell. The vacancy thereby created in an atomic shell is filled through an electron cascade process from outer orbits, accompanied by the emission of X-radiation.

The process was first discovered by Hahn [10] who observed a line spectrum in $\overset{\alpha}{\Lambda}$ magnetic $\overset{\beta}{\Lambda}$ spectrometer.

Since conversion and γ decay compete, a useful parameter associated with the process would be the conversion coefficient. It provides a measure of the relative probability in a given transition and is defined as

$$\alpha \equiv \frac{\lambda_e}{\lambda_\gamma} = \frac{N_e}{N_\gamma} \qquad (1.15)$$

where $\lambda_{e(\gamma)}$ and $N_{e(\gamma)}$ are the decay constant and number of electrons (photons). The partial internal conversion coefficients are normally used in connection with electron emission from specific orbital shells.

e.g.

$$\alpha_K = N_{eK} \,/\, N_\gamma \qquad (1.16)$$

is the coefficient for ejection of electron from K-shell while α_{L1} is the coefficient for the ejection from L1 shell. Their sum then gives the total conversion coefficient;

$$\alpha_K + \alpha_{L1} + \alpha_{L11} + \ldots = \alpha \qquad (1.17)$$

The possibility of decay of an excited state by internal conversion adds to its decay constant; thus the total decay constant λ is equal to the sum of the partial decay constants λ_γ and λ_e. As a consequence ;

$$\lambda = \lambda_\gamma + \lambda_e \qquad (1.18)$$

From the relation (1.15), thus

$$\lambda = \lambda_\gamma(1 + \alpha) \qquad (1.19)$$

The measurement of the internal conversion coefficients has been a useful spectroscopic tool in determining the multipolarity of a transition. This is achieved by comparing the experimental values with the theoretical calculations. Although, there existed several theoretical approaches to the calculation generally, the values of α increases with the increase in multipole order, L, and decreases with an increase in energy transition. Furthermore, the values of α also depend on Z, the proton number of the nucleus, since this determines the electron density at the nucleus.

In the calculation of Green and Rose [11] the finite charge distribution of the nucleus affects only the relativistic wavefunctions of the bound state and continuum state electrons. On the other hand, in the theory of Sliv and Band[12] the nuclear current distribution was based on a simple surface current model. A modification to these approaches was later done by Church and Weissner [13] who considered the 'penetration' effect of the shell electrons into the nucleus.

The calculations of Hager Seltzer [14] and Pauli and Alder [15] using this later approach is so far the most recent and reliable data for K, L and M shells. These tables will be used in the present work in determining the multipolarities of transitions with known experimental α . Lengthy discussion are also available in several texts [16, 17].

1.5 β^- decay.

The emission of negative or positive electrons or capture of atomic electrons constitute the main method for restoring nuclides to the stability line throughout the periodic table. The first method is referred to β^- decay, where a

neutron is being changed into a proton. This results in an increase in the nuclear charge by one unit but leaves the atomic number unchanged.

The kinetic energy (E) of the negatrons (negative electrons) emitted in this β^- decay cover a continuous range from zero up to a maximum (E_0) value. In very many cases, the observed β^- spectrum is rather complex, a superposition of the spectra for the various possible transitions arising from more than one final nuclear state. This occur when the daughter nucleus is left in an excited state rather than in its ground state.

The probability of a β^- decay is given by [18],

$$\beta^- \text{ decay probability} = \frac{\ln 2}{t} = C\ f(Z,E_0) \qquad (1.20)$$

where

t is the half-life of the β^- decay,

C is a constant which depends on nuclear wavefunction and

$f(Z,E_0)$ is an integral given by:

$$f(Z,E_0) = \int_0^{P_0} F(Z,E)p^2\ (E_0-E)^2\ dp \qquad (1.21)$$

The factor F(Z,E) is a coulomb correction factor resulting from an interaction of the orbital electron with daughter nucleus, p is the momentum of the electron emitted and dp is a given momentum interval. The upper limit of integration, $p_0 = (E_0^2 - 1)^{\frac{1}{2}}$, is the maximum momentum in the electron spectrum, expressed in units mc. For large values of E_0, $f(Z,E_0)$ is proportional to E_0^5.

Beta transitions can be classified as either allowed or forbidden. Allowed transitions are those in which the

emitted particles (electrons and neutrinos) do not carry away any orbital angular momentum i.e. s-wave. This means that the parity of the decaying nucleus does not change. If in the decay the parity of the nuclear states changes, then the particles cannot be emitted as an s-wave. The angular momentum carried now is no longer zero. Such a transition is termed as forbidden transition.

It is customary to define the 'comparative half-life' of a beta transition, ft, by:

$$ft = f(Z,E_0) \times t \qquad (1.22)$$

On the basis of the ft values, it is possible to group, the known beta decays into allowed, first-forbidden, second-forbidden and etc.

Table (1.1) shows some useful classification of beta transitions according to the ft values. The parentheses indicate whether there is a change or not in the parity. This table will be used later in deducing the possible spins and parities of the nuclear states. A formal treatment of the β^- decay theory are given in several texts [19, 20].

Table (1.1). Classification of Beta Transition according to ft values. The change in parity are given in parentheses.

Type	Selection rules	ft
Superallowed	$\Delta J = 0,\pm1$ (no)	1000 - 4000
Allowed	$\Delta J = 0,\pm1$ (no)	2×10^4 - 10
First Forbidden	$\Delta J = 0,\pm1$ (yes)	10^6 - 10^8
Unique First Forbidden	$\Delta J = \pm2$ (yes)	10^8 - 10^9
Second Forbidden	$\Delta J = \pm2$ (no)	2×10^{10} - 2×10^{13}
Unique Second Forbidden	$\Delta J = \pm3$ (no)	10^{12}

CHAPTER II

NUCLEAR MODELS

2.1 Nuclear shell model.

The idea of the shell model was first developed to explain the observed stability of nuclei having special numbers of protons or neutrons [22]. These numbers at 2, 8, 20 28, 50, 82 and 126 are commonly referred to as magic numbers [21].

The striking phenomena connected with definite numbers of protons and neutrons have been interpreted as an indication that neutrons and protons are arranged into shells within the nucleus, like electrons in atoms. Each shell is limited to a certain maximum number of nucleons of a given sort. When a shell is filled, the resulting configuration is particularly stable and therefore of low energy.

There exists several theories devised to describe the nature of these shells. The three notable shell models are the extreme particle model [23], the single particle model [24] and the independent particle model [25]. These models possess a common property that is the particles in the nucleus are assumed to move in a mean spherically symmetric potential independent of each other.

In the simplest form of the shell model, the extreme single particle model, the nucleons are supposed, in the ground state, to have dynamically paired motions so that many of the nuclear properties are due only to the last unpaired nucleon. It is also assumed that the neutron and proton states fill independently. In such a system, every even-even nuclide has zero spin and every odd-A nuclide has the angular momentum of the unpaired particle. The overall average potential of either infinite harmonic oscillator potential or infinite rectangular well potential satisfactorily predict the lowest of the magic numbers 2, 8, 20 but thereafter fail to meet the challenge of accounting for the higher distinctive numbers 28, 50, 82 and 126. This was accomplished through the introduction of an attractive spin-orbit force into the nuclear potential.

On the basis of single particle model, the assumption of strong spin-orbit coupling was also used. The low energy properties of a nuclide are attributed to its 'loose' particles outside closed shells. Thus, the nucleus is considered as a core of completely filled closed shells containing the maximum allowed number of nucleons and unfilled shells containing the remaining number of nucleons.

The reduced transition probability $B(\sigma L)$ for the gamma-rays transition was estimated by Weisskopf [26] as:

$$B(EL) = \frac{(1.2)^{2L}}{4\pi} \left\{\frac{3}{L+3}\right\}^2 A^{2L/3}\, e^2 (fm)^{2L} \qquad (2.1)$$

and

$$B(ML) = \frac{10}{\pi} (1.2)^{2L-2} \left\{\frac{3}{L+2}\right\}^2 A^{(2L-2)/3}\, U_N{}^2 (fm)^{2L-2} \qquad (2.2)$$

where A is the mass number of the nucleus and U_N is the nuclear magneton. It can be seen that these estimates are independent of the energy of the transition and thus form a rough estimate of the transition probabilities.

The independent-particle model is based on the assumption that each nucleon moves independently of all nucleons in a common potential field. This field represents the average effect of all interactions with other nucleons, and it is the same for each particle. Every nucleon is then considered as an independent particle, and the presence of other particles moving in the same field exerts its influence only by means of the requirements of the Pauli principle, which excludes identical particles from occupying the same quantum state.

The calculations for single particle states in a deformed potential was later developed by Nilsson [27]. The level order was found to vary from that deduced from d_Λ potential with spherical symmetry. Many properties of odd-A nuclei, as a function of deformation were predicted with great success.

2.2 Collective model.

A most significant failure of the shell model approach to nuclear structure is its inability to explain the very large quadrupole moments, Q. The first attempt to set up a theory which would explain this anomaly for even nuclei in the region $150 \leqslant A \leqslant 190$ and $A \geqslant 220$ was made by Rainwater[28]. He emphasised that a single nucleon moving in an independent orbit, especially if it has a high angular momentum, will exert a centrifugal force against the inner surface of the nucleus thus tending to distort the nuclear shape from the spherical to ellipsoidal. This distortion contributes to the large value of Q.

For a closed shell nucleus, the various nucleon orbits are oriented at random so that the overall nuclear shape is spherical.

A single loose nucleon beyond a closed shell will tend to have its orbit in plane, thus setting up a slight oblate spheroidal deformation. As the number of loose particles outside the filled nucleon shells increases, there is competition between the shape deforming tendencies of the loose nucleons and the pairing force interaction. The latter effect represents the tendency of two nucleons of the same kind to couple to form states of zero angular momentum which are of course, spherically symmetric. Thus, the equilibrium shape of the nucleus depends on the relative strengths of the two effects.

For nuclei with only a few loose particles, the pairing force dominates and the nuclear shape is very nearly spherical. The simplest collective motion of such a system is a simple harmonic vibration of the surface about equilibrium.

On the other hand, nuclei with many loose particles are strongly deformed as the deforming effect of the loose nucleons is a coherent one.

2.2.1 Collective vibrations.

Classically, this model is similar to an incompressible liquid drop; where the instantaneous form of the surface may be described generally by an expansion in terms of spherical harmonics.

The surfaces of constant density may hence be described by [29]

$$R = R_0 \left[1 + \sum_{LM} \alpha_{LM} Y_{LM} (\theta,\phi)\right] \qquad (2.3)$$

where the Y_{LM} are the spherical harmonics and θ and ϕ are polar angles with respect to some arbitrarily chosen space fixed axis. Any collective motion will be described by the variation of the coefficients α_{LM} with time. Assuming small oscillations, in the quadratic approximation, the kinetic energy of collective motion will be

$$T = \tfrac{1}{2} \sum_{LM} B \left|\dot{\alpha}_{LM}\right|^2 \qquad (2.4)$$

likewise, the potential energy may be written as

$$V = \tfrac{1}{2} \sum_{LM} C \left|\alpha_{LM}\right|^2 \qquad (2.5)$$

The total energy (E) may be written in terms of a force parameter C, and a mass parameter, B [30],

$$E = \tfrac{1}{2} C \alpha^2 + \tfrac{1}{2} B \dot{\alpha}^2 \qquad (2.6)$$

with an oscillation frequency given by

$$\omega = \sqrt{C/B} \qquad (2.7)$$

The notation α represents the displacement amplitude from equilibrium.

If the oscillations are quantized the energies have the values

$$E(n) = n\hbar\omega \qquad (2.8)$$

where

n is the number of quadrupole phonons.

The total angular momentum permitted for a given n is determined by the occupation numbers allowed by the Bose-Einstein statistics.

The systematic appearance of the 2^+ single phonon vibrational state is an outstanding feature of the spectra of even-even nuclei, and the triplet of a 2-phonon state 0^+, 2^+, 4^+ at approximately double the energy of the first excited state is also frequently seen [30].

Thus the energy spectrum takes the sequence

$$E_1,\ 2E_1,\ 3E_1\ \ldots\ldots$$

For higher spins, this sequence is violated due to the effect of centrifugal forces on the equilibrium shape.

Octupole phonons have an energy approximately twice that of a quadrupole vibration, and the single-phonon octupole state, 3^-, is found in the spectrum of even-even nuclei near the two phonon quadrupole states. The collective 3^- excitation is another prominent features of the low lying states.

2.2.2 Collective rotation.

It was known that deformed nuclei show rotational like spectra [31]. The spectrum depends on the nuclear equilibrium shape.

For axially symmetric nuclei, there are no collective rotations about the symmetric axis and the rotational wavefunction is completely specified by the quantum number I, K and M. Here I is the angular momentum with M as its projection in the Z direction and K as its component along the nuclear symmetry axis.

The energy spectrum is given by a simple expression:

$$E(I) = E_0 + \frac{\hbar^2}{2\mathcal{I}_0} I(I+1) \qquad (2.9)$$

where $\mathcal{I}_0$ is the effective moment of inertia and E_0 is an energy scale constant.

More generally, the rotational energy can be expressed as a function of I(I+1). For sufficiently small values of I, one can employ an expression in powers of I(I+1)

$$E(I) = E_0 + AI(I+1) + BI^2(I+1)^2 \qquad (2.10)$$

where A is the moment of inertial independence while B is the corresponding higher-order inertial parameter.

This deviation of equation (2.10) from the leading order rotational energy (Eqn.2.9) may be viewed as the result of rotation-vibration coupling. The effect can be seen in the heaviest deformed region.

Equation (2.9) implies that the ratio between the energies of the first two excited states in ground-state band is:

$$E_{4_1^+} / E_{2_1^+} = 10/3 \qquad (2.11)$$

This provides a good indicator as to whether the nuclei exhibit

rotation or vibration spectra.

In general, if the transition operator $M(\sigma L)$ is given for the transition, the $B(\sigma L)$; which is the reduced transition probability is given by:

$$B(\sigma L;\ I_i \rightarrow I_f) = \frac{1}{(2I_i+1)} \left[< f|M(\sigma L)|i > \right]^2 \qquad (2.12)$$

where $< f|M(\sigma L)|i >$ is the reduced matrix element.

Specifically, the reduced matrix element for E2 transitions within a band is given as

$$< KI_f|M(E2)|KI_i > = (2I_i+1)^{\frac{1}{2}} < I_iK20|I_fK > X \left(\frac{5}{16\pi}\right)^{\frac{1}{2}} eQ_0 \qquad (2.13)$$

which gives the reduced transition probability:

$$B(E2;\ I_i \rightarrow I_f) = \frac{5}{16\pi} e^2Q_0{}^2 < I_iK20|I_fK >^2 \qquad (2.14)$$

where

Q_0 is the intrinsic quadrupole moment and

$< I_iK20|I_fK >$ is the vector addition coefficient representing the coupling of the angular momenta in the intrinsic frame.

2.2.3 Generalised collective model.

The collective models described in the preceding sections are based on a classical picture where the nucleus is described by a liquid drop or a similar object which has a

definite shape. The collective states are then given by oscillations and rotations of this drop and normally the deformation is restricted to the quadrupole type. These models (rotator, vibrator) were simple. More refined models such as rotation-vibration (RVM) [32] were based on the kinetic energy of Bohr and Mottelson and restricted the potentials to a triaxial potential minimum and prolate or oblate minimum respectively.

The first generalisations were put forward by Kumar and Baranger [33], and later by Gneuss et al. [34], and Gneuss and Greiner [35]. However, for numerical reasons the potential and kinetic energies in the Gneuss-Greiner model were restricted to special forms.

Hess et al. [36] has presented a generalised version of the Gneuss-Greiner approach which led to a generalised collective model. The numerical solution of the collective Schrodinger equation is very simple: the Hamiltonian is diagonalised within the basis of the five dimensional harmonic oscillator, whose eigenfunctions were constructed analytically.

The collective properties are determined by the mass parameter and by the potential energy surface (PES) which gives a vivid representation of the dynamical collective properties of the nucleus. Thus, for example, two minima in the potential will tell us that an isomeric structure of the nucleus exists, or a γ-unstable valley in the potential will indicate softness with respect to the triaxiality.

The collective variables of this model are the components α_{2m} of an irreducible quadrupole tensor α, which is defined via the expansion of the nuclear surface terms of spherical harmonics. The conjugate momenta π_{2m} are introduced by requiring the canonical commutation relations:

$$[\pi_{2m}, \alpha_{2m'}] = -i\hbar\delta_{mm'} \qquad (2.15)$$

Other variables used are the deformation coordinates β and γ

together with the Euler angles describing the orientation of the intrinsic system.

The collective Hamiltonian has the following form

$$H = T + V \qquad (2.16)$$

where

T is the kinetic energy which consists of a harmonic term proportional to $[\pi\times\pi]^{(0)}$ and two α-dependent terms which correspond to deformation-dependent masses,

V is the potential energy surface (PES), a function of β and $\cos 3\gamma$

In deriving the quadrupole operator, Q_{2m}, the following assumptions are made:

a) Constant charge distribution ($\rho(r) = \rho_0$)

b) incompressibility of nuclear matter

c) Expansion in α only up to second order

d) no distinction between protons and neutrons.

The quadrupole operator is given by:

$$Q_{2m} = \rho_0 R_0^5 (\alpha_{2m} - \frac{10}{\sqrt{220}} [\alpha\times\alpha]^{(2)}) \qquad (2.17)$$

2.3 Boson Expansion Technique (BET).

The geometrical models no doubt are simple but there is no well-defined procedure for making transitions between the different models e.g. the transition from a spherical vibrator to a deformed rotor. Attempts were made to describe the collective properties of nuclei in terms of boson

degrees of freedom [37, 38], instead of fermion degrees of freedom. Unfortunately, most of these methods involve infinite expansions, i.e. boson operators of ever-increasing order [39]. Thus in order to describe the nuclei, the expansion has to be truncated at certain orders. This has been shown by Tamura et al. [40] in the Boson Expansion Technique.

The Hamiltonian taken as a starting point is given as a sum of a single-particle Hamiltonian, a particle-hole type quadrupole-quadrupole interaction, and a pairing interaction of both monopole and quadrupole types [41, 42].

$$H = H_{s.p.} + H_{ph} + H_{pair} \qquad (2.18)$$

where

$H_{s.p.}$ is the single-particle Hamiltonian

H_{ph} is the particle-hole Hamiltonian and

H_{pair} is the pairing Hamiltonian.

Taking first the single-particle Hamiltonian and the monopole type pairing interaction, the transformation is made, so that the original shell model type single-particle system is replaced by a system of quasiparticles.

After this transformation is made, the Hamiltonian is written in a form which is quadratic in the quasiparticle pair creation and scattering operators. An orthogonal transformation is then made so as to isolate a collective particle-hole operator.

These fermion-pair operators are expanded in an infinite series of boson operator products. The coefficients of this expansion are then determined so that all the commutation relations, satisfied by the fermion pairs, are satisfied by their boson expanded form as well. Since the boson-expanded form is infinitely long, satisfaction of the commutation relations is required to hold order by order.

After the expansion coefficients are obtained, the fermion pair operators in the Hamiltonian are replaced by their boson-expanded forms and thus the boson Hamiltonian emerges.

The Hamiltonian is then diagonalised in a space spanned by products of the collective bosons. The basis states in this space classified [43] by irreducible representations of the chain of groups; $SU(5) \supset R(5) \supset R(3)$, i.e. by the set of quantum numbers N, ν, γ and I. Here N is the number of collective bosons, ν is the seniority (the number of bosons that are not coupled pairwise to spin zero), and I is the angular momentum. The extra quantum number γ, enumerates R(5) states that are degenerated for a pair of values of ν and I.

2.4 Interacting Boson Model (IBM).

Another approach to the problem of infinite boson expansion was proposed by Arima and Iachello [44-48]. In this model, which has the virtue of being simple, the collective properties are described in terms of pairs of nucleons coupled to angular momentum of L=0 and L=2; which are treated as bosons. The pairs with L=0 are called s-bosons and those with angular momentum L=2 are called d-bosons. The total number of bosons (N) in a given even-even nucleus is the sum of the neutron (N_ν) and proton (N_π) pairs. If more than half of the shell is full, $N_{\pi(\nu)}$ is taken as the number of hole pairs.

The model where proton and neutron bosons are explicitly introduced is usually referred to as the Interacting Boson Model-2 [49] to distinguish from IBM-1 which made no distinction between proton and neutron pairs.

IBM-1

In this model, one assumes that low-lying collective quadrupole states can be generated as states of a system of [N] bosons able to occupy two levels; one with angular momentum L=0, called s and with angular momentum L=2 called d.

For the case in which the two levels are degenerate

and in the absence of any interaction between the bosons, the five (u=0, ±1, ±2) components of the d-boson and the single component of the s-boson span a linear vector space which provides a basis for the representation of the group SU(6). This is characterised by the symmetry properties of the wave-function. For these bosons, the only allowed representation are the totally symmetric ones, belonging to the partition [N] of SU(6) group.

The energy difference, $\varepsilon=\varepsilon_d-\varepsilon_s$, and the boson-boson interaction lift the degeneracy and give rise to definite spectrum. The spectrum is defined by ε, the two-body matrix elements and the partition [N] of SU(6) to which it belongs. Thus, in this approach, each nucleus is characterised by a set of parameters. The positive parity energy levels can be obtained by diagonalising the model Hamiltonian [50]:

$$H_{sd} = \varepsilon \times n_d + \frac{ELL}{2}(\underset{\sim}{L}.\underset{\sim}{L}) + \frac{QQ}{4}(\underset{\sim}{Q}.\underset{\sim}{Q}) + PAIR(\underset{\sim}{P}.\underset{\sim}{P}) - 10\sqrt{7}\,\frac{OCT}{2}(\underset{\sim}{T}_3.\underset{\sim}{T}_3)$$

$$+ 30\,\frac{HEX}{2}(\underset{\sim}{T}_4.T_4) \qquad (2.19)$$

where

$$n_d = [d^\dagger.\tilde{d}],$$

$$\underset{\sim}{P} = \tfrac{1}{2}[\tilde{d}.\tilde{d}] - \tfrac{1}{2}[\tilde{s}.\tilde{s}],$$

$$\underset{\sim}{L} = \sqrt{10}\,[d^\dagger \times \tilde{d}]^{(1)},$$

$$\underset{\sim}{Q} = [d^\dagger \times \tilde{s} + s^\dagger \times \tilde{d}]^{(2)} - \tfrac{1}{2}\sqrt{7}\,[d^\dagger \times \tilde{d}]^{(2)},$$

$$\underset{\sim}{T}_3 = [d^\dagger \times \tilde{d}]^{(3)}$$

$$\underset{\sim}{T}_4 = [d^\dagger \times \tilde{d}]^{(4)}$$

The $s^\dagger(\tilde{s})$ and $d^\dagger(\tilde{d})$ are the creation (annihilation) operators for s and d bosons respectively. The number in the parentheses

denotes the angular momentum couplings. Thus, n_d is the number of d-bosons and $(\underset{\sim}{L}.\underset{\sim}{L})$, $(\underset{\sim}{Q}.\underset{\sim}{Q})$ and $(\underset{\sim}{P}.\underset{\sim}{P})$ are the angular momentum, quadrupole-quadrupole and pairing interactions respectively. The parameters ELL, QQ and PAIR characterise their respective magnitudes. The remaining two parameters, OCT and HEX, refer to the magnitude of the octupole $(\underset{\sim}{T}_3.\underset{\sim}{T}_3)$ and hexadecapole $(\underset{\sim}{T}_4.\underset{\sim}{T}_4)$ interactions respectively.

In addition to energies, one can also calculate other properties such as electromagnetic transition rates. In order to do so, one must specify the transition operators. If one assumes that these are atmost one-body operator:

$$T^{(\ell)} = \sum_{i=1} t_i^{(\ell)} \tag{2.20}$$

From the most generalised second quantized form, the few possible transition operators are [30]:

$$T(E2) = E2SD\ (s^{\dagger}\tilde{d}+d^{\dagger}\tilde{s})^{(2)} + \frac{E2DD}{\sqrt{5}}\ (d^{\dagger}\tilde{d})^{(2)} \tag{2.21}$$

$$T(M1) = (M1+M1N\times\hat{N}+M1ND\times\hat{n}_d)\hat{L} + M1E2[\hat{T}(E2)\times\hat{L}] \tag{2.22}$$

The constants are written in the same manner as program FBEM (see chapters IV and V).

Once the transition operators have been given, electromagnetic transition rate can be calculated by taking reduced matrix elements of $\hat{T}^{(\ell)}$ between initial (J_i) and final (J_f) states $< J_f|\hat{T}^{(\ell)}|J_i >$. The $B(E\ell)$ and $B(M\ell)$ values are then obtained as:

$$B(\sigma\ell\ ;\ J_i \rightarrow J_f) = \frac{1}{(2J_i+1)}\ [\ < J_f|\hat{T}^{(\ell)}|J_i >\ ]^2 \tag{2.23}$$

In order to generate the negative parity states an $f(L^{\pi}=3^{-})$ boson should be coupled with the s-d bosons space. The total Hamiltonian will then be:

$$H = H_{sd} + H_{f} + H_{df} \tag{2.24}$$

where

H_{sd} is defined by equation (2.19)

H_{f} is the Hamiltonian of an f-boson while

H_{df} is the Hamiltonian resulting from the coupling of d and f bosons. These Hamiltonians are defined as follows:

$$H_{f} = HBAR3 \times n_{f} \tag{2.25}$$

$$H_{df} = FELL(\underset{\sim}{L}_{d}\cdot\underset{\sim}{L}_{f}) + FQQ(\underset{\sim}{Q}_{d}\cdot\underset{\sim}{Q}_{f}) \tag{2.26}$$

where HBAR3 is the magnitude of the f-boson energy and FELL and FQQ are the magnitude of the angular momentum and quadrupole-quadrupole interactions of d and f-bosons respectively.

Although for a detailed comparison with experiment it may always be necessary to perform numerical calculations, it is of interest to consider special situations for which all properties of the system can be calculated in compact, analytic form. These special or limiting situations provide the framework for a semi-quantitative understanding of the observed spectra without resorting to numerical calculations. Since the interacting boson model has a very definite group structure, that of the group SU(6), the problem of finding all the possible analytic solutions to the eigen-value problem of H can be solved in a rigorous and complete way.

Analytic solutions correspond to dynamical symmetries of the Hamiltonian H, that is, to situations in which it

is possible to write the Hamiltonian in terms of invariant operators of a complete chain of subgroups of SU(6). There are three and only three possible chains which hence give rise to three limits, SU(5), SU(3) and O(6). However, the model is in no way limited to these symmetries only. Indeed, one of its most attractive aspects is its ability to treat complex transitional regions,such as SU(3) $\rightarrow$ O(6) or SU(5) $\rightarrow$ SU(3) case extremely simply. The characteristics of a nucleus lying in this transitional region can then be specified in terms of the ratio of the coefficients of the characteristic terms for the two limits.

2.4.1 The rotational limit SU(3)[46].

The Hamiltonian used to describe the positive parity states can be written as:

$$H_{sd} = \frac{ELL}{2} (\underset{\sim}{L}.\underset{\sim}{L}) + \frac{QQ}{4} (\underset{\sim}{Q}.\underset{\sim}{Q}) \qquad (2.27)$$

The eigen-states of this limit $|[N], (\lambda,\mu), K, L, M,>$ are labelled by the group reduction $SU(6) \supset SU(3) \supset O(3)$ for which the quantum numbers are; [N] the total number of bosons, L, the angular momentum with M as its z-projection, and K, the projection of L along the axis of nuclear symmetry. The (λ,μ) denote SU(3) irreducible representations.

The values of (λ,μ) contained in each [N] are given by:

$$[N] = (2N,0) + (2N-4,2) + (2N-8,4) + ... \qquad (2.28)$$

The values of K in each (λ,μ) group ranges as:

$$K = \min(\lambda,\mu) \ , \ \min(\lambda,\mu) - 2, \ .... \ 1 \text{ or } 0 \qquad (2.29)$$

The allowed values of L in each K are

$$L = K,\ K+1,\ K+2,\ \ldots.\ K+\max(\lambda,\mu) \qquad (2.30)$$

with the exception of K=0 for which:

$$L = \max(\lambda,\mu)\ ,\quad \max(\lambda,\mu) - 2\ ,\ \ldots.\ 1 \text{ or } 0 \qquad (2.31)$$

Thus the ground state is represented by $|[N],\ (2N,0),\ K=0,\ L>$ while the β- and γ-bands are represented by $|[N],\ (2N-4,2),\ K=0,\ L>$ and $|[N],\ (2N-4,2),\ K=2,\ L>$ respectively.

Analytically, the energy states derived from the pure SU(3) limit can be written as

$$E = (-\frac{3QQ}{16}+\frac{ELL}{2})L(L+1) + \frac{QQ}{4}(\lambda^2+\mu^2+\lambda\mu+3(\lambda+\mu)) \qquad (2.32)$$

The degeneracy of γ- and β-bands may be removed by including the fourth term of equation (2.19).

The corresponding E2 operator is given by

$$T(E2) = \alpha[(s^{\dagger}\tilde{d}+d^{\dagger}\tilde{s})^{(2)} + (R/\sqrt{5})(d^{\dagger}\tilde{d})^{(2)}] \qquad (2.33)$$

where α = E2SD and $R = \frac{E2DD}{E2SD}$ of equation (2.21). The constant α simply has the effect of multiplying all calculated B(E2) values by α^2. Thus the only parameter which affects relative B(E2) values is R. In pure SU(3) limit, R takes the value $-\sqrt{35}/2$, equal to -2.958, and with such a value E2 transitions between the different (λ,μ) representations are forbidden. Since R takes the value 0 in the O(6) or SU(5) limits, its overall range can be expected to lie between 0 and -2.958.

If the contributions from the $\Delta n_d = \pm 1$ and $\Delta n_d = 0$ terms of the E2 operator are defined to be [52] :

$$M_1 = (2I_i+1)^{-\frac{1}{2}} < K_f I_f || (s^\dagger \tilde{d} + d^\dagger \tilde{s})^{(2)} || K_i I_i > , \tag{2.34}$$

$$M_0 = (2I_i+1)^{-\frac{1}{2}} < K_f I_f || (d^\dagger \tilde{d})^{(2)} / \sqrt{5} || K_i I_i > \tag{2.35}$$

then

$$< K_f I_f || T(E2) || K_i I_i > = (2I_i+1)^{\frac{1}{2}} (M_1 + R M_0) \tag{2.36}$$

giving

$$B(E2;\ I_i \longrightarrow I_f) = (M_1 + R M_0)^2 \tag{2.37}$$

The requirement that an inter-representation transition vanishes in the SU(3) limit for R=-2.958, implies either

$$M_1 = 2.958\ M_0 \tag{2.38}$$

or

$$M_1 = M_0 = 0 \tag{2.39}$$

The reduced E2 matrix element in the first case becomes

$$< K_f I_f || T(E2) || K_i I_i > = (2I_i+1)^{\frac{1}{2}}\ M_1 \left[1 + \frac{R}{2.958}\right]$$

Thus the ratio of the matrix elements of any two inter-representation transitions is independent of R.

For transitions with the same I_i the ratio becomes

$$\frac{< K_f I_f || T(E2) || K_i I_i >}{< K_f I_f' || T(E2) || K_i I_i >} = \frac{M_1}{M_1'} \tag{2.41}$$

The relative strengths of inter-representations transitions can therefore be deduced simply from the matrix elements M_1.

An analytical solution for B(E2) value for transitions within GSB is given by

$$B(E2;\ L+2 \rightarrow L) = \alpha^2 \tfrac{3}{4} \frac{(L+1)(L+2)(2N-L)(2N+L+3)}{(2L+3)(2L+5)} \qquad (2.42)$$

which implies

$$\frac{B(E2;\ 4_1^+ \rightarrow 2_1^+)}{B(E2;\ 2_1^+ \rightarrow 0_1^+)} = \frac{10}{7} \frac{(N-1)(2N+5)}{N(2N+3)} \xrightarrow[N \rightarrow \infty]{} \frac{10}{7} \qquad (2.43)$$

The quadrupole moment of the first excited state ($Q_{2_1^+}$) is given by

$$Q_{2_1^+} = -\alpha\sqrt{\frac{2\pi}{5}} \times \frac{2(4N+3)}{7} \qquad (2.44)$$

In the periodic table, there are two regions which correspond to the SU(3) limit. One comprises of nuclei in the middle of the N=82-126, Z=50-82 and the second consists of nuclei in the shells above N=126, Z=82.

2.4.2 γ-unstable O(6) limit [47].

The Hamiltonian which describes the pure O(6) limit is made up of second, fourth and fifth terms of equation (2.19).

The eigen states $|[N],\ \sigma,\ \tau,\ \nu_\Delta,\ L,\ M>$ are labelled by the group reduction $SU(6) \supset O(6) \supset O(5) \supset O(3)$ for which the quantum numbers are [N], the total number of bosons, L, the angular momentum with M as its z-projection.

The values of quantum number σ contained in each [N] are given by

$$\sigma = N, N-2, \ldots 0 \text{ or } 1, \text{ for } N = \text{even or odd} \tag{2.45}$$

The quantum number τ characterises the totally symmetric irreducible representation of O(5) which can take the value in each σ as:

$$\tau = \sigma, \sigma-1, \ldots 0 \tag{2.46}$$

A quantum number ν_Δ, counts d-boson triplets coupled to zero angular momentum. The values are given by:

$$\nu_\Delta = 0, 1 \ldots \leq |\tau/3| \tag{2.47}$$

The values of L contained in each τ are given by:

$$L = 2\lambda, 2\lambda-2, 2\lambda-3, \ldots \lambda \tag{2.48}$$

where λ is limited by

$$\lambda = \tau - 3\nu_\Delta > 0 \tag{2.49}$$

Analytically, the excitation energies derived from the pure O(6) Hamiltonian is given by:

$$E([N], \sigma, \tau, n_\Delta, L) = \tfrac{1}{2} \text{ PAIR } (N-\sigma)(N+\sigma+4) + 15 \text{ OCT} \times \tau(\tau+3) + \frac{(\text{ELL-OCT})}{2} L(L+1) \tag{2.50}$$

Some important characteristic features of an O(6) spectrum are:

(i) For each value of σ, the level spacing are exactly repeated commencing at successively higher bandhead energies. The same level spin repeat, except for the effects of a spin 'cut-off' which limits states to spin value < 2σ.

(ii) Repeating $0^+ - 2^+ - 2^+$ sequence

(iii) For higher τ-values, one notes other level groupings. One in particular are 4^+, 5^+, 6^+ levels.

For a pure O(6) limit, the parameter E2DD in the E2 operator of equation (2.21) is zero. This reduces the equation to:

$$T(E2) = E2SD\ (d^{\dagger}\tilde{s} + s^{\dagger}\tilde{d})^{(2)} \qquad (2.51)$$

This gives rise to two selection rules for E2 transitions.

(i) $\Delta\sigma=0$, which states that the matrix elements connecting states with different values of the quantum number σ simply vanish in the O(6) limit.

(ii) $\Delta\tau = \pm 1$

Also derived from equation (2.51) above, the B(E2) ratios for transitions originating from same initial spin are independent of the E2 parameters.

The analytical solution for B(E2) values in GSB (σ=N) is given by

$$B(E2;\ L+2 \rightarrow L) = (E2SD)^2\ \frac{L+2}{2(L+5)}\ \frac{(2N-L)(2N+L+8)}{4} \qquad (2.52)$$

Thus the ratio

$$\frac{B(E2;\ 4_1^+ \rightarrow 2_1^+)}{B(E2;\ 2_1^+ \rightarrow 0_1^+)} = \frac{10}{7}\,\frac{(N-1)(N+5)}{N(N+4)} \xrightarrow[N \rightarrow \infty]{} \frac{10}{7} \qquad (2.53)$$

The M1 transition matrix element of equation (2.22) becomes [53]:

$$< K_f I_f | T(M1) | K_i' I_i > = M1ND \sqrt{I_i(I_i+1)(2I_i+1)}\ < K_f I_f | n_d | K_i' I_i >$$

$$\delta_i \delta_f - M1E2\ f(I_i I_f) < K_f I_f | T(E2) | K_i I_i > \qquad (2.54)$$

where

$$f(I_i I_f) = \left[\frac{1}{40}\,(I_i+I_f+3)(I_f-I_i+2)(I_i-I_f+2)(I_i+I_f-1)\right]^{\frac{1}{2}} \qquad (2.55)$$

The n_d term of the quation obeys the selection rule $\Delta\sigma=2$, $\Delta\tau=0$, while the E2 operator obeys the rule $\Delta\sigma=0$, $\Delta\tau=\pm1$. Thus for transitions between the $\sigma=N-2$ and $\sigma=N$ groups of levels, the $\Delta\tau=0$, $I \rightarrow I$ transition might be expected to be dominantly M1 in character, with relative absolute strengths distributed according to the spin dependence of the first term of equation (2.54). In addition the ratio of these M1 transitions to M1 branches involving $\Delta\sigma=2$, $\Delta\tau=\pm1$ should be large.

There exists two regions which are postulated to exhibit the O(6) limit characters. These regions occur towards the end of the neutron shells 50-82 and 82-126.

2.4.3 Vibrational limit SU(5) [48].

The Hamiltonian of this limit can be written in the form:

$$H = \varepsilon \times n_d + \sum_{L=0,2,4} \tfrac{1}{2}\sqrt{2L+1}\, C\left(\frac{L+2}{2}\right) [(d^{\dagger}\tilde{d})^{(L)} \times (\tilde{d}\tilde{d})^{(L)}] \qquad (2.56)$$

The resulting eigen-values resulting from diagonalising this Hamiltonian are given as:

$$E(n_d, \nu, n_\Delta, L, M) = En_d + \tfrac{1}{2}\alpha(n_d)(n_d-1) + \beta(n_d-\nu)$$

$$(n_d+\nu+3) + \gamma[L(L+1)-6n_d] \qquad (2.57)$$

where the parameters in equation (5.27) are related to that in equation (5.26) by

$$\begin{aligned} C1 &= \alpha + 10\beta - 12\gamma \\ C2 &= \alpha - 6\gamma \\ C3 &= \alpha + 8\gamma \end{aligned} \qquad (2.58)$$

As written in equation (5.27), the states are uniquely classified by five quantum numbers. Three of them are trivial, the d-boson number n_d, the angular momentum L and its z-component M. The fourth is the boson seniority ν. Instead of ν, one can introduce another quantum number n_β which counts boson pairs coupled to zero angular momentum. n_β is related to ν by:

$$\nu = n_d - 2n \qquad (2.59)$$

The fifth quantum number is n_Δ which counts boson triplets coupled to zero angular momentum.

The total number n_d is partitioned by n_β and n_Δ as;

$$n_d = 2n_\beta + 3n_\Delta + \lambda \qquad (2.60)$$

and the values of the total angular momentum for each n_d, n_β, n_Δ are given in terms of λ by;

$$L = \lambda, \lambda+1, \lambda+2, \ldots. 2\lambda-2, 2\lambda \qquad (2.61)$$

To identify the region of SU(5) a necessary but not sufficient condition is that the forbidden $\Delta n_d=2$ transition be small, and that a vibration like two phonon pattern is present with 0^+, 2^+, 4^+ states in the neighbourhood of twice the energy of the first excited state. The most favourable condition seems to be when N(orZ) is only 4-6 particles away from the closed shell and Z(or N) is 8-10 particles away from it.

2.4.4 Transitional Regions.

The three limiting cases discussed above are useful since they provide a set of analytic solutions which are easily tested by experiment. However, only few nuclei can be described by the limiting cases. Most nuclei display spectra intermediate between the limiting cases. For the purpose of classification, the transitional nuclei can be divided into four classes.

A. nuclei with spectra intermediate between SU(3) and SU(5)

B. nuclei with spectra intermediate between O(6) and SU(3)

C. nuclei with spectra intermediate between O(6) and SU(5)

D. nuclei with spectra intermediate among all three limiting cases.

Nuclei in the transitional class D are difficult to treat from a phenomenological point of view, because they require the use of all the operators n_d, $\underset{\sim}{P}.\underset{\sim}{P}$, $\underset{\sim}{L}.\underset{\sim}{L}$, $\underset{\sim}{Q}.\underset{\sim}{Q}$, $\underset{\sim}{T}_3.\underset{\sim}{T}_3$

and $\underset{\sim}{T}_4 \cdot \underset{\sim}{T}_4$ appearing in equation (2.19). Much simpler studies can be done for nuclei belonging to the transitional classes A, B and C.

The Hamiltonian of class A can be written as

$$H = H[SU(3)] + \varepsilon \times n_d \qquad (2.62)$$

where the first term on the R.H.S. is the Hamiltonian of SU(3) limit. It is clear that, when ε is large, the eigenfunctions of H will be those appropriate to the SU(5) symmetry, while when ε is small, they will be those appropriate to SU(3) limit. For intermediate situations, they will be somewhat intermediate between the two limits. Similar changes also occur in the electromagnetic transition rates. Particularly important is the ratio

$$R = \frac{B(E2;\ 2_2^+ \rightarrow 0_1^+)}{B(E2;\ 2_2^+ \rightarrow 2_1^+)} \qquad (2.63)$$

which changes from

$$R = 0 \ , \quad \text{in SU(5)} \qquad (2.63\ a)$$

to

$$R = \frac{7}{10} \quad \text{in SU(3)} \qquad (2.63\ b)$$

The Hamiltonian of class B can be written in the form

$$H = H[O(6)] + \frac{QQ}{4} (\underset{\sim}{Q} \cdot \underset{\sim}{Q}) \qquad (2.64)$$

Again, when QQ is small the eigenfunctions of H are those appropriate to O(6) limit, while when QQ is large they are those appropriate to symmetry SU(3). The changes in electromagnetic transition rates can be seen from the ratio R,

defined in equation (2.63) whereby

$$R = 0 \quad \text{in } O(6) \tag{2.65}$$

and

$$R = \frac{7}{10} \quad \text{in } SU(3) \tag{2.66}$$

In the case of transitional class C, the Hamiltonian can be expressed as

$$H = H[O(6)] + \varepsilon \times n_d \tag{2.67}$$

Thus when ε is large the eigenfunctions of H are those of SU(5) limit, while when ε is small they are those appropriate to O(6) limit.

2.4.5 Program codes PHINT and FBEM.

These two programs were used during the course of present work to predict the nuclear structure properties in the context of the Interacting Boson Model. They are coded in FORTRAN IV and were designed to calculate the energy levels and transition probabilities.

The program PHINT calculates the energies and eigen vectors for the positive and negative parity states. These resulted from an exact diagonalisation of the IBA Hamiltonian (H) defined as:

$$H = H_{sd} + H_f + H_{df} \tag{2.68}$$

where the appropriate definition of the Hamiltonian were given by equations (2.19), (2.25) and (2.26). In calculating the Hamiltonian the spherical SU(5) basis is used;

$$|\psi> = |[N], n_d, n_\beta, n_\Delta, L_d, n_f, L> ,$$

where N = total number of bosons
n_d = number of d-bosons,
n_β = number of pairs of d-bosons coupled to L=0,
n_Δ = number of triplets of d-bosons coupled to L=0,
L_d = total angular momentum of d-bosons,
n_f = number of f-bosons; =0 for positive parity states
=1 for negative parity states.
L = total angular momentum of the state.

The program FBEM calculates the transition probabilities, as a result of acting the transition operator on the wavefunctions generated by PHINT. An example of such an operator was given earlier in equation (2.21), used to calculate B(E2) values.

The calculation procedures which involve the two programs will be briefly discussed. Both programs are available at the University of London CDC 7600 computer.

The important step in calculating the positive parity states of a nucleus is first to determine its 'strategy' i.e. the IBM Limit which can represent the nucleus. This will enable an appropriate form of the Hamiltonian to be specified during the diagonalisation procedure. The quick and easy way to identify the limit is to calculate the experimental energy levels ratio $E_{4_1}^+ / E_{2_1}^+$. If the ratio is approximately in the region of 3.0, the appropriate limit to start with is SU(3). When the ratio lies between 2.0 and 2.5, an O(6) description is more suitable while the ratio less than 2.0 indicates an SU(5) characteristic.

Figure (2.1) shows the typical energy level spectrum for the different types of symmetries. The arrows between the levels specified the allowed γ-transitions.

The second step is to estimate the values of the parameters used in the Hamiltonian. The parameters that have to be included are:

SU(3) : (QQ, ELL) and EPS, PAIR, OCT, HEX

O(6) : (PAIR, OCT, ELL) and EPS, QQ, HEX

SU(5) : full Hamiltonian.

The parameters in the brackets are for the exact (pure) limit and the other parameters are in order of assumed decreasing importance. The bracketed parameters can be estimated from the specific analytical solutions. The method is to equate a few experimental energy levels with the appropriate analytical solution. The values (in MeV) obtained from this 'hand' fitting will constitute the initial values for the parameters used during the diagonalisation of H.

The total number of bosons, specified by option NPHMAX, are deduced from the number of nucleons outside the closed shell. When the shells are more than half-filled, the bosons are counted as hole pairs. In its standard version the program can handle up to 16 bosons. The maximum spin value that can be computed by PHINT is twice the number of bosons. Normally, this spin value is specified in order to reduce the computing problem. By setting the option IAM equals to a certain number, the program will stop executing when it reaches this spin value. If not, the execution will only terminate after a default value of 2 X NPHMAX is reached.

The negative parity states can be calculated by assigning IPPM=2 instead of 1. This will instruct the program to take the Hamiltonian defined by Equation (2.68). The option NEIG specify the number of eigenvectors to be calculated for each J. Some other options available include, WRTAPE which tells the program to write the eigenvectors on the diskfile "TAPE 10". This diskfile will be used by FBEM to calculate the transition probabilities. The option PRINTP enables the resulting levels to be drawn schematically. The detailed type of options available are given in the program package PHINT [50].

The program FBEM needs two sets of inputs in order to calculate the transition probabilities. The first set consists of the values of the parameters for which the transi-

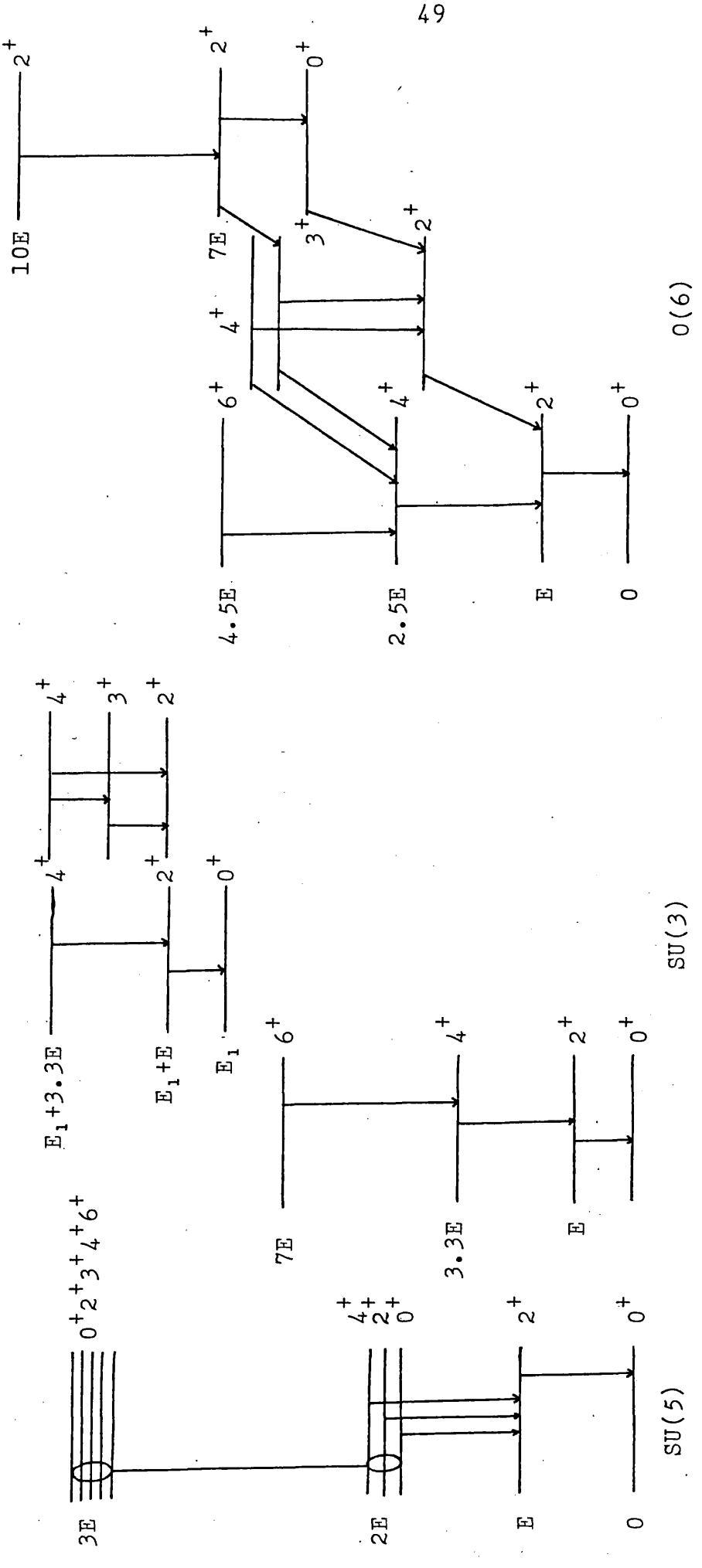

Figure (2.1) Theoretical level spectrum in the SU(5), SU(3) and O(6) limits. The arrows indicate allowed γ-transitions.

tion probabilities are to be calculated. For example, the parameters E2SD and E2DD are used to calculate the B(E2) values. The values of the parameters can be estimated using the analytical solutions i.e. by equating few known experimental values with the solutions.

The second set of the inputs consists of several options which enables the program to select the transition's mode. For example option ALL=λ will instruct the program to calculate all the possible transitions with multipolarity Eλ and Mλ. If only few transitions are needed, an option ONLY must be used.

It is important to note that FBEM cannot function independently without program PHINT but not vice versa.

2.5 Pairing-Plus-Quadrupole Model (PPQM).

This model has been used in recent years in attempts at understanding nuclear structure. The combination of two forces leads naturally to the most important residual effects in nuclear structure, namely pairing effects and quadrupole deformation. The nucleus find its shape as a result of the competition of these two forces, the quadrupole force attempting to deform it and the pairing force trying to keep it spherical.

The Hamiltonian (H) of the model consists of three parts [54]:

$$H = H_s + H_p + H_Q \qquad (2.69)$$

where

H_s is the Hamiltonian for the spherical, single-particle energy,

H_p is the Hamiltonian of the pairing force and

H_Q is for the quadrupole force.

The simplest approach to this Hamiltonian is to treat it in a self-consistent approximation [55]. The pairing effects and field effects are treated on the same footing. The assumptions made are:

a) The contribution of the pairing force to the self-consistent field is neglected.

b) The contribution of the quadrupole force to the pairing potential is neglected.

c) The exchange term coming from the quadrupole force is also neglected.

These approximations are essential in bringing out great simplifications in the formalism.

The approach was used by Baranger and Kumar [54] for the single-j shell analysis i.e. a nuclear shell consisting of one single particle level, whose angular momentum is j.

The validity of the model was later discussed [56] whereby a correction is introduced to take into account the different number of protons and neutrons. The criteria for choosing the values of each parameters in the Hamiltonian were also described. The parameters include the harmonic oscillator length b, the number of levels that should be included in the calculation, the quadrupole strength and also the strength of the pairing force.

A further test on the model was made by Kumar and Baranger whereby the properties of the rare-earth nuclei were calculated [57]. The calculations were done within the framework of Bohr's collective Hamiltonian [58]. The seven functions (six kinetic energy functions and one potential energy function) are calculated microscopically starting from a spherical shell model plus residual interaction [59]. The pairing plus quadrupole model of residual interaction was used. The seven functions determine the coupling between rotational motion, β-vibration and γ-vibration.

CHAPTER III

EXPERIMENTAL ARRANGEMENT

3.1 Singles spectra measurements.

The gamma-rays emitted by the radioisotopes were detected using different types of detectors: their efficiencies, equivalent volumes and measured performance characteristics are tabulated in Table (3.1). Each of these detectors are equipped with cooled FETs low noise preamplifiers, except for the NE102A plastic counter.

Two types of detectors were used in the singles spectra measurements. An intrinsic Germanium detector was employed to detect gamma-rays of energies less than 300 keV and 12 % efficient Ge(Li) measured the whole energy range of gamma-rays observed in the decay of the isotopes. These two combinations provide an overlap energy region between zero to 300 keV and constitutes a good check-up procedure, not only for the presence of gamma-rays with energies less than 300 keV but also their relative intensities.

In obtaining the singles, the output signals from the preamplifier were fed into a spectroscopic amplifier (Ortec 572). The signal-to-noise ratio was optimised by setting the shaping time constant of the amplifier at 2 μsec and the Baseline Restorer (BLS) at AUTO mode. The output signals from the amplifier were then fed to the Analogue Digital Converter (ADC) whose output was taken to the memory unit having 4096 channel numbers.

The source-to-detector distance was fixed at 25 cm and the source activity was chosen to give a count rate of less than 2000 counts per sec. in order to minimise the pile-up effects.

Table (3.1) Specifications of the detectors used in this work.

Type	Approx. Volume	Relative Efficiency♦	Energy Resoln.† (keV)	Peak-Compton ratio
Ge(Li)	70 cc.	12 %	2.21(5)	36
Ge(Li)	60 cc.	10 %	1.94(5)	38
Intrinsic Ge	2.5cm² × 2.5cm		1.62, 0.5*	37
NE102A Plastic	1'' × 1''			

† : FWHM of 1332 keV ^{60}Co.

* : FWHM of 122 keV.

♦ : at 1.33 MeV

3.2 Energy and efficiency calibration.

The energy calibration was determined by a least-squares fit to an n-th degree polynomial to the γ-ray energies. The energies used in the fitting were the 511 and 1275 keV of ^{22}Na and the 1173 and 1332 keV of ^{60}Co together with few prominent γ-rays of the isotope under study. The uncertainties in their calibrated energies were taken from Ref: [61]. The centroid of these energy peaks were determined by the fitting procedure of program SAMPO [60] which uses the Gaussian-plus-exponential representation of the shape function for the photopeaks. Essentially the uncertainties in the energy determination can be attributed to two main reasons, the energy response of the preamplifier and the ADC and also due to the listed calibration uncertainty. The nonlinearities of the preamplifier and the ADC may add up to few parts in a thousand and is assumed to be a continuous function of energy. A third order polynomial was found to give the best fit.

The efficiency curve for the detector was constructed using gamma-ray sources over the energy range from 30 keV to 2.0 MeV. The sources are chemical standard sources [62] which

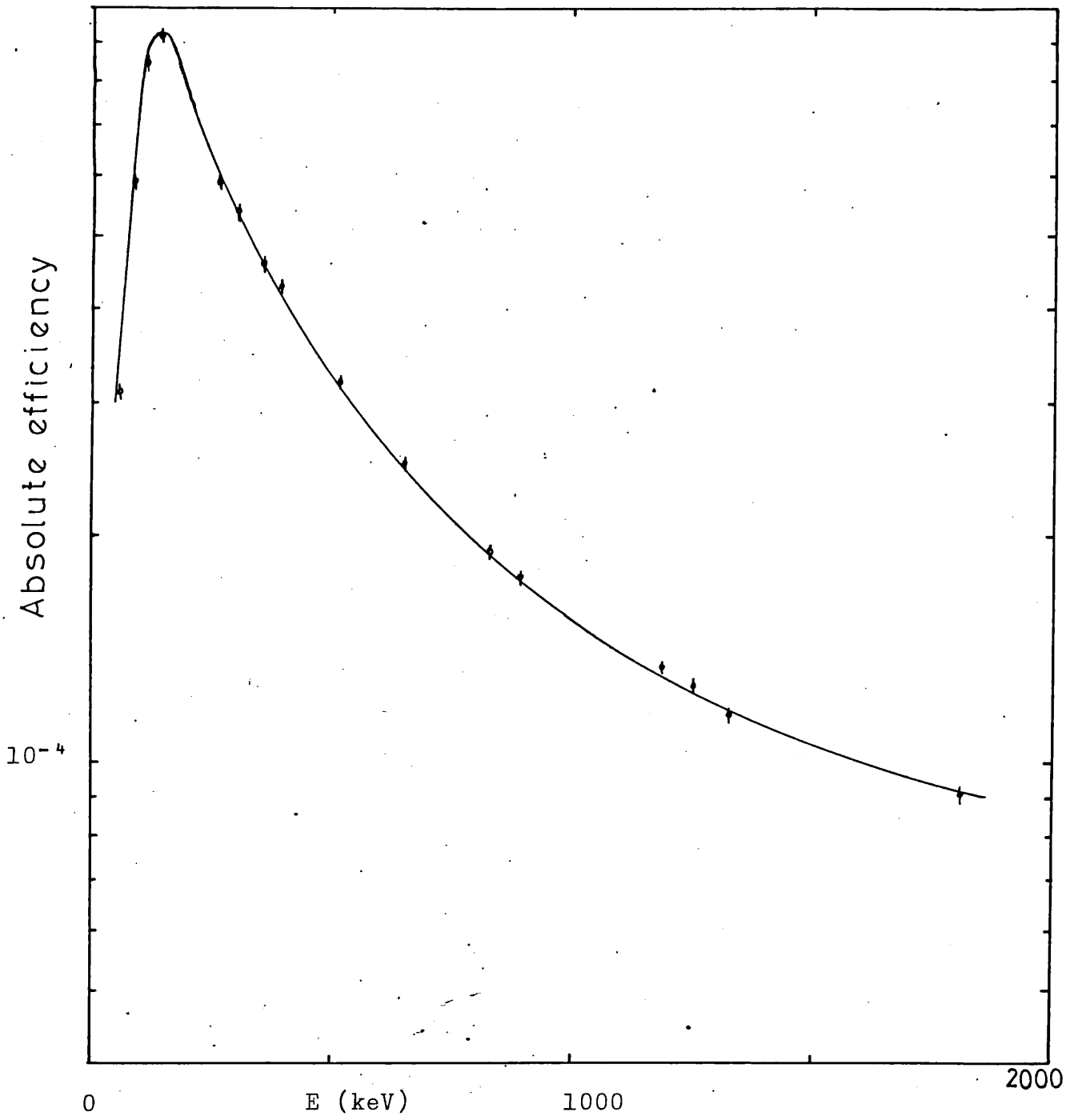

Figure (3.1) The absolute efficiency-energy relationship for the 12 % efficient detector.

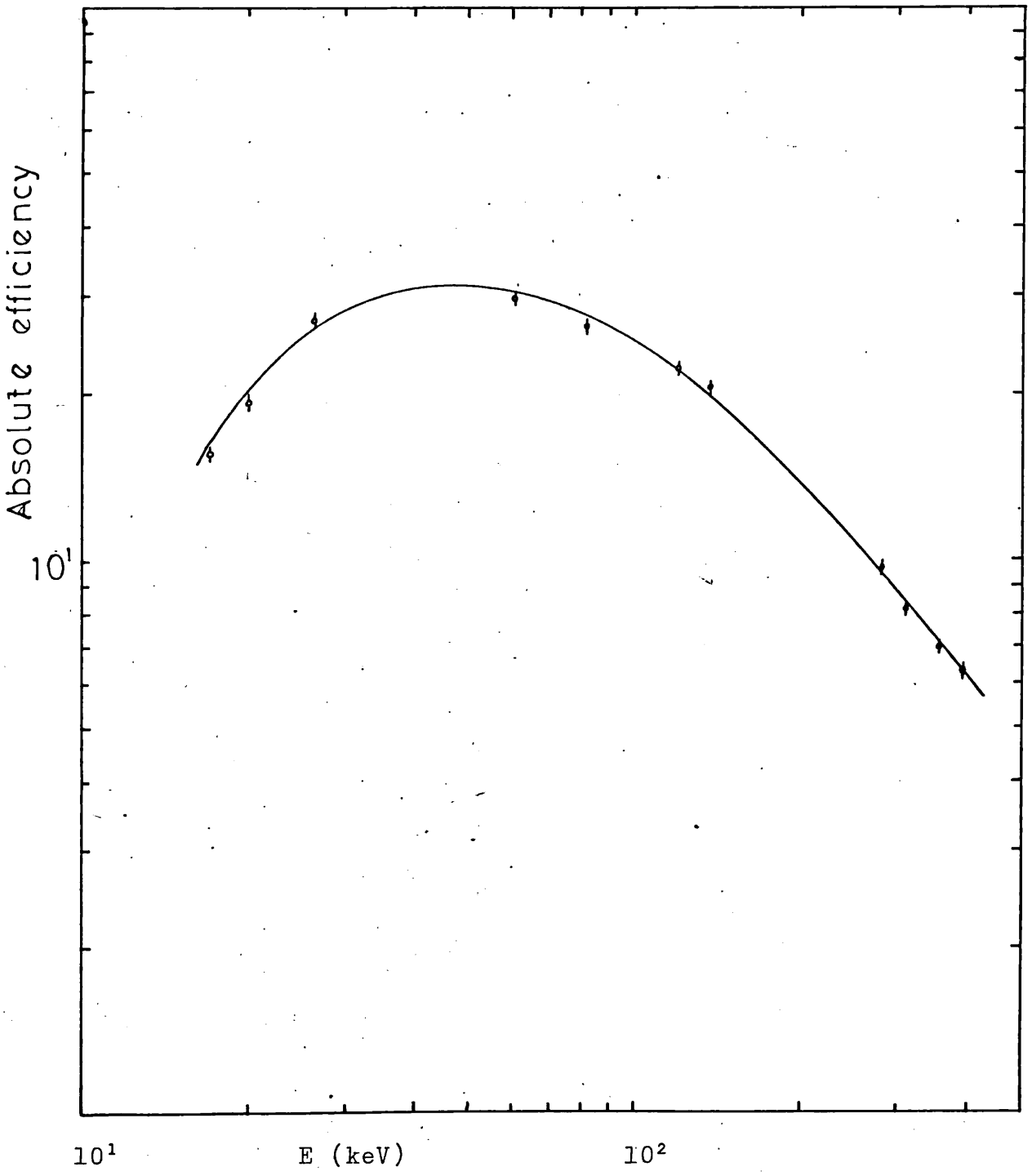

Figure (3.2) The absolute efficiency-energy relationship for an intrinsic Germanium detector.

include ^{241}Am, ^{133}Ba, ^{57}Co, ^{60}Co, ^{132}Cs, ^{54}Mn, ^{88}Y and ^{22}Na. The efficiency ε of the detector was taken as a function of the energy E to be:

$$\varepsilon = P_1[E^{P_2} + P_3 \exp(P_4 E)] \qquad (3.1)$$

where E is expressed in keV. The four parameters P_1-P_4 were determined by a least-squares minimisation procedure carried out by the program SAMPO [60], modified to run on the University of London CDC 6600 computer. The error in the efficiency calibration was attributed to the error in the peak area of the γ-rays as determined by the peak fitting procedure of SAMPO. The error in the efficiency calibration was estimated to be in the region of 2 %.

Figure (3.1) shows the efficiency curve for the 12 % Ge(Li) detector as a function of energy. The efficiency curve for the pure Germanium detector is shown in Figure (3.2).

3.3 γ-γ coincidence method.

When two γ-radiations are emitted successively by a nucleus, they are correlated either in space or in time. The measurement of the time correlation which involves the determination of the number of transitions of the first γ-transition following (or preceding) the other enables a level scheme of a nucleus to be constructed. These coincidences are measured by a system having resolving time greater than the delay between the 'birth' and 'death' of the two transitions. The system uses two detectors, one selects an 'energy channel' and measures the energy spectrum in the other detector of the coincidence radiations.

3.3.1 Fast-slow coincidence system.

Basically the system consists of 'fast' and 'slow' branches, the fast refers to the timing arm and the slow represents the energy section.

Figure (3.3) shows the conventional fast-slow coincidence system.

The two detectors were arranged at 90^0 to one another in order to minimise the possible scattering effects of the crystals inside the detectors. There are two outputs from each of the detectors. One was for the timing and another for the energy. In the fast branch of the system, the 12 % efficient Ge(Li) detector was used to initiate the START pulse while the 10 % efficient Ge(Li) provides the STOP signal to the Time Pulse Height Converter (TPHC). The output of the TPHC gives a time distribution for the events in the two detectors.

The timing pulses from the two detectors were initially shaped and amplified by two units, Constant Fraction Discriminator (CFD) and Timing Filter Amplifier (TFA), before being fed to the TPHC. The timing distribution obtained depends on the combination of settings of these units. The accuracy of any coincidence experiment depends on this time distribution as a timing correlation for the coincidence gate. Generally, this time distribution can be affected by the contribution from undesired events such as chance and background coincidences.

The chance coincidences depend on the resolving time τ defined as the FWHM of the timing peak. The ratio of the true-coincidence to chance coincidence is inversely proportional to τ [62]. Thus for small value of τ, the ratio is expected to be high. The value of τ obtained is much affected by time walk and jitter noises in the electronics.

Walk effect is a time variation in producing time signals [63]. It arises from pulses which triggers the discriminator at fixed threshold with varying amplitudes and risetime. This variation in risetimes and amplitudes of the pulses is indeed expected to occur especially in the solid state detectors used. These detectors possess finite charge collection time depending on the position of electron-hole pair being created. In order to minimise this time walk

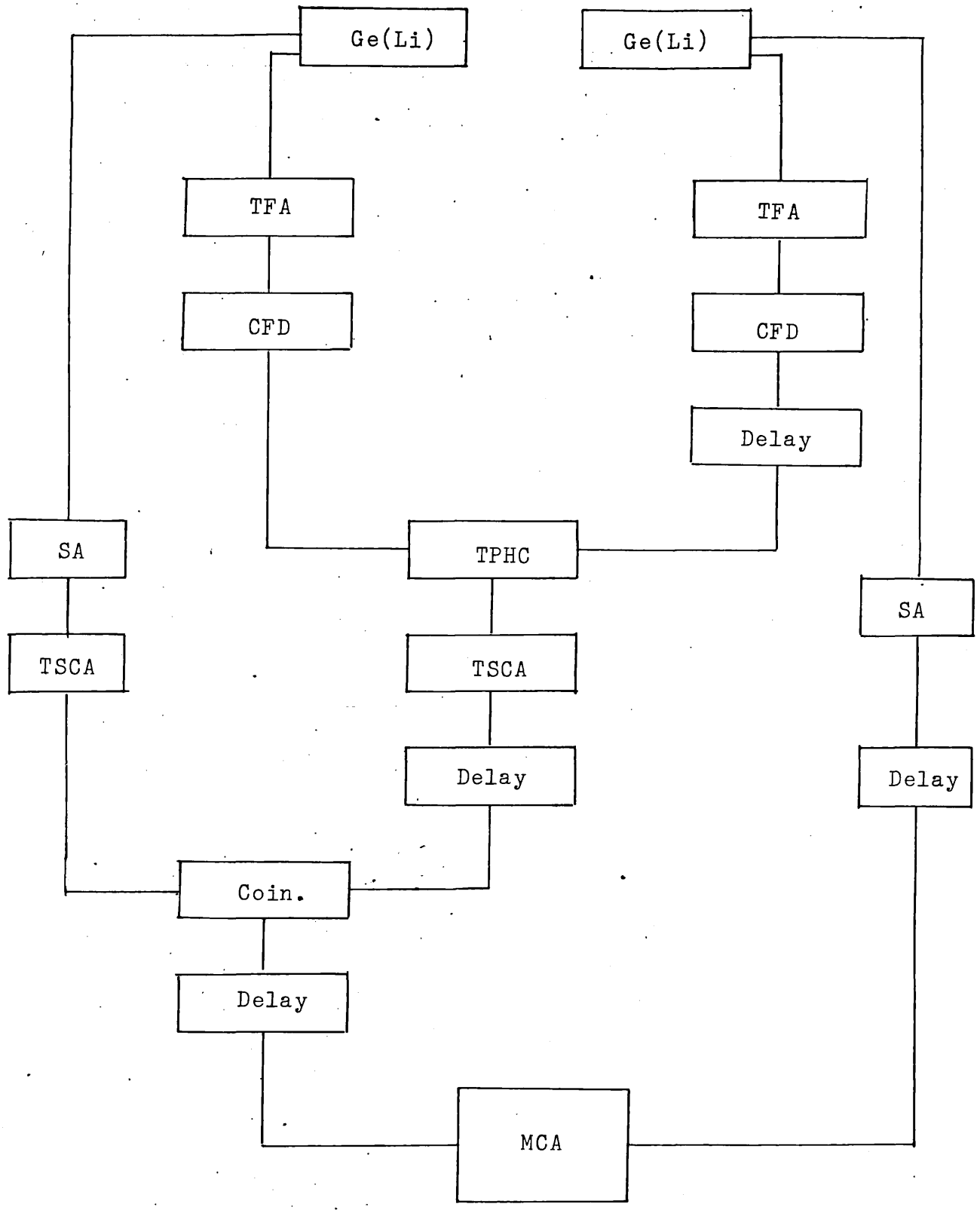

Figure (3.3) Block diagram of the conventional fast-slow system.

problem, a method of constant fraction timing mode [64, 65, 66] was used. Here, the input pulse is initially attenuated by a factor 20 % of the original height. The full amplitude, being delayed by time (t_d), is then inverted and added to the attenuated pulse. The timing signal is derived at the zero-crossing point of the pulse and will be the same for all pulses.

Jitters on the other hand are noise signals superimposed on the real signals. They are statistical fluctuations of the signals from the detector and can cause discriminator to response either sooner or later than it should be. This problem can be resolved by setting the constant fraction discriminator level well above the noise level.

The Timing Single Channel Analyser (TSCA) was used to select the true part of the timing spectrum generated by the TPHC. The window settings ΔE of the TSCA were adjusted to lie across the peak of the timing spectrum.

In the slow branch, the gating energy was chosen by another TSCA, from the energy pulses of the 10 % Ge(Li) detector. The output of both TSCA were delayed and fed into a slow coincidence unit.

The output is then taken to the Pulse Stretcher (PS) and to the coincidence part of the Multichannel Analyser (MCA).

The 12 % detector provides the total spectrum which was first delayed and fed to the high level of the MCA. By setting the MCA to coincidence mode, the coincidence data was then accumulated until sufficient counts were obtained.

The conventional fast-slow system is relatively of low efficiency due to two main factors:

- In selecting the true coincidence part of the timing spectrum, the region ΔE was narrowed down as much as possible. This could lead to some useful information being lost and therefore resulting in poor coincidence spectrum.

- The background coincidences were not corrected for. This is very important especially for gating peaks with low energies where the background is high.

3.3.2 Dual Parameter Energy-Time Spectrometer (DPETS).

The spectrometer [67] provides an alternative system to the conventional fast-slow coincidence system. The high efficiency of the DPETS enables large amounts of data to be accumulated within a short time period. The spectrometer has a 4096 by 4096 coincident gamma-gamma spectra from two Ge(Li) detectors stored in a large capacity magnetic tape.

Figure (3.4) shows a schematic diagram of the spectrometer.

The difference between the spectrometer and the conventional fast-slow system is the introduction of a Dual Parameter Collection System (DPDCS) which contributes to the high efficiency of the spectrometer.

Figure (3.5) shows the block diagram of the dual-parameter data collection system attached to the fast-slow branch.

The DPDC system used a dual-parameter interface between the coincidence branch and the magnetic tape storage and is called the write interface. The interface between the magnetic tape and memory unit is the read interface.

In the fast branch there is also a modification being made. The output of the TPHC is fed to two separate TSCAs. One TSCA selects the total part of the timing spectrum and the other chooses the chance region. The output of these TSCAs then trigger the Pulse Generator (GPG), an output of which was used to gate the two ADCs. The two ADCs, one for the spectrum and one for the gating are coupled to the write interface of the DPDC system (Figure: 3.5).

A pulse from the fast system indicates an event which can be either total or chance. This pulse then opens the gate

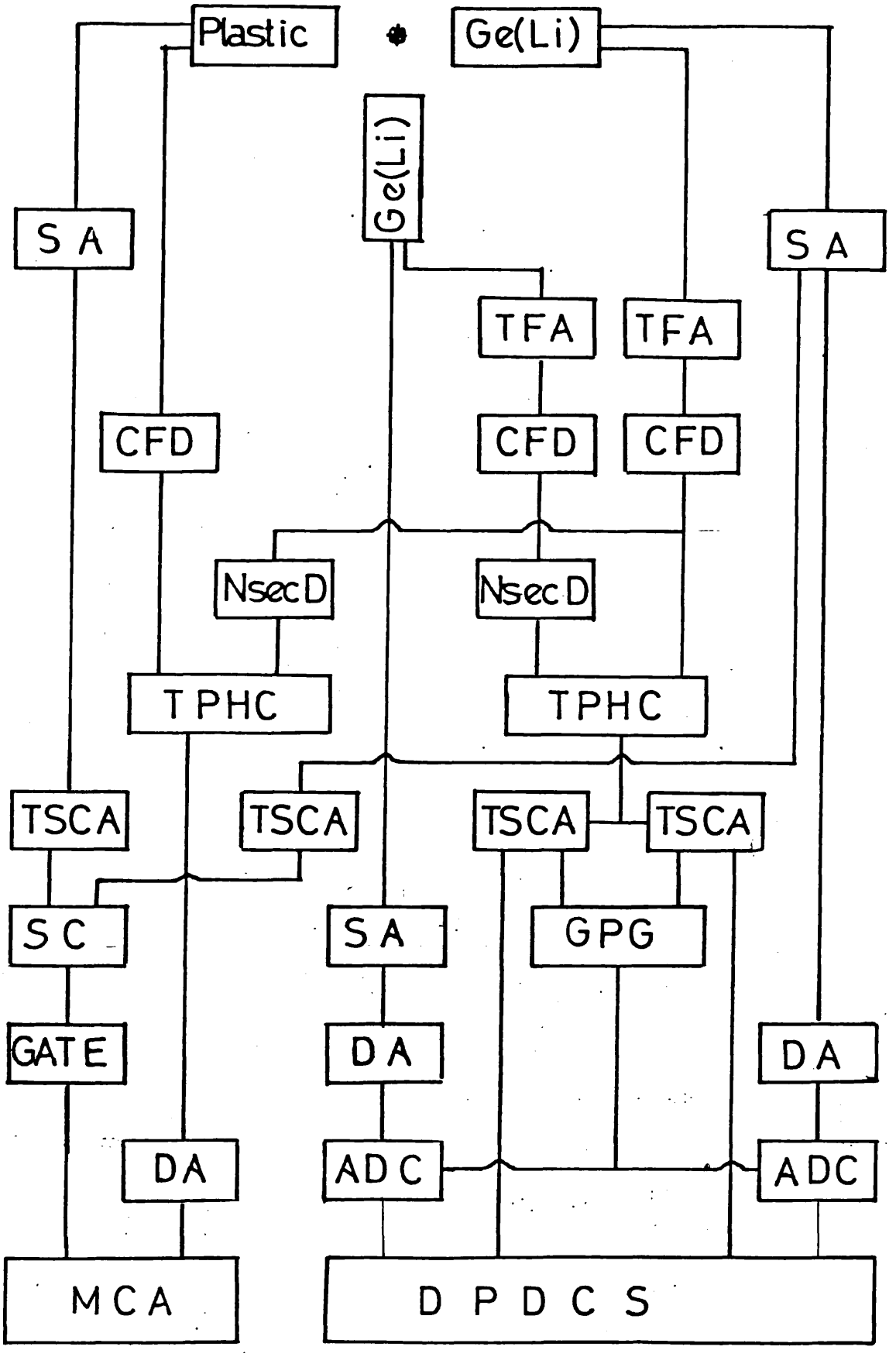

Figure (3.4) Block diagram of the Dual-Parameter Energy-Time Spectrometer.

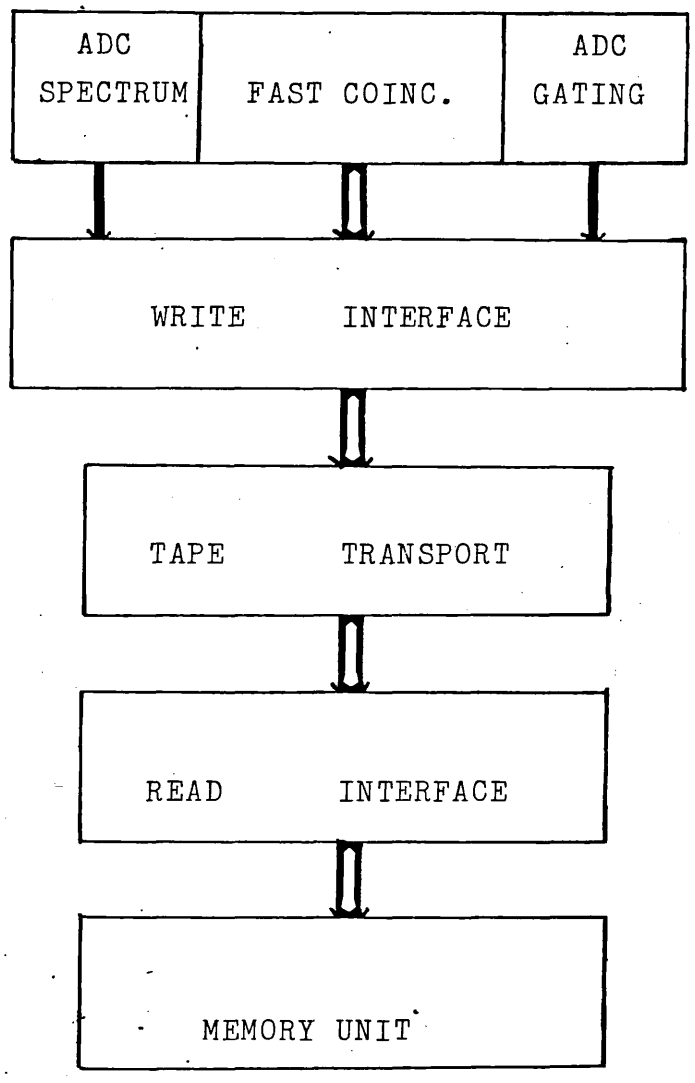

Figure (3.5) Block diagram of the dual-parameter data collection system.

of the respective gating and spectrum ADCs enabling the linear signals from the two detectors to be digitised. At the same time, the pulse is suitably delayed to take into account of the time required for the conversion process in the two ADCs. The recording process will be initiated as soon as this conversion has been completed.

The binary addresses from the ADCs are converted into binary-coded-decimal (BCD). The multiplexer unit converts the parallel data into serial form and then stored temporarily in a storage buffer. The buffer can contain up to a maximum of 2048 bytes. Since one event correponds to nine bytes, the buffer can store approximately 227 coincidence events before dumping the contents on to the tape.

The ½" wide tape has seven tracks assigned as 1-2-4-8-A-B-P. The parity P has been chosed to be odd and is not used in the present work.

For every coincidence event, nine words are written along the tape with each 7-bit word recorded on the corresponding track. The first word identifies whether the coincidence comes from total or chance. Suppose it comes from the total, then tracks 1248 of the tag word will have zeros while tracks ABD will have only ones in them. For chance coincidence then ABP becomes (010) and tracks 1248 still remain as zeros. The remainder eight words correspond to the two ADC addresses, four for each ADC.

In the read interface, shift register was used to convert the serial data back to parallel form suitable for the memory unit of the MCA. The output of the register were divided into two sections, one corresponds to addresses of the gating ADC and the other for the spectrum ADC. The former were connected to the comparator units (thumbwheels).

To obtain a coincidence spectrum, these thumbwheels (upper and lower windows) were set to a certain region of interest i.e. gating peak. The spectrum is then read through the READ mode of the system. During the reading process the

incoming data (on the tape) were simultaneously compared with the window boundaries. Any coincidence with the window will thus be registered and stored in the memory unit.

The resulting coincidence spectrum is a combination of three types of coincidences, true, chance and background coincidences. The last two types have to be eliminated to obtain a true coincidence spectrum. The elimination can be achieved by the subtraction mode of the MCA.

The chance coincidence was removed by switching the TOTAL-CHANCE toggle of the DPDCS to the CHANCE position. The coincident data (on the magnetic tape) was then read to generate chance coincidence spectrum. Since the MCA was in the subtraction mode, the chance coincidence was then subsequently eliminated from the previously obtained coincidence spectrum.

The background coincidence was subtracted by resetting the toggle back to the TOTAL position. The digital windows were then set to a region corresponding to the background of the gating peak. With the MCA still in its subtraction mode, the coincidence data was then read. The background coincidence is therefore being eliminated and the resulting spectrum is the CORRECTED coincidence spectrum, free from both the chance and background coincidences.

3.4 Timing Spectrometer.

Figure (3.6) shows the set up for the fast branch of the spectrometer. The complete set up is incorporated with the Dual Parameter Energy Time Spectrometer of Figure (3.5).

The most critical circuitary of the fast coincidence system is that which derives the time information from the output of the photomultiplier or the Ge(Li) detector. The direct detector pulses in general have relatively long rise-times and vary in amplitudes. They must be processed to produce regularised pulses of constant amplitude and rather fast rise-times, for presentation to the TPHC.

The amplitude of the anode pulse from plastic

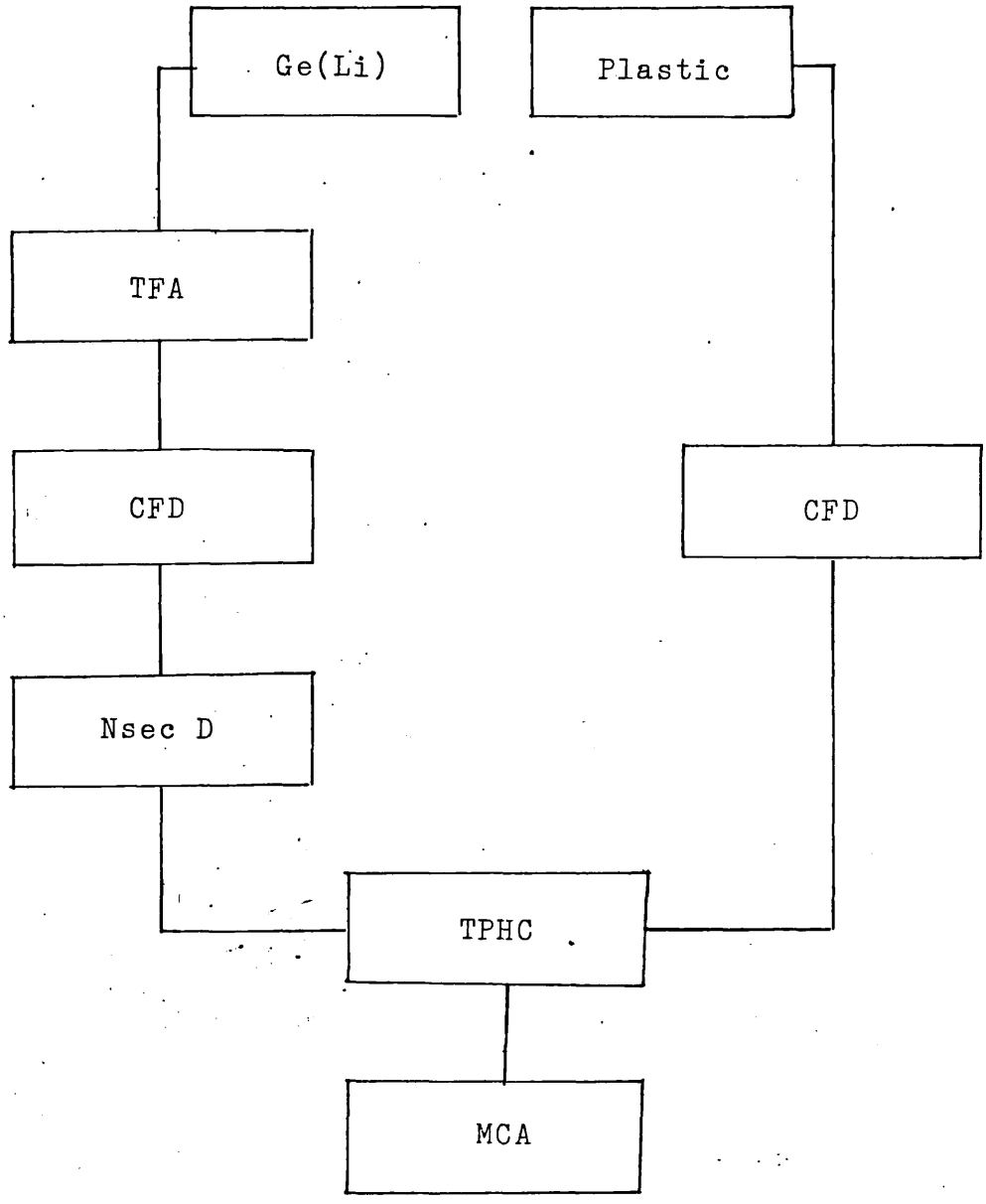

Figure (3.6) Block diagram for the fast-part of the lifetime spectrometer.

scintillation counter is approximately in the range of 5 V with ~2-3 nsec rise-time. The timing pulse of the Ge(li) detector has an amplitude of ~0.1 V with longer rise-time in the range of 60-100 nsec. The pulses from the latter detector have to be amplified by TFA before being taken to CFD. In the case of the pulses from plastic counter, they were fed directly to the CFD. The high amplitude of the pulses are sufficient enough to trigger the discriminator without being initially amplified.

The output of CFD (Ge(Li) branch) was delayed by a Nanosecond Delay unit which then fed the pulse to the STOP input of TPHC. The output of CFD from plastic branch was fed directly to the START of TPHC.

The characteristics of a delayed-coincidence system are most often given in terms of the response of the arrangement to a prompt coincidence. Although the shape of the spectrum (output of TPHC displayed on MCA) depends on the properties of the detectors, it may be roughly characterised by a FWHM and an apparent half-life ($T_{\frac{1}{2}}$) of the slope. In addition, the shape also depends on the combination of electronic settings especially the TFAs and CFDs. In general, the width of the prompt curve is a result of the time dispersions of two detectors and if the detectors do not have equal response, the prompt curve generally will not be symmetric.

The time distribution of an excited state was measured by gating the timing spectrum (TPHC output) with the gamma ray which depopulate this state. The energy arms of both detectors were fed into a slow coincidence unit (Figure 3.6) . The output was fed to the MCA.

The data was accumulated for several weeks until the counts in the spectrum peak reach the order of 10^4 counts. This large number of counts will result in a small statistical error of ~1 %.

The half-life of the excited state was estimated by a slope-method [63]. Here, the life-time of the level is defined as the time taken by the count rate to drop half of the initial

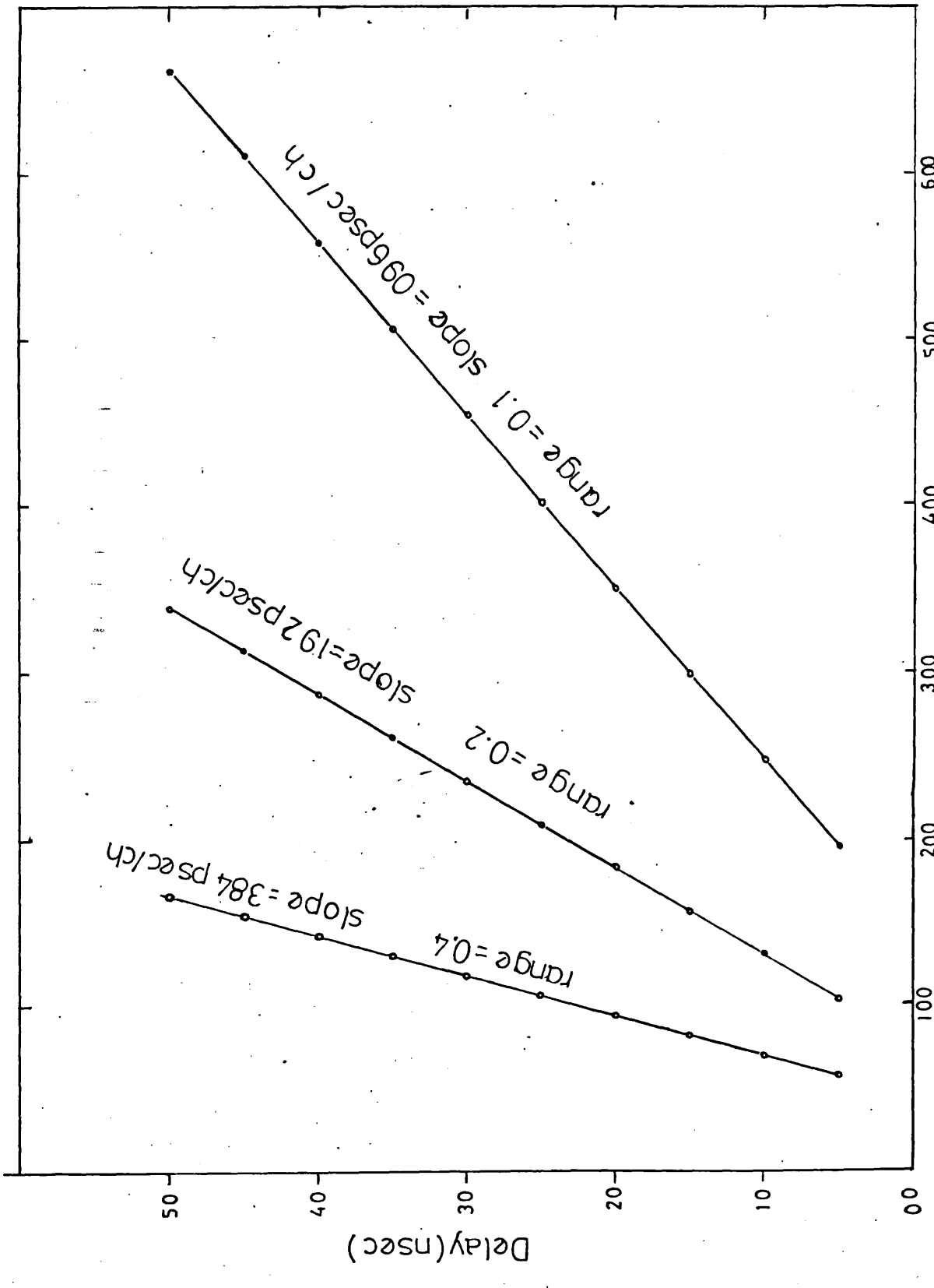

Figure (3.7) The time calibration of the MCA for different TPHC ranges.

value. This drop in the count number is a function of channel numbers. Thus timing calibration is essential to convert the channel numbers into time lapse.

Figure (3.7) shows the result of the calibration for 1048 conversion gain of the MCA at different TPHC time range. The expected linearity between delayed time and channel numbers were observed.

The coincidence count rate (N_γ) is related to the source strength by an expression [68]:

$$N_\gamma = \frac{N_1 N_2}{N}$$

where N_1 and N_2 are the count rates of the two detectors and N is the source activity. The smaller the source activity is, the higher will the coincidence rate be. In addition, the ratio of true to chance coincidence (N_t/N_c) will also increase [63]

$$\frac{N_t}{N_c} \propto \frac{1}{2\tau N}$$

where τ is the time resolution of the spectrum (FWHM).

Hence it is important to choose a small activity for the radioisotope used.

3.6 Performance of the system.

3.6.1 Timing Spectrometer.

The performance of the spectrometer was checked by using two standard radioactive sources: ^{22}Na and ^{60}Co. The ^{22}Na source was used to measure the lifetime of positrons in Lucite (perspex) material while ^{60}Co source provides a prompt

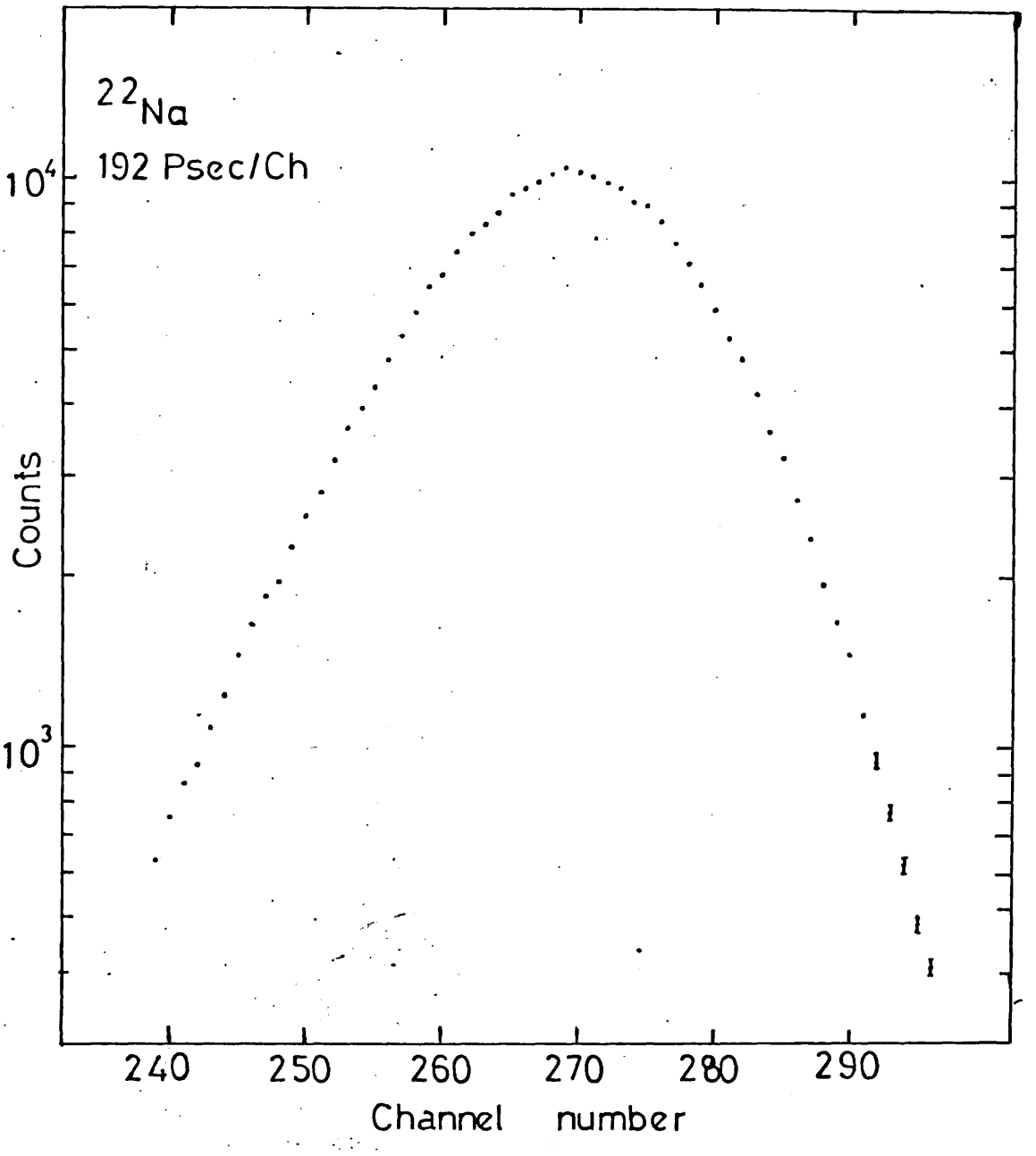

Figure (3.8) The lifetime spectrum of positrons in Lucite (perspex) sample.

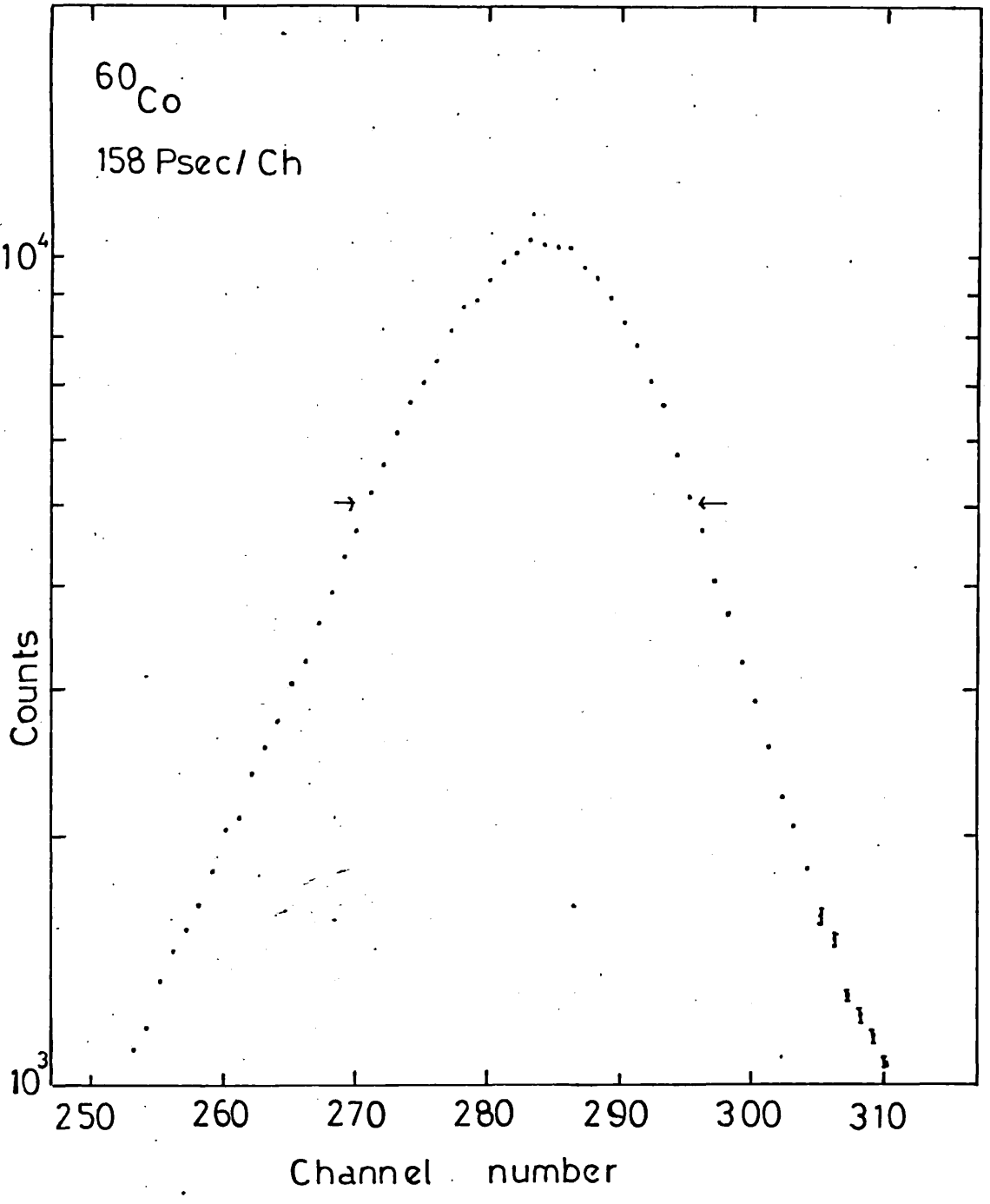

Figure (3.9) The prompt timing spectrum of ^{60}Co.

timing spectrum.

Figure (3.8) shows the lifetime spectrum of positrons in Lucite material.

The Ge(Li) detector was used to select the 511 keV peak of the ^{22}Na spectrum while the plastic detector selects the Compton plateau region for this peak. These selections were done by setting the TSCAs windows at the appropriate levels. The output signal from these TSCAs were fed to the input of the slow coincidence unit, the output of which is then used to open the gate of the MCA.

The half-life ($T_{\frac{1}{2}}$) of the positron measured from the slope of figure (3.8) was 1.35 ± 0.05 nsec., in agreement with the values of 1.32 ± 0.03 nsec. of Ref: [69] and 1.18 ± 0.14 nsec. of Ref: [70]. The lifetime spectrometer time resolution measured using the prompt gamma-rays of ^{60}Co is shown in Figure (3.9) and FWHM of 3.91 ± 0.05 nsec. was obtained.

3.6.2 DPETS.

The performance of the spectrometer was checked by measuring the coincidence spectra of the decay of ^{110m}Ag. The detectors used were the 12 % and 10 % efficient Ge(Li) detectors. The former actsas a spectrum detector while the latter was used as the gating detector.

The activity of the source, produced by $^{an}_{\Lambda}(n,\gamma)$ reaction, was 10 μCi. The distance between the source and both detectors were adjusted to give a count rate of less than 2000/sec in each of the detectors.

The total coincidence was collected for three weeks, a reasonable time to acquire data of sufficiently good statistics.

Figure 3.10 shows part of the total spectrum of ^{110}Ag.

A total of 4 gating peaks were chosen to build the

decay scheme of ^{110}Cd. The energies were 658, 765, 818 and 884 keV. Apart from their high relative intensities, these peaks were chosen due to their interrelationship in the decay scheme.

For each of these gates, initially the UNCORRECTED coincidence spectrum was taken by setting the appropriate windows. Later, the CHANCE and BACKGROUND coincidences were subtracted using the subtract mode of the MCA. The coincidence spectrum that resulted is the TRUE (or CORRECTED) coincidence spectrum of the specified gate.

The coincidence spectrum for all these gates are shown in Figures: 3.11 – 3.18. For the 818 and 884 keV gates, only the CORRECTED coincidence spectrum were shown.

The program SAMPO was used to determine the relative intensities of peaks observed in the CORRECTED coincidence spectrum. Table (3.2) shows the summary of the coincidence results. The entries VS (Very Strong), S (Strong) and W (Weak) signifies the degree of coincidences. The classification of these entries were based on their relative intensities of the transitions. VS indicates that the relative intensity is more than 1.5 times the standard relative intensity (relative intensity in total spectrum). If it is between 1-1.5, it is considered as Strong (S) and if it is less than 1, a Weak (W) coincidence is established.

The same criteria were adopted for the rest of the studies (see Chapter IV and V).

Figure (3.19) shows the partial decay scheme of ^{110}Cd established from the γ-γ coincidence measurements.

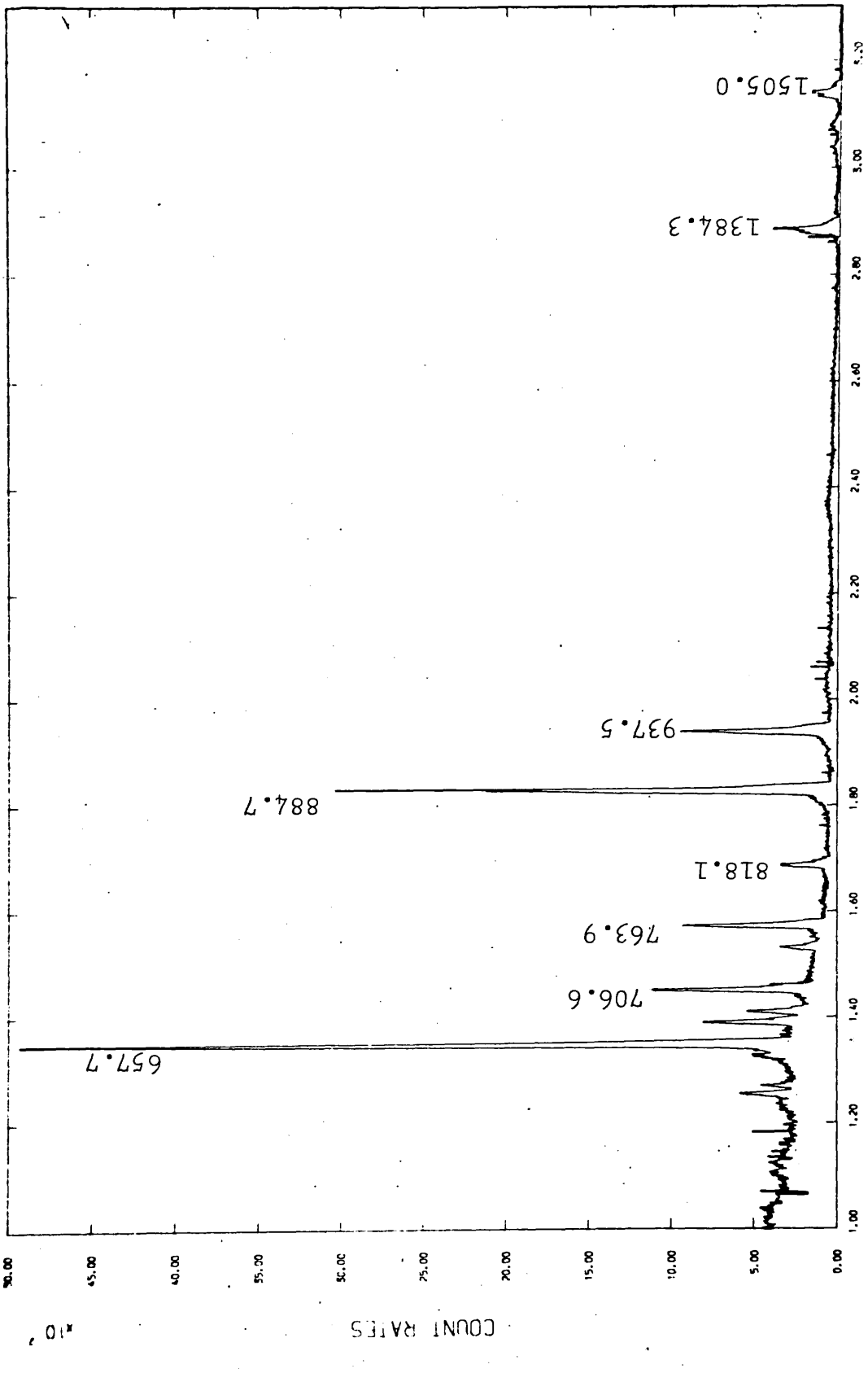

FIG. 3.10 110M-AG TOTAL SPECTRUM

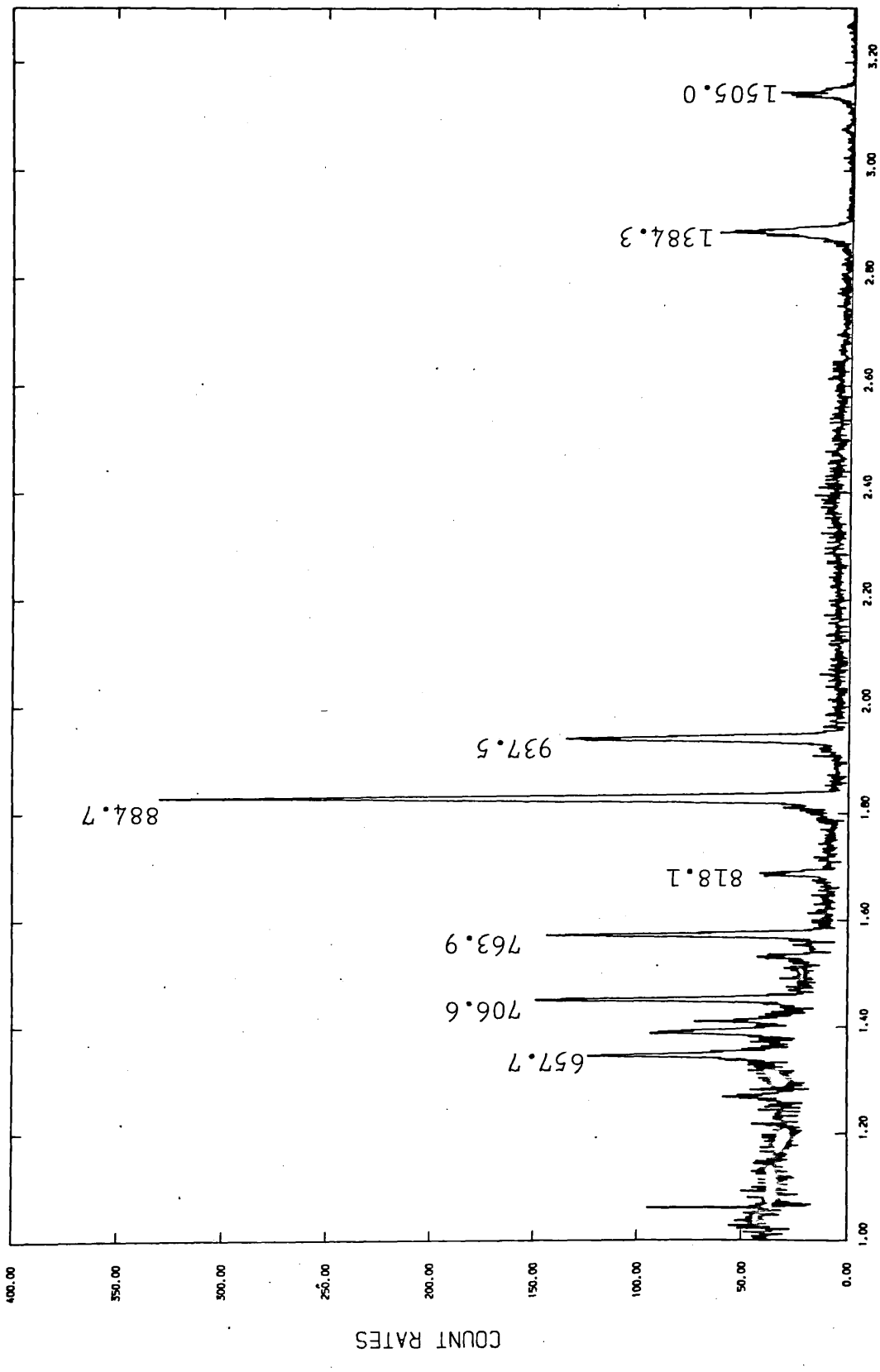

FIG (3.10 UNCORRECTED SPECTRUM OF AG-110M IN COINCIDENCE WITH 658 KEV

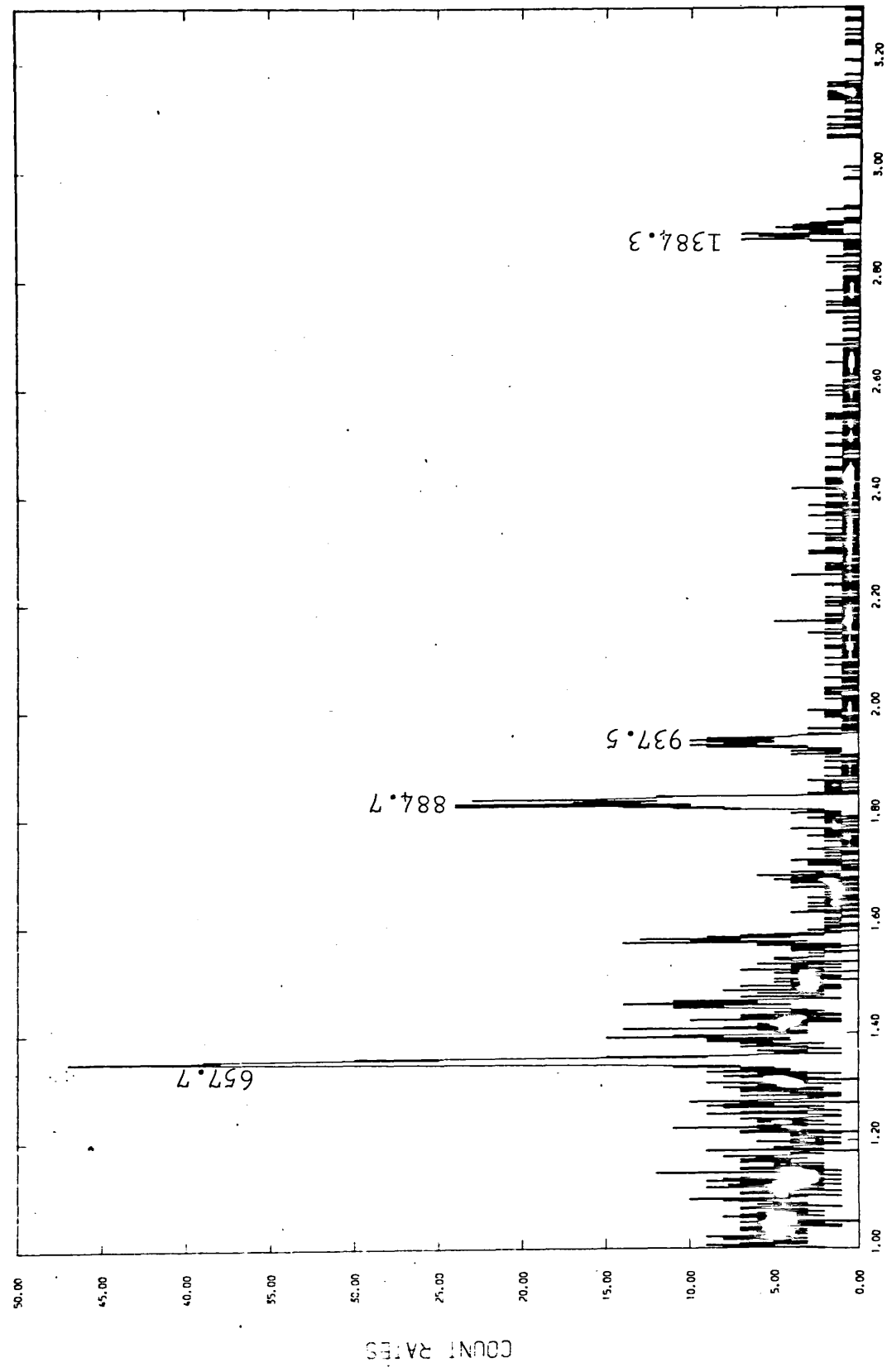

FIG (3.12) BACKGROUND SPECTRUM OF AG-110M IN COINCIDENCE WITH 658 KEV

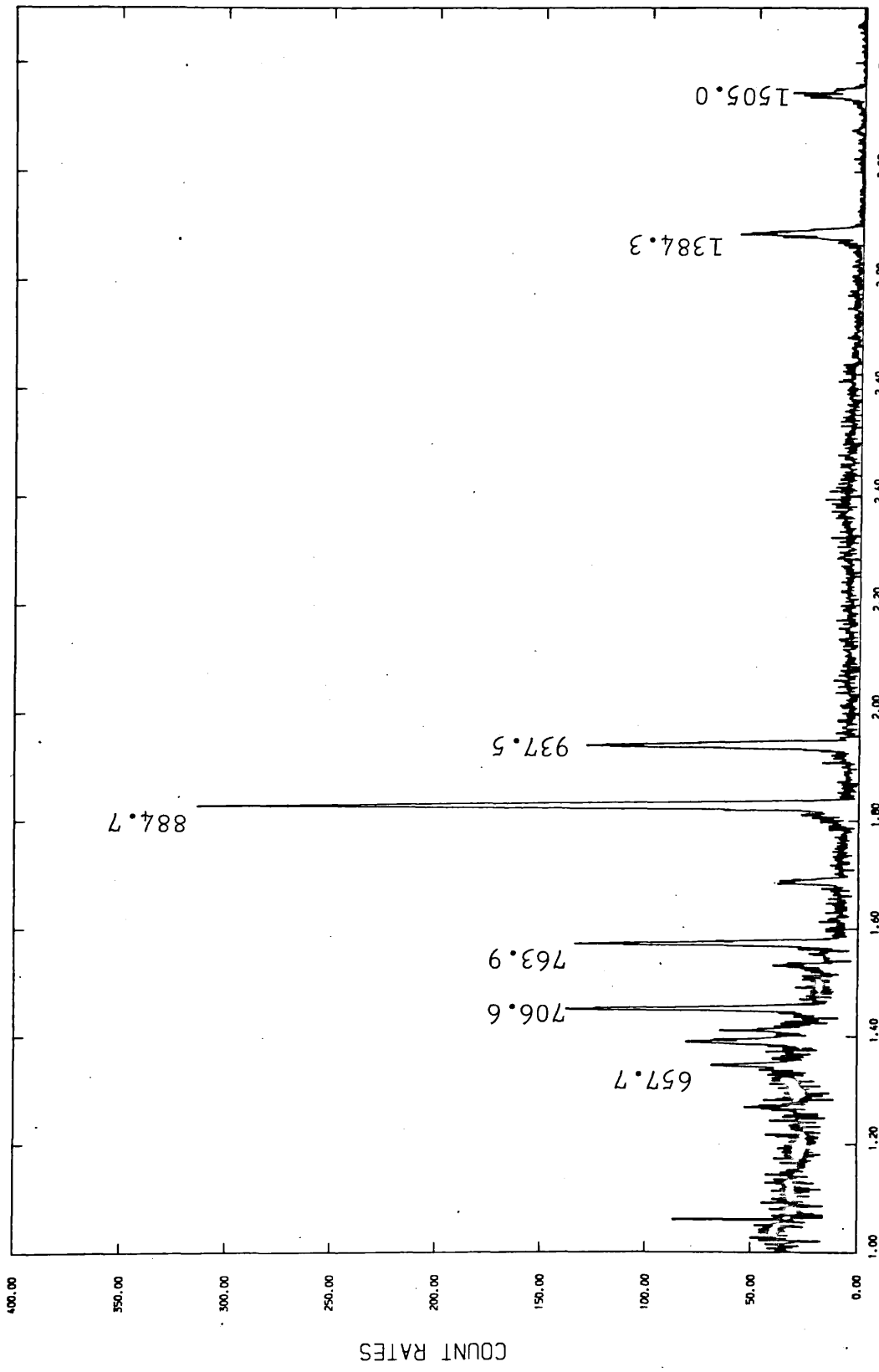

FIG (3.13) CORRECTED SPECTRUM OF AG 110M IN COINCIDENCE WITH 658 KEV

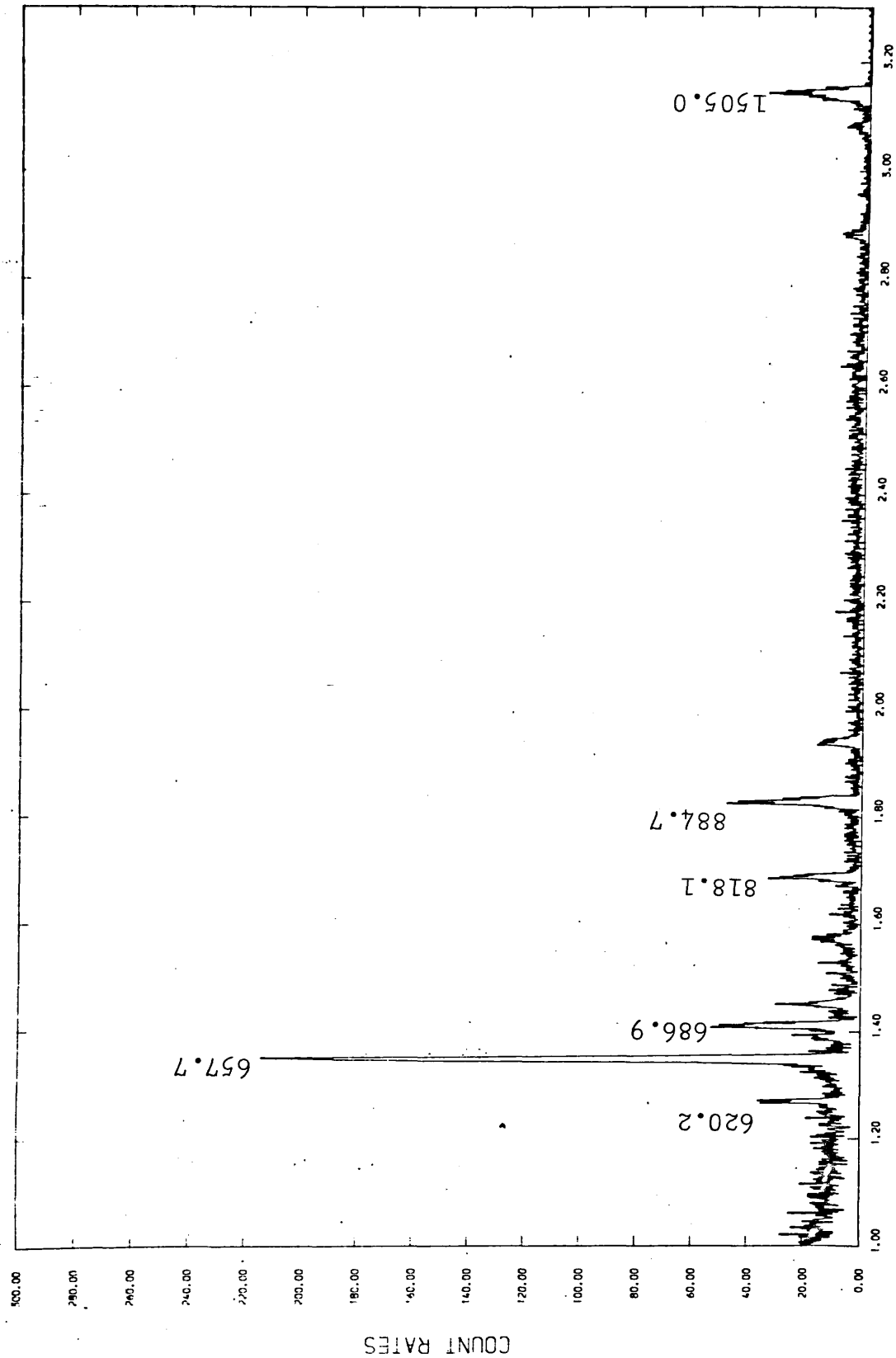

FIG(3.14) UNCORRECTED SPECTRUM OF AG-110M IN COINCIDENCE WITH 764 KEV

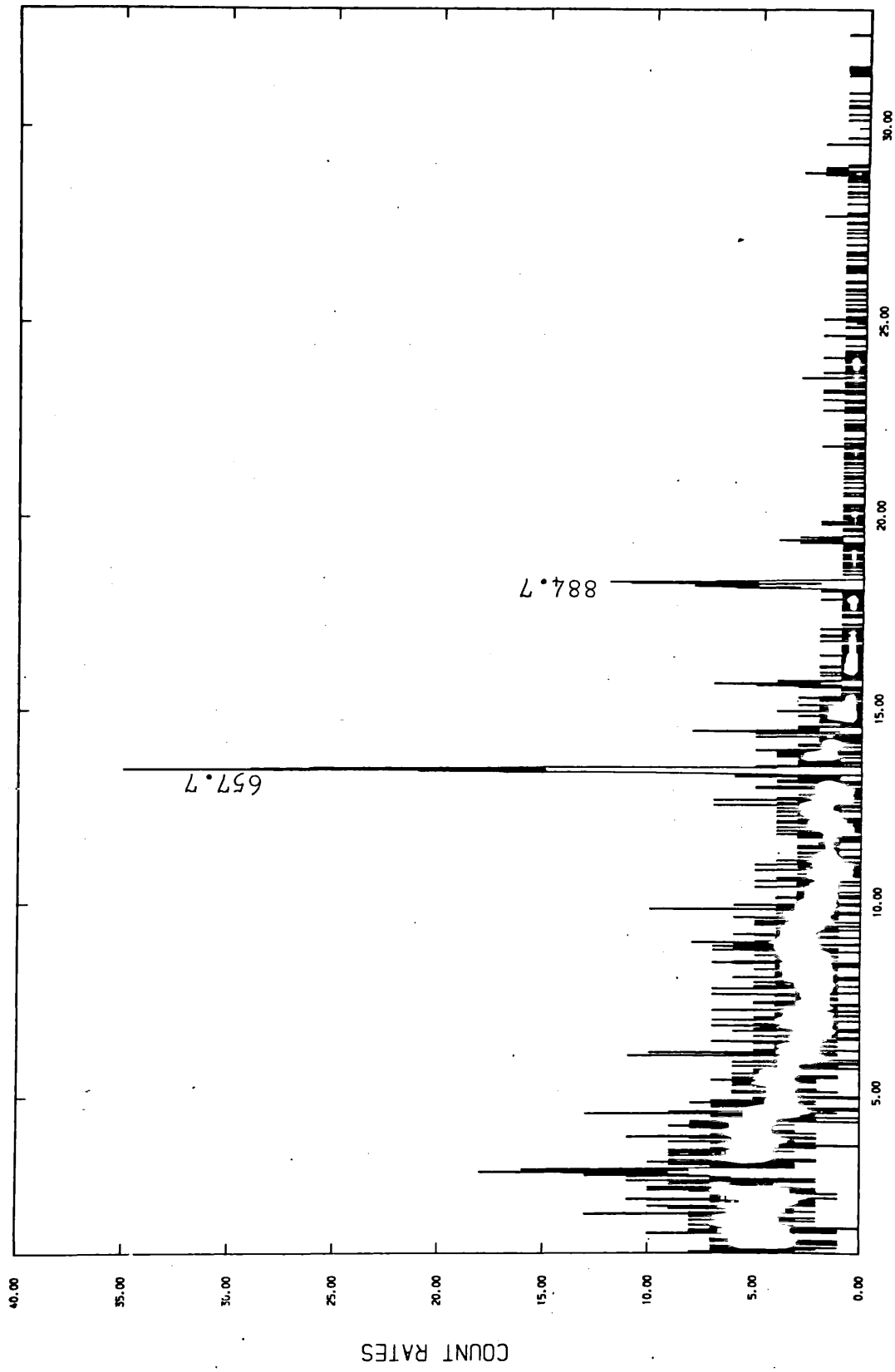

FIG(3.15) BACKGROUND SPECTRUM OF AG-110M IN COINCIDENCE WITH 764 KEV

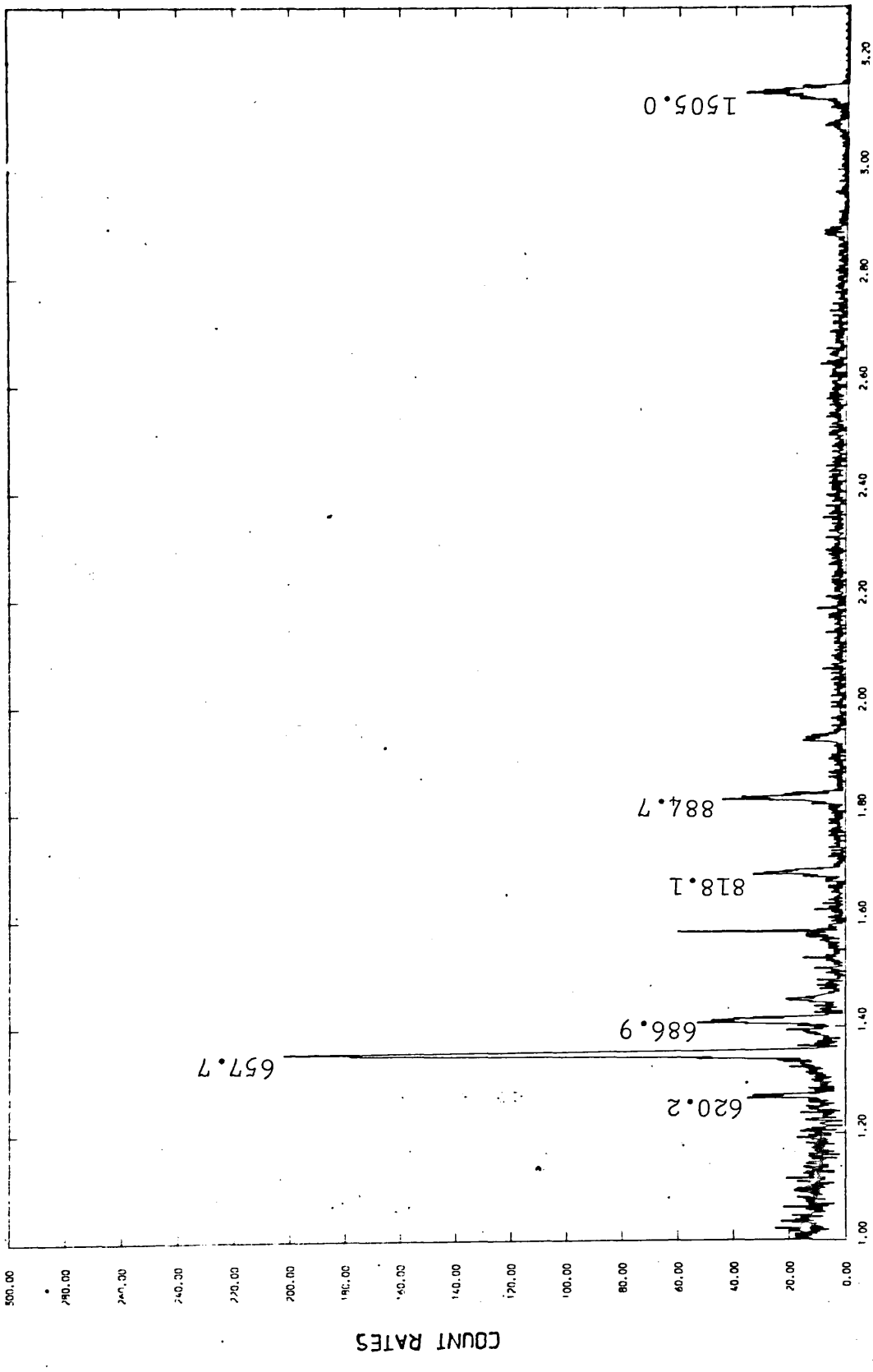

FIG (3.16) CORRECTED SPECTRUM OF AG-110M IN COINCIDENCE WITH 764 KEV

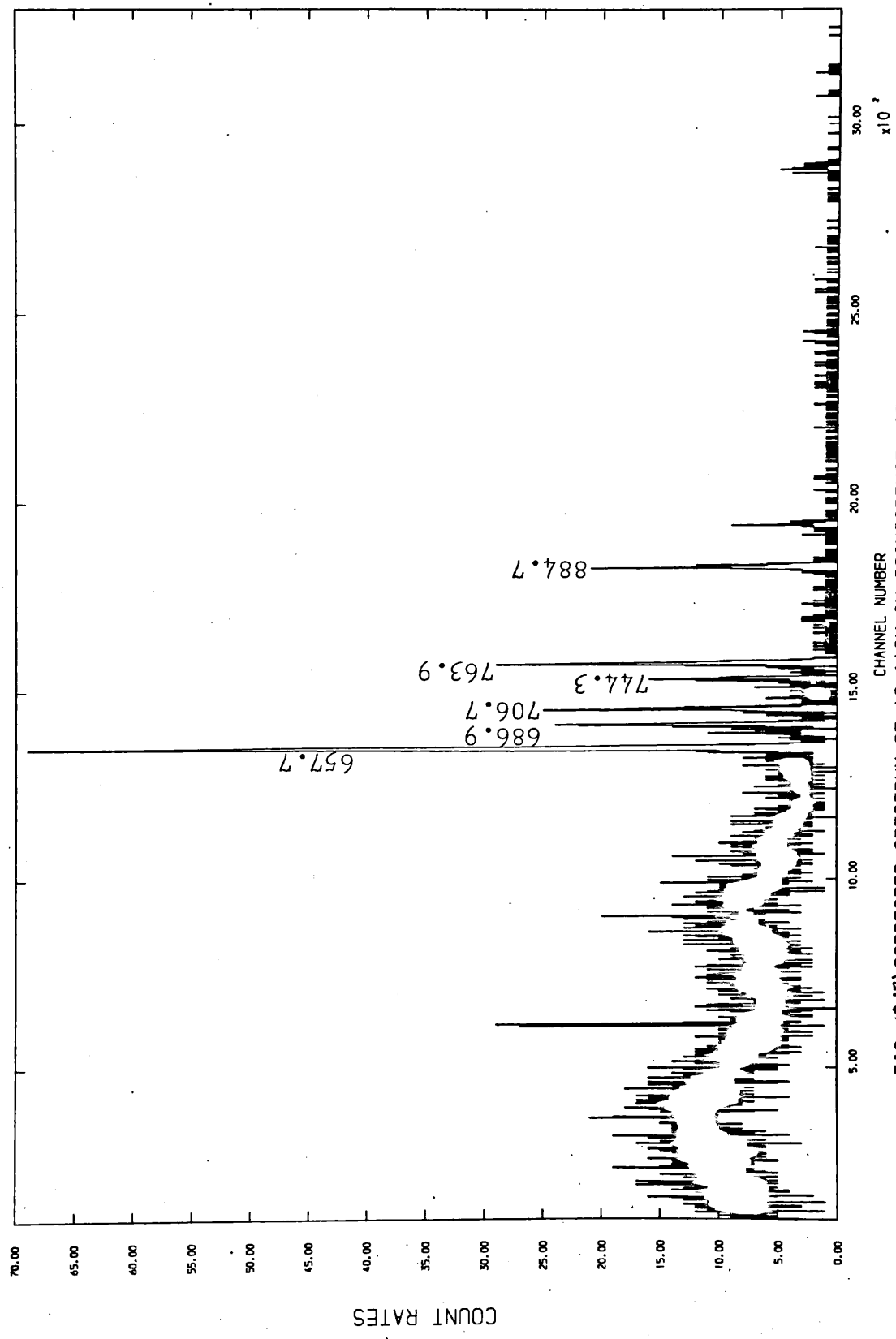

FIG (3.17) CORRECTED SPECTRUM OF AG-110M IN COINCIDENCE WITH 818 KEV

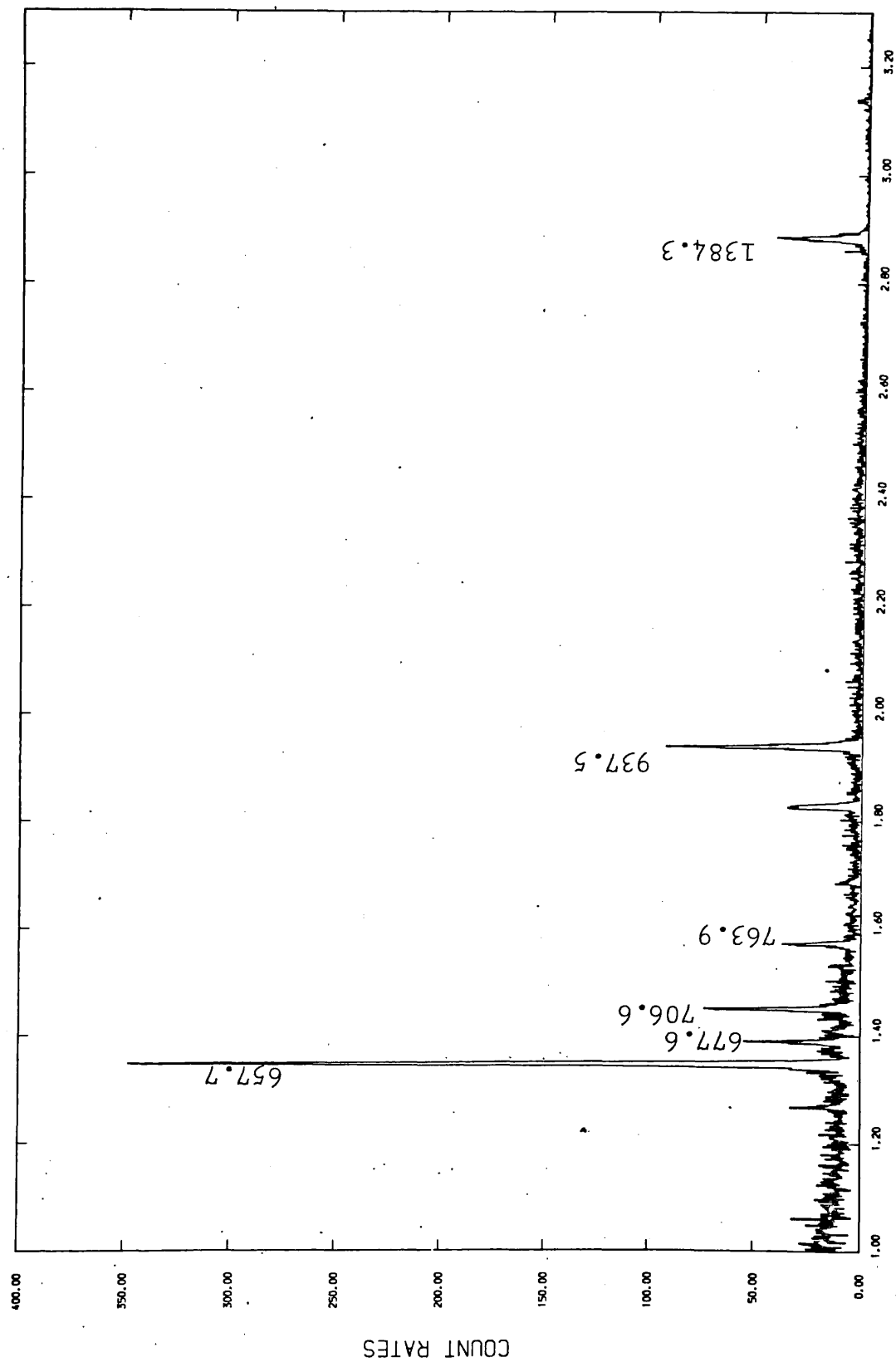

FIG (3.19) CORRECTED SPECTRUM OF AG-110M IN COINCIDENCE WITH 884 KEV

Table (3.2) Summary of γ-γ coincidence, for prominent γ-rays, in the decay of ^{110m}Ag.

Energy (keV)	Intensity†	Gate (keV)			
		658	764	818	884
620.24(2)	2.96(10)	W	VS	-	S
657.70(2)	100 (3)	-	S	VS	VS
677.58(2)	11.25(36)	W	-	-	VS
686.98(2)	6.87(22)	S	VS	VS	-
706.67(2)	17.53(55)	W	-	W	W
744.27(2)	4.95(16)	W	-	VS	-
763.94(2)	23.47(73)	S	-	VS	S
818.06(2)	7.78(24)	VS	S	-	-
884.73(2)	77.77(239)	VS	W	-	-
937.55(2)	36.57(113)	VS	-	-	VS
1384.28(2)	26.90(83)	S	-	-	VS
1475.74(2)	4.39(14)	-	-	-	-
1504.96(2)	14.40(45)	VS	VS	-	-
1562.18(2)	1.31(5)	W	-	-	-

† Intensity normalised to I_γ(658 keV) = 100.

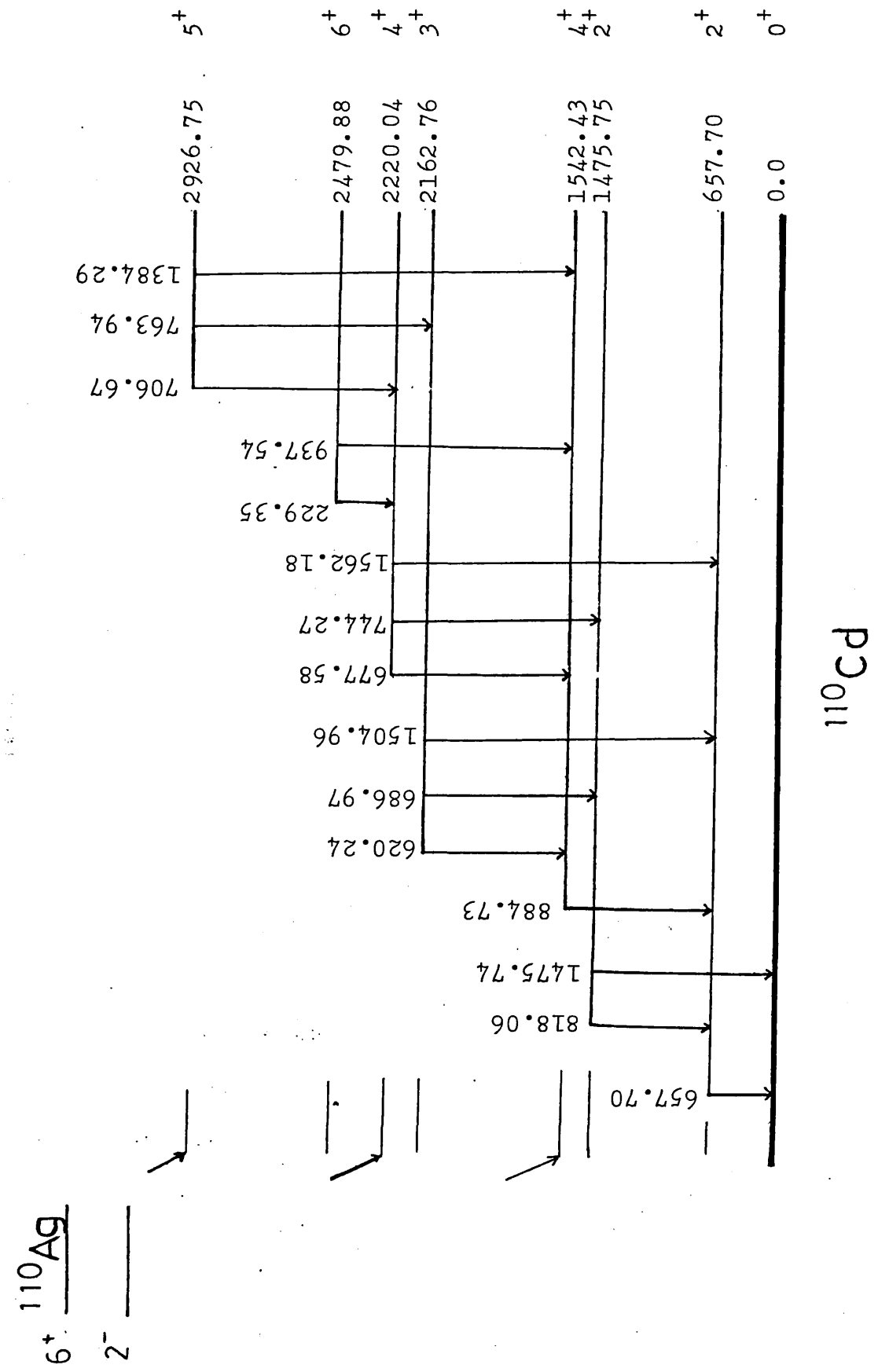

Figure (3.19) The partial decay scheme of ^{110}Cd.

CHAPTER IV

THE ^{160}Dy NUCLEUS.

4.1 Introduction.

The doubly even nuclide ^{160}Dy lies in the region of strongly deformed nuclei[71]. Thus on the basis of the collective nuclear model, it is to be expected that this nucleus would exhibit a ground state rotational spectrum[28]. In addition, quadrupole and octupole vibrational states are likely to occur at higher excitation energies, and associated with these states would find a rotational sequence. This has been particularly true for the low spin states of ^{160}Dy, together with the neighbouring ^{154}Gd and ^{152}Sm nuclei as has been observed by Ofer[72].

On the other hand, for higher spin states Kumar [73] observed a decrease in the level spacing. The Pairing-Plus-Quadrupole model (PPQM)[73] was introduced to describe this phenomena and it could also explain the backbending effect in the GSB.

Apart from the rotational I(I+1) spacing condition of the states, the applicability of a collective rotational model to describe ^{160}Dy could also be studied by observing the branching ratios for transitions connecting different states. These ratios, both for inter- and intra-band transitions, should obey the rule of Alaga[74].

The B(E2) ratios as measured by Gunther et al. [75], for transitions connecting states of gamma-band and GSB, reveal that such a rule was violated. The experimental ratios were not in agreement with the theoretical predictions [74]. To account for these deviations, the First Order Perturbation (FOP) theory of Lipas[76] was incorporated into the theoretical calculations [75]. This was further supported by the work of Marshalek [77] who suggested that the ^{160}Dy nucleus is similar to the deformed ^{166}Er and ^{168}Er nuclei.

The advancement in the field of nuclear detectors

has led to more precise energy and relative intensity measurements being made. The subsequent works of Ludington et al. [78], Keller and Zganjar [79], McAdam and Otteson [80], Dasmahpatra [81] and Hamilton [82] on the B(E2) ratios found that the FOP theory [76] indeed could not explain the deviation, in contradiction to the previous observations[75,77].

Dasmahpatra [81] and Hamilton [82] went a step further by considering the possibility of the inclusion of a Second Order Perturbation (SOP) theory to explain the observed discrepancies. The results of both workers disagree with one another. While Hamilton [82] found that such SOP could possibly explain these deviations, the calculations of Dasmahpatra [81] revealed no such possibility.

Theoretically, it has not been possible to understand the level spacing of the negative parity states in ^{160}Dy. The branching ratios of the E1 transitions depopulating such states do not follow the geometrical model. Although the occurrence of pairs of states with spin/parity 2^-, 3^- and 4^- suggests the presence of two rotational bands [75], the energy spacing between members within both bands do not follow the simple rotational formula [83].

The calculations of energy levels by Kocbach and Vogel [84], using band-mixing theory with $\Delta K=1$, did not give satisfactory results. A similar approach was taken by Krane [85] to calculate the B(E1) ratios. The results show that the method of band-mixing could only explain the low energy E1 transitions but not higher ones.

The introduction of the IBM by Arima and Iachello has prompted many investigations especially for nuclei lying in the region of deformation. The nucleus of ^{160}Dy, with the energy ratio $E_{4_1^+}/E_{2_1^+} = 3.03$, is classified as belonging to the symmetry group SU(3) [46]. The main characteristics of this group are to give a degeneracy to the gamma- and beta-bands as well as to forbid E2 transitions connecting states of gamma-band with states of GSB. Experimentally, gamma- and beta-bands are observed to be non-degenerate and there exist strong E2

transitions between gamma-band and GSB. Warner et al. [86] as a result of his studies on the deformed ^{168}Er nucleus suggested that a small O(6) perturbation to the SU(3) Hamiltonian could possibly account for the observed features exhibited by deformed nuclei.

A very interesting feature about ^{160}Dy is the number of nucleons present. The proton number (Z=66) is exactly mid-way between the shell closure at 50 and 82 resulting in a neutron number (N) of 94. In context of a recently discovered subshell closure at Z=64 [87], the work of Casten et al. [88] on Ba-Gd isotopes conclude that this proton closure effect will vanish for nuclei having neutron number more than 88. The subsequent use of "hybrid parameters", referring to a Z=64 shell for N<88 and Z=82 shell for N>90, in the interacting boson approximation enabled Gill et al. [89] to reproduce the behaviour of energy ratio $E_{4_1^+}/E_{2_1^+}$. However, detailed quantitative agreement was not found for nuclei with N>90 in particular $^{146}_{56}Ba_{90}$, suggesting that the Z=64 subshell effect was still effective. This has led Ibrahim and Stewart [90] to suggest a retarded dissipation of this shell gap to occur in $^{160}_{66}Dy_{94}$ nucleus.

The energy levels of ^{160}Dy can be populated either by β^- decay of ^{160}Tb or EC/β^+ decay of ^{160}Ho. Hence, previous workers have used both modes to establish the level scheme of ^{160}Dy. Other possible reactions like (d,d′) [91] and (p,t) [92] are rarely employed.

In the present work, the decay mode chosen was through β^- decay of ^{160}Tb. The long half-life (70 days) of ^{160}Tb enable large amount of data to be collected. Furthermore the radioactive ^{160}Tb can be easily prepared through (n,γ) reaction using ^{159}Tb metal. The β^- decay was first studied by Burson et al.[93,94] and Cork et al. [95]. Later several techniques such as γ-γ correlation, β-γ coincidence and nuclear orientation were applied to study the decay in greater depth. Typical examples of γ-γ directional correlation and β-γ coincidence works were those of Nathan [71], Ofer [72] Reddy et al.[96] and Jaklevic et al. [97]. The first nuclear orientation work was that of Johnson et al. [98] and Postma et al. [99]. The

technique has been improved recently by Krane [85]. Among these techniques the one that really concerns us is the γ-γ coincidence studies which enable a level scheme of ^{160}Dy nucleus to be constructed. Experimentally, there still existed several discrepancies with regard to the observed energies and their intensities, and also the placement of levels.

The earliest comprehensive work on γ-γ coincidence from ^{160}Tb decay was that of Jaklevic et al. [97]. A 2mm depth Ge(Li) detector and a 7.6 cm X 7.6 cm NaI(Tl) counter were used to detect the γ-rays emitted. A total of four energy gates at 87, 197, 215 and 298 keV were taken to establish the level scheme of ^{160}Dy. Only 20 out of 21 transitions observed could be placed between 9 energy levels.

Ludington et al. [78] in his work using the curved crystal and Ge(Li) spectrometer observed a total of 35 transitions, 8 of which at 237, 242, 246, 349, 432, 1005, 1069 and 1300 keV are new. Another five additional transitions which have been reported in only one or two works but were previously unconfirmed in later works have been measured with energies 176[95,100], 379[95,100], 486[100], 871[101] and 1285[100] keV. The coincidence results were able to establish three new levels of 1155, 1288 and 1535 keV.

Further work by Gunther et al. [75] employing 4mm thick Ge(Li) detector confirm the presence of 6 out of 8 new transitions suggested by Ludington et al. [78]. The two energies which were not seen were 246 and 1005 keV. Instead another five weak transitions at 320, 420, 658, 1299 and 1447 keV were reported. Their intensities were not uniquely defined. From the coincidence measurement, employing 4mm Ge(Li) and 7.6cm X 7.6cm NaI(Tl) counter, no evidence was found for a proposed level at 1288 [78] keV.

The most recent work on the β^- decay of ^{160}Tb was by Mc Adam and Otteson [80]. Two Ge(Li) detectors were used in the energy and intensity measurements. A total of 34 γ-rays were observed, one which at 1285 keV is suggested to be new. This transition was weakly observed by Ludington et al. [78] who suggested that it results from the depopulation of 1286 (3^-)

keV level to the ground state. From the coincidence studies conducted by a 4cm planar Ge(Li) and a 3' X 3' NaI(Tl) counter enable Mc Adam and Otteson [80] to suggest a new level at 1285 keV with spin/parity 1^-. The newly observed transition at 1285 keV is indeed resulting from the depopulation of this level to the ground state.

The controversies pertaining to this ^{160}Dy nucleus do not only apply to energies, relative intensities and level scheme but also to the measurement of the lifetime for the first excited state. Further experimental work was needed to clarify the level properties of ^{160}Dy in order to give reliable information which could result in a more satisfactory theoretical explanation of the nucleus; in particular fuller IBM tests.

4.2 Single spectra.

The radioactive source was prepared by a neutron capture Tb^{159} (n,γ) Tb^{160} reaction at the University of London Reactor Centre (ULRC). The target material is in the form of metal with 99.999% purity. An amount of 3 mg were irradiated in a neutron flux of 10^{12} n/sec/cm^2 for 7 hours to obtain 10 μCi of ^{160}Tb. The source was left for a week to enable the background radiation to decay.

Two detectors were used to measure the single spectra. The 12% efficient coaxial Ge(Li) detector was used to measure the gamma rays covering an energy range of 80 to 1600 keV. The source was placed at 25cm from the detector and the spectrum was collected using a 4096 channels MCA.

The other detector used was an intrinsic Ge. It covers the lower energy region up to a maximum of 350 keV. Hence the combination of these two measurements provide an overlap for energy region between 80 to 350 keV which gives a good cross-check to be made of the measured gamma ray energies and relative intensities.

Figure (4.1) shows the gamma ray singles spectrum following the beta decay of ^{160}Tb .

Table (4.1). Energies (keV) and relative intensities I_γ in the decay of ^{160}Tb.

Energy	Intensities normalised I_γ(879keV)=30.0			
(keV)	Present	Ref: [78]	Ref: [79]	Ref: [80]
86.76(06)	13.6 (3)	13.7 (20)	14.0 (6)	13.0 (7)
93.95(03)	0.045 (13)	0.067(10)		0.054(4)
112.24(17)	0.004 (1)			
148.64(19)	0.006 (1)			
176.24(19)	0.005 (1)	0.005(1)		
197.05(03)	5.37 (30)	5.22 (29)	5.16 (9)	5.22 (25)
215.64(02)	3.99 (18)	3.93 (22)	3.91 (9)	4.00 (20)
230.62(04)	0.089 (4)	0.071(7)	0.062(9)	0.082(6)
237.71(06)	0.010 (1)	0.007(3)		0.012(8)
242.42(02)	0.026 (6)	0.004(3)		0.021(8)
246.37(14)	0.019 (4)	0.018(4)		0.026(3)
298.53(01)	27.55 (125)	27.1 (16)	27.0 (7)	27.3 (14)
309.52(02)	0.957 (38)	0.90 (4)	0.82 (3)	0.918(47)
320.54(19)	0.009 (4)	<0.02		
337.35(04)	0.387 (14)	0.33 (3)	0.34 (3)	0.355(21)
349.94(18)	0.019 (2)	0.014(3)		0.018(6)
379.30(03)	0.020 (3)	0.014(4)		0.017(6)
392.46(04)	1.46 (6)	1.36 (5)	1.36 (6)	1.40 (7)
432.55(04)	0.023 (9)	0.013(4)		0.024(5)
454.96(36)	0.007 (4)			
485.99(21)	0.102 (22)	0.080(7)	0.096(15)	0.088(5)
518.84(22)	0.003 (1)			
574.32(07)	0.028 (5)			
621.75(45)	0.018 (9)			
682.38(06)	0.621 (23)	0.545(50)	0.537(30)	0.617(31)
704.35(29)	0.012 (6)			
707.44(30)	0.018 (7)			
728.09(05)	0.025 (3)			
765.28(06)	2.10 (7)	2.03 (18)	1.93 (5)	2.16 (11)
872.01(03)	0.207 (46)	0.174(35)	0.285(39)	0.207(14)
879.36(03)	30.0	30.0	30.0 (5)	30.0 (15)
962.46(05)	10.03 (43)	10.2 (7)	10.6 (5)	9.42 (49)
966.15(04)	25.94 (92)	24.7 (15)	25.5 (5)	24.8 (12)
1002.95(04)	0.94 (92)	0.98 (5)	1.01 (7)	1.02 (5)
1069.00(04)	0.102 (5)	0.076(8)	0.113(9)	0.104(10)
1102.63(05	0.529 (21)	0.50 (3)	0.561(30)	0.557(28)
1115.13(05)	1.52 (6)	1.50 (9)	1.52 (5)	1.48 (8)
1143.35(27)	0.008 (2)			
1177.91(06)	15.3 (6)	14.8 (5)	15.7 (4)	15.0 (8)
1199.81(05)	2.23 (11)	2.24 (9)	2.48 (7)	2.37 (12)
1251.17(06)	0.095 (5)	0.094(8)	0.096(9)	0.10 (8)
1271.82(05)	7.72 (23)	7.4 (2)	7.81 (30)	7.48 (38)
1285.58(07)	0.013 (2)	0.011(3)		0.015(2)
1299.13(23)	0.0043(15)	0.005(3)		0.006(4)

— continued —

Energy	Intensities normalised I_γ(879keV)=30.0			
(keV)	Present	Ref: [78]	Ref: [79]	Ref: [80]
1311.93(05)	2.85 (14)	2.79 (17)	3.00 (12)	2.87 (15)
1338.13(17)	0.005 (2)			
1349.30(19)	0.005 (2)			
1420.42(19)	0.006 (1)			
1448.36(19)	0.005 (1)			
1507.58(19)	0.003 (1)			

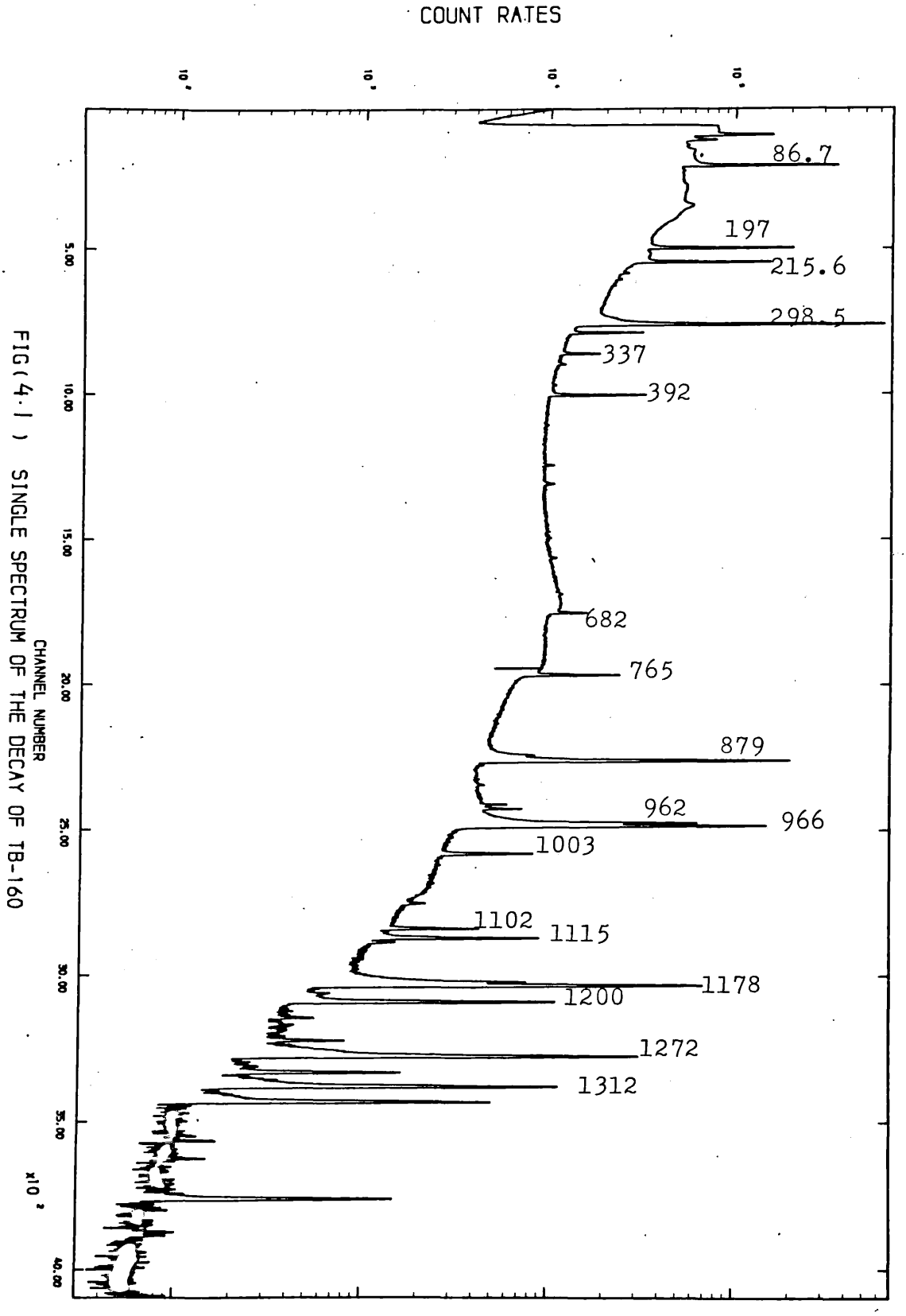

FIG(4.1) SINGLE SPECTRUM OF THE DECAY OF TB-160

The energies of all the gamma ray observed were listed in Table (4.1). The relative intensities were shown in comparison with previous workers Ludington et al. [78]. Mc Adams [80] and Keller [79]. The energies and relative intensities for gamma rays less than 350 keV were taken from the mean of Ge(Li) and Ge(I) detectors measurements.

A total of fifty gamma rays were observed; ten of which were seen for the first time from ^{160}Tb decay. Another four transitions (628, 704, 707, 728 keV) were also observed for the first time in this decay but have been seen previously [102] from EC/β^+ decay of ^{160}Ho.

4.3 Coincidence measurement.

Two coaxial Ge(Li) detectors were used to collect the γ-γ coincidence data. They were arranged at 90^0 geometry in order to minimise the backscattering effect. The 12% efficient detector was used for the total spectrum while the 10% detector was used for the gating. The data were acquired for three weeks on three magnetic tapes through the WRITE mode of the DPDCS.

A total of six gates at; 87, 197, 215, 309, 879 and (962 + 966) keV were taken. Apart from their high intensities, these energy gates were chosen because of their special reasons.

The first excited state in the ^{160}Dy nucleus is at 87 keV. Thus we expect most of the transitions from higher states will either populate directly or in cascade with this level. Hence, the 87 keV gate is very important in constructing the level scheme of this nucleus.

The 197 keV gate was taken to confirm the presence of a level at 1288 keV observed by Ludington [78]. This suggestion, based on a strong coincidence of 246 keV transition with 197 keV gate, was never observed in the subsequent works of Keller [79] Mc Adams [80].

The need for the 215 keV gate was to search for the possibility of higher energy levels since it depopulates the

1264 keV. The gate at 309 keV was chosen in order to establish and confirm a level at 1507 keV. The energy which depopulates this level and is in cascade with the 309 keV transition is the energy transition at 148 keV. Hence we expect a strong coincidence to exist between the 148 keV transition and the 309 keV gate.

A wider gate at (962 + 966) keV was taken since these two intense peaks lying close to one another could not be separated. In order to identify the peaks which are in coincidence with either 962 or 966 keV energy gate, another energy gate at 879 keV was taken. The energy transitions at 879 and 966 keV depopulates the common level at 966 keV. Thus, the populating energy transitions to this common level are expected to be in coincidence with both the gates; 879 and (962 + 966) keV. By comparing the two coincidence results and through the process of elimination the energies which are in coincidence with either 962 or 966 keV gate can be deduced.

The coincidence spectrum for the six gates are shown in Figures: 4.2, 4.3, 4.4, 4.5, 4.6, 4.7.

The summary of the coincidence results are shown Table: 4.2. The energy gates are listed at the top while the entries VS(Very Strong), S(Strong) and W(Weak) refer to the strength of the coincidence. These results were used to build the decay scheme of ^{160}Dy. Most of the energy transitions observed in the decay of ^{160}Tb are in coincidence with the gates listed. The transitions which are not in coincidence with any of the gates are either transitions which directly go to the ground state or transitions which are too weak to be seen in the coincidence spectra.

4.4 Lifetime of the 87 keV level.

The lifetime of the first excited state (87 keV level) in ^{160}Dy has been measured by several workers with varying degree of accuracy. The work of Fossan and Herskind [103] using plastic-plastic counters combination obtain a value of 1.92±0.05 nsec. A slightly higher value was obtained by Abou-Leila et al.[104] who used a 2.54cm X 2.54cm plastic counter

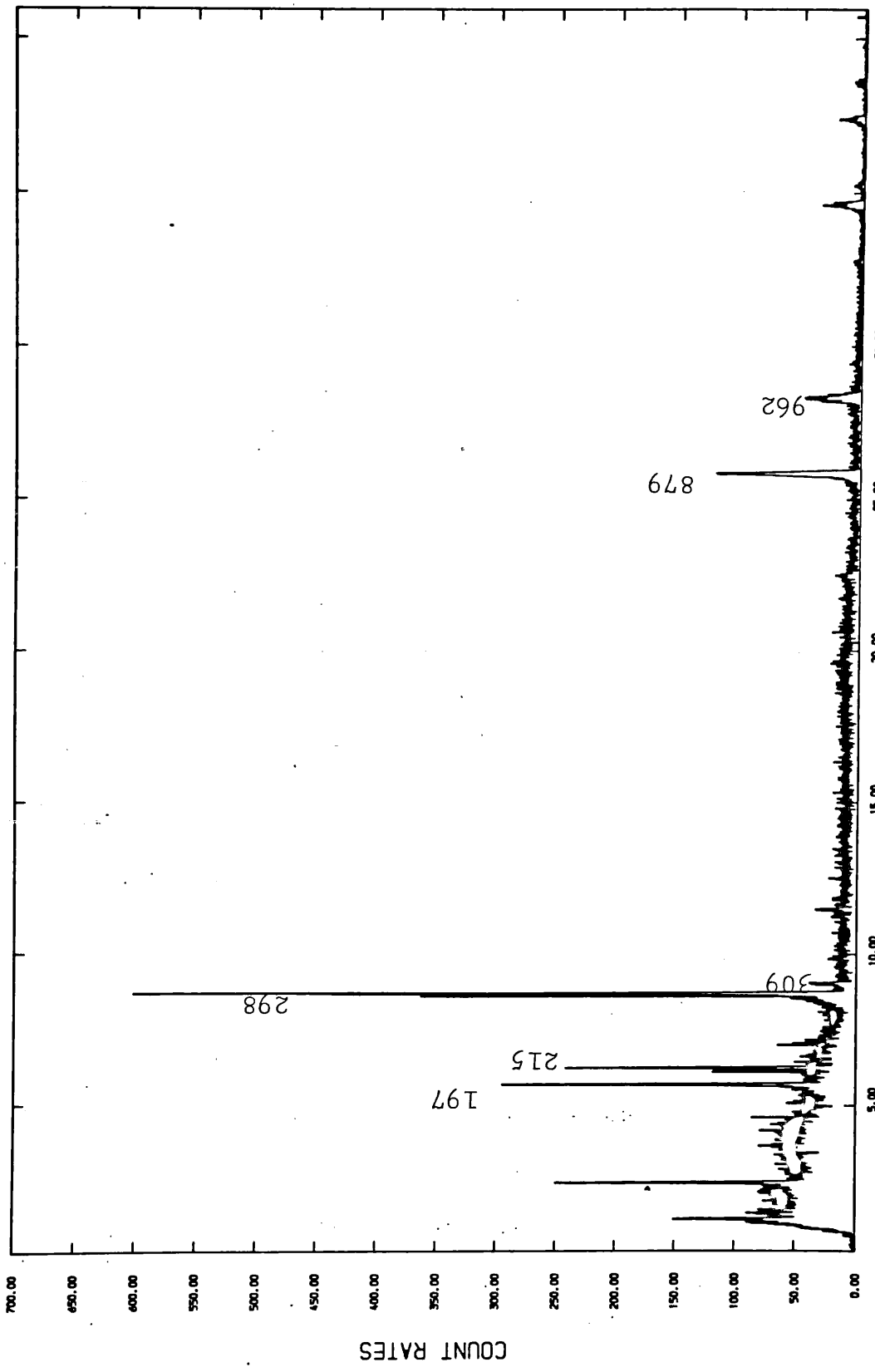

FIG (4-2) 86 KEV IN COINCIDENCE WITH TB-160

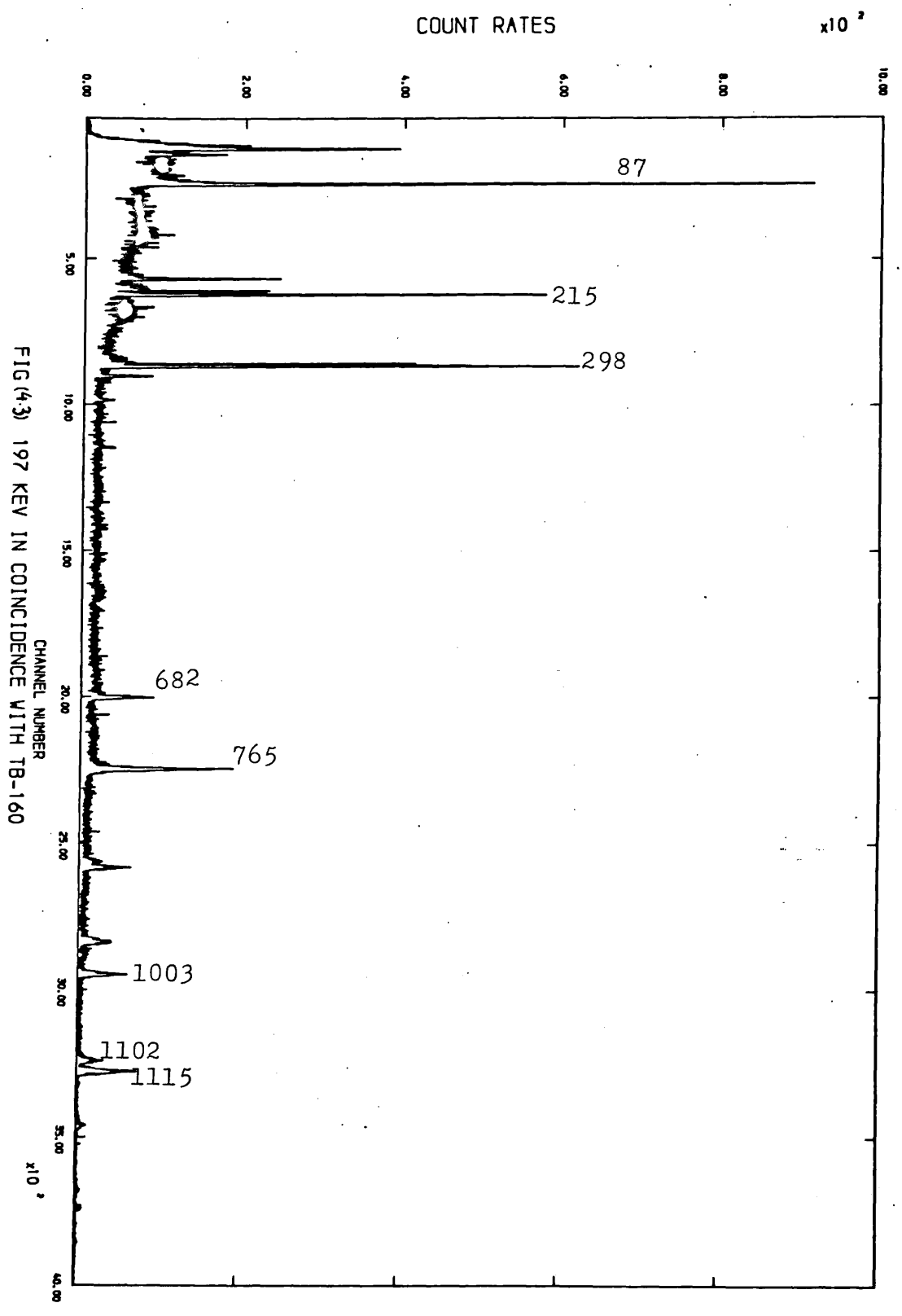

FIG(4.3) 197 KEV IN COINCIDENCE WITH TB-160

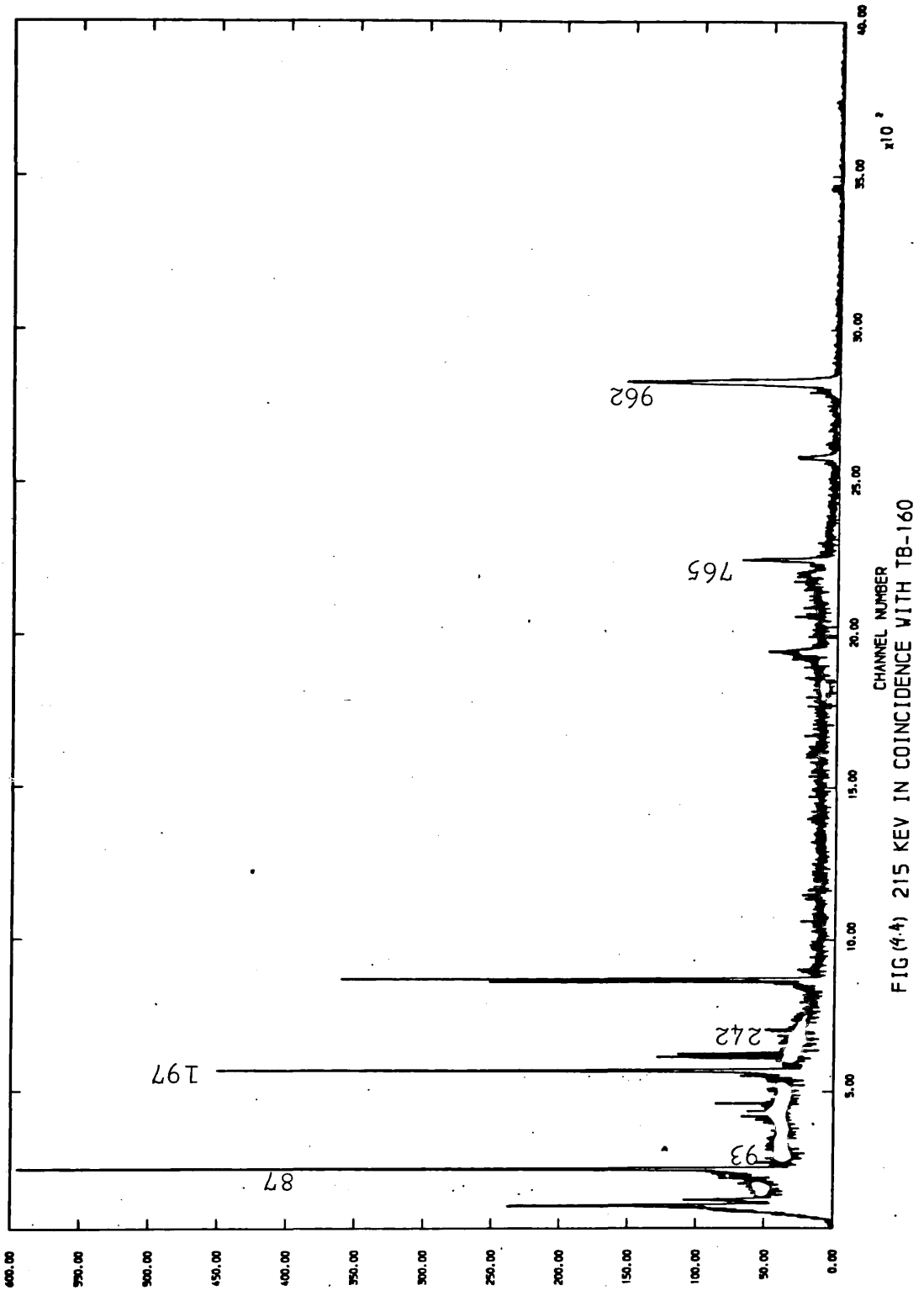

FIG (4.4) 215 KEV IN COINCIDENCE WITH TB-160

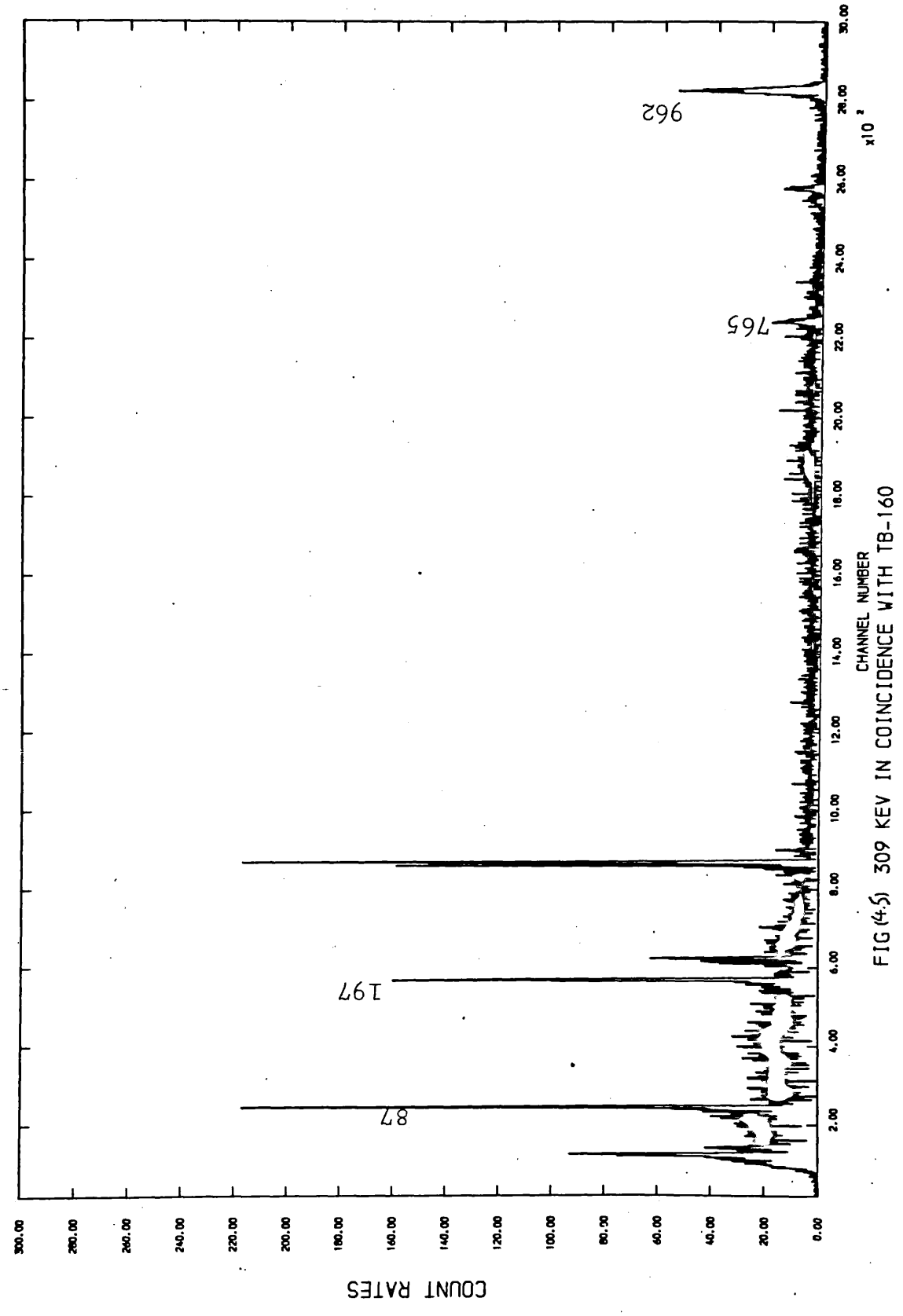

FIG (4.5) 309 KEV IN COINCIDENCE WITH TB-160

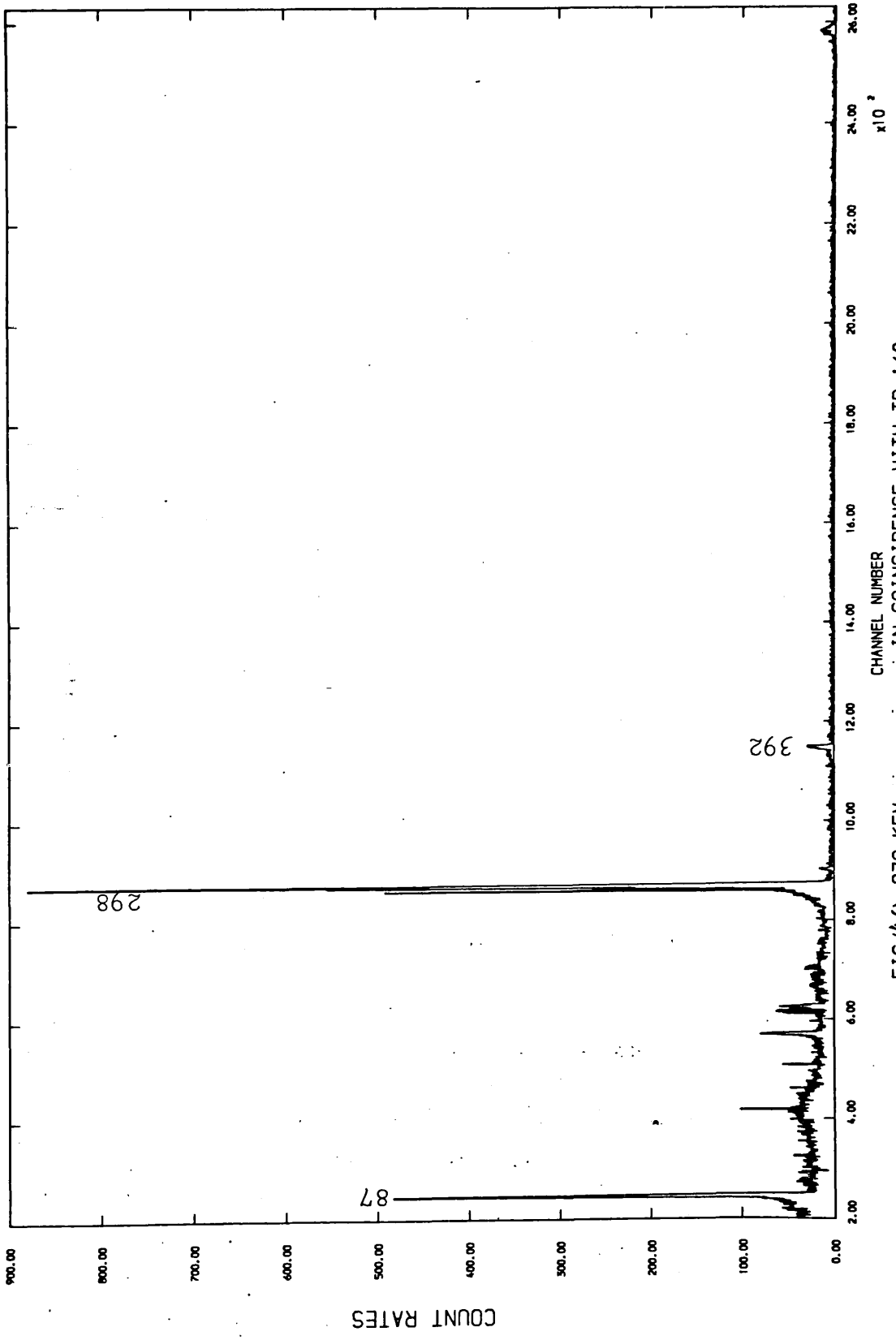

FIG (4.6) 879 KEV IN COINCIDENCE WITH TB-160

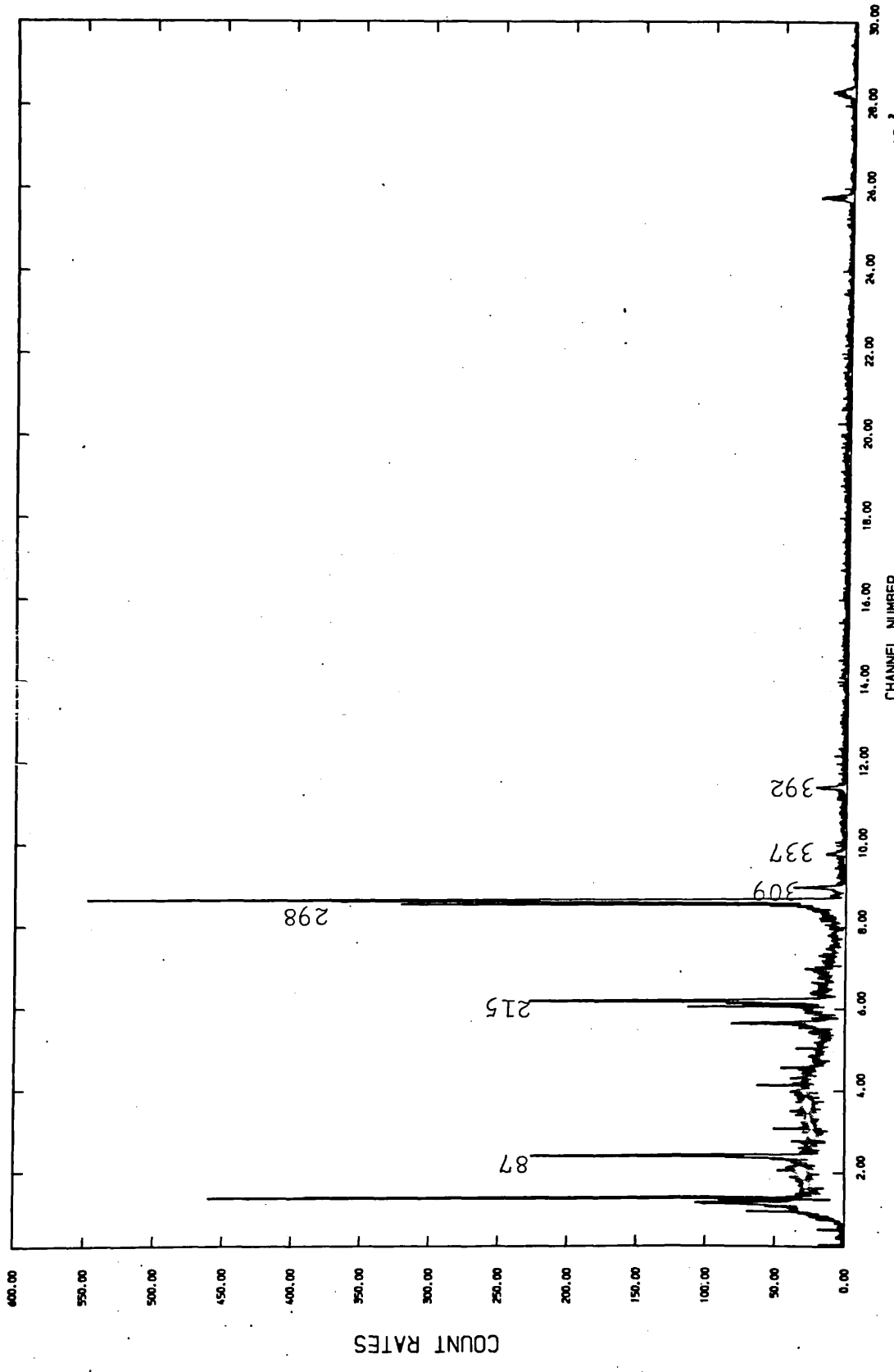

FIG (4.7) 962 KEV AND 966 KEV IN COINCIDENCE WITH TB-160

Table (4.2). Summary of γ-γ coincidence in ^{160}Dy.

Transition	Gate (keV)					
(keV)	86	197	215	309	879	962+966
86		VS	VS	W	S	W
93	W		S			
112		W				
148				S		
176			W			
197	VS		VS	W		W
215	S	VS				S
230	W	W				
237		W				
242		W				
246		S				
298	VS	S			VS	VS
309	W	W				S
320					W	W
337	W					W
349						W
379		W				W
392	W	W			VS	S
432					W	
485		W				
518	W					
621						W
682	S	VS				
704					W	
728					W	
765	W	S				
872	W	S				
879	S					
962	S		S	S		
1002	W	VS				
1069	S					
1102	W	S				
1143	W					
1115		S				
1177	S					
1199	S					
1251		W				
1271	W					
1299	W					
1311	S					
1420	W					
1448	W					

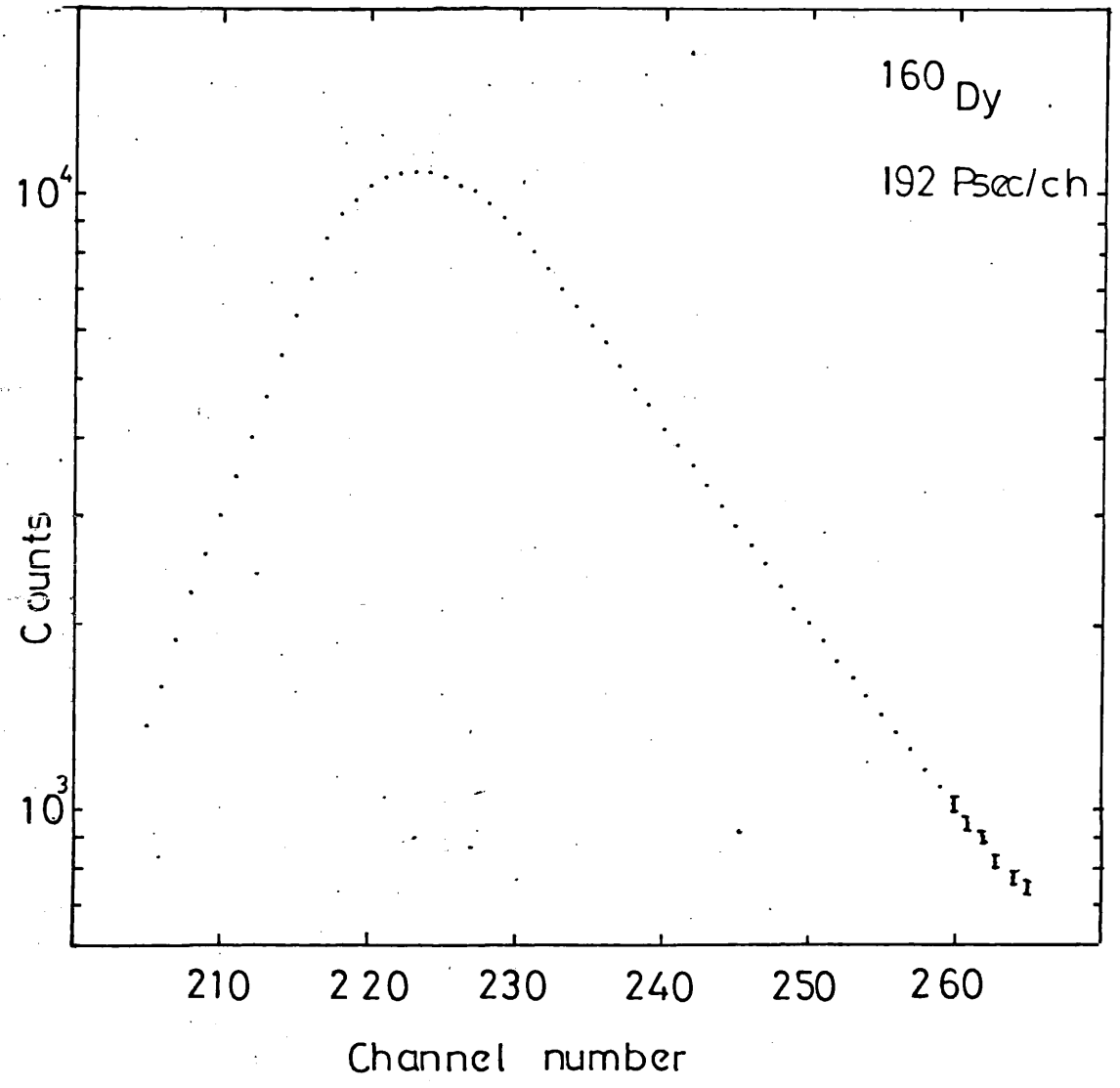

Figure (4.8) . Lifetime spectrum of the 87 keV level.

with magnetic double lens spectrometer. The value obtained was 1.97±0.04 nsec. The most recent measurement by Ismail et al.[105] obtained a value of 2.19±0.08 nsec.

In the present work, the lifetime of the 87 keV level was measured by a method of delayed coincidence. A plastic scintillation counter and a 10% efficient Ge(Li) detector were used. The detectors were arranged at 180° geometry and a complete set up of the spectrometer is shown in Fig:(3.4) together with the dual parameter data collection system. The function of the electronics has been previously discussed in section (3.4). The fast timing spectrum was gated by the 87 keV γ-ray which depopulates the 87 keV level to the ground state.

Fig:(4.8) shows the lifetime spectrum of the first excited state in ^{160}Dy. A slope method was used to calculate the lifetime and the value obtained is 1.98±0.04 nsec.

The value obtained is consistent with that of Ref:[103] and Ref:[104]. The value quoted in Ref:[105] is higher than that obtained in the present work.

4.5 Decay scheme and Level properties.

The decay scheme of the ^{160}Dy nucleus established from the results of coincidence and energy sum relations (Table: 4.3) is shown in Fig. 4.9. The level energy (keV), branching ratios, log ft values, spins and parities are given on the left of the figure. The number at the base of the arrow indicates the energy of the transition in keV. The transitions marked by dagger (†) indicate two placements and the one marked by asterisk (*) refer to transition suggested as a result of coincidence measurements.

Table: 4.4 shows the Branching Ratios (B.R's), the log ft values for the β^- decay of ^{160}Tb and the deduced spins and parities. The B.R's were computed from the total intensity balance between the decay and feeding γ-rays for each level. The log ft values were calculated according to the relations

Table (4.3). Sum energy relations in ^{160}Dy.

Energy of transition(keV)	Energy sum(keV)	Energy level(keV)
86.76	86.76	86.76
86.76+ 197.06	283.82	283.82
86.76+ 197.06+ 682.38	966.20	
86.76+ 879.37	966.13	966.16
966.15	966.15	
86.76+ 197.06+ 765.28	1049.10	
86.76+ 962.46	1049.22	1049.16
86.76+ 197.06+ 872.01	1155.83	
86.76+1069.01	1155.77	1155.80
86.76+1143.35	1230.11	1230.11
86.76+ 197.06+ 765.28+215.65	1264.75	
86.76+ 197.06+ 682.38+298.53	1264.73	1264.72
86.76+1177.92	1264.68	
1285.58	1285.58	1285.58
86.76+ 197.06+ 765.28+237.71	1286.81	
86.76+ 197.06+ 682.38+320.54	1286.74	
86.76+ 197.06+1002.95	1286.77	1286.72
86.76+1199.81	1286.57	
86.76+ 197.06+(1005)	1288.82	1288.82
1338.13	1338.13	1338.13
1349.30	1349.30	1349.30
86.76+ 197.06+ 765.28+ 93.95	1358.70	
86.76+ 197.06+ 765.28+309.52	1358.62	1358.64
86.76+ 197.06+ 682.38+392.46	1358.66	
86.76+1271.83	1358.59	
86.76+ 197.06+ 872.01+230.62	1386.45	
86.76+ 197.06+ 765.28+337.35	1386.45	
86.76+ 197.06+1102.63	1386.45	1386.31
86.76+1299.13	1385.89	

—— continued ——

Energy of transition(keV)	Energy sum(keV)	Energy level(keV)
112.34+1285.58	1397.92	
86.76+ 197.06+ 872.01+242.42	1398.25	
86.76+ 197.06+ 765.28+349.94	1399.04	1398.60
86.76+ 197.06+ 682.38+432.55	1398.75	
86.76+ 197.06+1115.13	1398.95	
86.76+1311.93	1398.69	
86.76+ 197.06+ 765.28+215.65 + 93.95+ 148.64	1507.34	
86.76+1420.42	1507.18	1507.37
1507.58	1507.58	
86.76+ 197.06+ 765.28+215.65 + 93.95+ 176.24	1534.94	
86.76+ 197.06+(1005) +246.37	1535.19	
86.76+ 197.06+ 872.01+379.30	1535.13	1535.08
86.76+ 197.06+ 765.28+485.99	1535.09	
86.76+ 197.06+1251.17	1534.99	
86.76+1448.36	1535.12	
86.76+ 197.06+ 765.28+621.75	1670.85	
86.76+ 197.06+ 682.38+704.35	1670.55	1670.70
86.76+ 197.06+ 682.38+728.09	1694.29	1694.29
86.76+1143.35+ 574.32	1804.43	
1349.30+ 454.96	1804.26	1804.37
1285.58+ 518.84	1804.42	

Table (4.4). Summary of the level properties in ^{160}Dy.

Energy level (keV)	E_β (keV)	I_γ (pop)	I_γ (depop)	B.R.%	logft	Deduced J
87	1752	74.24	74.58	0.34	12.1	2
283	1555	6.016	6.545	0.51	11.8	4
966	872	29.558	56.561	26.8	9.0	2
1049	789	5.624	12.13	6.45	9.42	3
1155	682	0.135	0.309	0.17	10.76	4
1230	608	0.028	0.008	-	-	0,2
1264	574	0.176	47.475	46.99	8.18	2
1285	553	0.0045	0.0259	0.021	11.40	1
1286	552	0.0043	3.178	3.15	9.23	3
1288	549	0.019	-	-	-	5
1338	498	-	0.0048	0.0047	11.82	1,2
1349	489	0.0074	0.005	-	-	0,2
1358	479	0.011	10.34	10.25	8.44	2
1386	452	-	1.01	0.99	9.4	4
1398	439	-	4.35	4.3	8.7	3
1507	331	-	0.0142	0.14	10.71	2
1535	303	-	0.26	0.25	9.41	4
1670	168	-	0.030	0.029	9.46	2,3,4
1694	145	-	0.026	0.025	9.25	2,3,4
1804	34	-	0.037	0.036	6.71	2,3,4

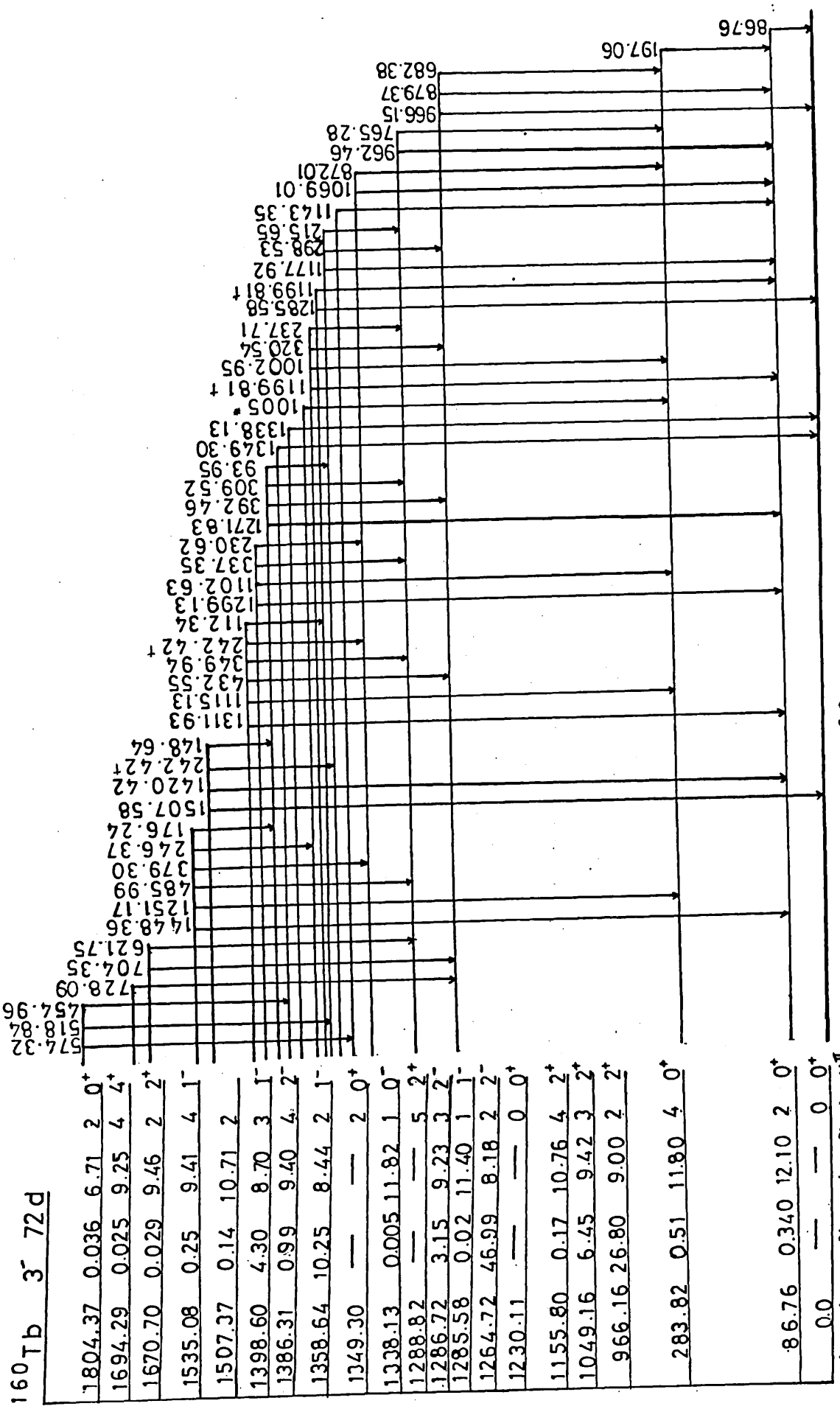

Figure (4.9) Decay scheme of ^{160}Dy.

given by Moskowski[106,107], the end point energies of the β^- decay were calculated using the given Q_{β^-} value of 1.838 MeV[108] for ^{160}Tb. The spins/parities were deduced according to the β^- decay selection rules. The results for B.R!s and log ft values obtained in the present work were comparable to that compiled by Tuli[102].

The spin/parity of the ground state of the ^{160}Tb is 3^- and therefore the β^- decay will primarily populate levels with spins/parities of $2^\pm, 3^\pm$ or $4^\pm$. Thus levels with spins/parities 0^+ or 5^+ can only exist through γ-ray population since β^- decay to these levels will violate the β^- decay selection rules.

The total intensity of the γ-ray feeding the 1230 keV level is greater than the depopulating intensity. According to the intensity balance this level will thus have no branching ratio and therefore there is no direct β^- feeding. This observation exclude the spins 2,3 or 4 assignment to this level. The spin/parity 0^+ assignment is more appropriate and hence consistent with β^- decay selection rules. The zero B.R. obtained for the 1288 keV level confirms the spin/parity of 5^+ while a small B.R. of 0.005 (log ft = 11.82) deduced for a new level at 1338 keV is consistent with spin/parity assignment of 1^-. The log ft value of 10.71 obtained for another new level at 1507 keV suggests a spin/parity of 2^+.

Table (4.5) shows the comparison of experimental and theoretical k-shell conversion coefficients (α_k) for the γ-ray transitions from the β^- decay of ^{160}Tb. The experimental α_k values were computed using equation (1.16). The β^- electron intensities were taken from the work of Ewan et al.[109] while the relative intensities of the γ-transitions were taken from singles measurements reported in Table:(4.1). The multipolarity for each of the transitions was deduced by comparing the experimental α_k value obtained with the theoretical α_k value of Hager and Seltzer[110]. The multipolarities adopted for the transitions are given in the last column of the Table (4.5). The results clearly indicate that with the exception of the 93 keV transition all the transitions observed are of pure E2

Table (4.5). The comparison of experimental and theoretical α_k-conversion coefficients.

Energy (keV)	I_i	I_f	$\alpha_k X10^{-3}$ Exp	Theoretical E1	Theoretical E2	Theoretical M1	Adopted multipolarity
86	2	0	1691(151)	370	1600	3000	E2
93	2	2	1777(678)	315	1250	2450	M1/E2
196	4	2	154(12)	46	165	298	E2
215	2	3	34(3)	35	130	235	E1
298	2	2	13.5 (8)	15	49	100	E1
309	2	3	12.0 (7)	13.8	45	91	E1
337	4	3	9.3 (8)	10.8	35.5	72	E1
486	4	3	4.4 (23)	4.7	13.8	29.5	E1
392	2	2	7.8 (6)	7.8	23.7	47.5	E1
682	2	4	5.6 (4)	2.3	5.9	12.0	E2
765	3	4	4.81(25)	1.8	4.5	9.2	E2
879	2	2	3.36(12)	1.42	3.35	6.3	E2
962	3	2	2.77(12)	1.18	2.80	4.98	E2
966	2	0	2.73(11)	1.16	2.75	4.95	E2
1002	3	4	1.15(8)	1.08	2.56	4.50	E2
1115	3	4	0.99(5)	0.85	1.95	3.28	E1
1177	2	2	0.80(5)	0.81	1.88	3.15	E1
1199	3	2	0.83(6)	0.79	1.80	2.90	E1
1271	2	2	0.71(4)	0.72	1.60	2.62	E1
1311	3	2	0.78(5)	0.67	1.52	2.45	E1
112	3	3	< 79.3	190	943		E2
320	3	2	<114.9	12.5	35	70	E1
1285	1	0	< 49.5	0.65	1.6	2.5	E1

and E1 characters. These observations are in fact consistent with the results of a nuclear orientation works on β^- decay of ^{160}Tb by Krane[85] and Krane and Steffen[111]. The multipole mixing ratios (δ) for E2/M1 and E1/M2 transitions were found to be small. The only appreciable admixtures of M2 were found for the two transitions at 1177 and 1271 keV.

In the case of the 93 keV transition, the present result shows that there exists an E2/M1 admixture. This observation contradicts the results of Refs:[79,97,112]. Their calculations suggested an M1 character for the 93 keV transition. On the other hand the result of Ref:[78] establish the multipolarity of E2 for this transition.

It is important to note that the multipolarities of the three transitions at 112,320 and 1285 keV were deduced from the spins/parities of the levels which connect them and not from the results of experimental α_k values. The main reason for this is that the conversion electron intensities for these three transitions were not uniquely defined. Only the upper limits were given and therefore the possible multipolarities can take any characters. The 112 keV transition is suggested (see later) to decay from the level at 1398 (3^-) to that at 1285 (1^-) keV. The difference in the spins allows an angular momentum of either 2,3 or 4 to be carried off by the 112 keV γ-ray. Furthermore there is no change in the parity between the two levels. This suggests that the most probable multipolarity for the 112 keV would be E2. The experimental α_k value obtained for this transition was < 0.079 compared to the theoretical α_k of 0.943 for an E2 transition. For the case of 320 keV transition, the initial and final levels connecting transition are 1286 (3^-) and 966(2^+) keV respectively. Again from the spin's difference the possible value of the angular momentum could either be 1,2,3,4 or 5. The change in parity between the initial and final levels allows an assignment of either E1 or M2 multipolarity for the 320 keV transition. The α_k(experimental) value of < 0.1149 confirms the multipolarity E1. The theoretical α_k value for an E1 transition is 0.0125 well below than the value 0.1149. The transition at 1285 keV connects the 1285 (1^-) kev level with the ground state 0^+. Thus the only possible angular momentum that could be carried off

by the 1285 keV γ-ray is 1. There is also a change in parity between the initial and final levels and therefore the most probable multipolarity for the transition 1285 keV is E1. The experimental α_k value is < 0.0495 while the theoretical α_k value is 0.00065.

The results concerning the well established levels are consistent with the latest work on ^{160}Tb decay [80]. The levels include 87 (2^+), 283 (4^+), 966 (2^+), 1049 (3^+), 1155 (4^+), 1264 (2^+), 1286 (3^-), 1358 (2^-), 1386 (4^-), 1398 (3^-) and 1535 (4^-) keV. The establishment of these levels were confirmed from the coincidence results. Their respective spins/parities were deduced from the adopted multipolarities of the depopulating transitions. For example a strong coincidence of the 197 keV transition with the 87 keV gate confirms a level at 283 keV. The E2 character deduced for the 197 keV transition suggests a 4^+ spin/parity for the 283 keV level which is further confirmed by a log ft value of 11.80.

In the remainder of this section the present results pertaining to new transitions and levels will be discussed together with points regarding the discrepancies with previous workers, in particular the observation of transitions.

The results of the singles measurements confirm the presence of two of the five transition energies reported earlier [75]. The energies are 320 and 1447 keV. Their relative intensities are now uniquely defined at 0.009 and 0.005 respectively. These intensities are normalised to 30.0 for the 879 keV transition. The measurement by Gunther et al. [75] could not define the intensities of these two transitions. Instead, the upper limits were suggested at 0.02 for both the transitions. These two transitions were not seen by any other workers who worked after Gunther et al.

The energy transition at 1285 keV, which was reported for the first time by McAdam and Otteson [80], was also seen in the singles measurements.

A total of four energies at 621, 704, 707 and 728 keV

were seen to exist for the first time in the β^- decay of ^{160}Tb. These energies were initially observed in the EC/β^+ decay of ^{160}Ho.

In the EC/β^+ decay of ^{160}Ho the transition at 1199 keV which also exists in ^{160}Tb decay is considered to be a doublet.[113]. One component deexcites from the level at 1286 keV while another component arises from the deexcitation of the 1285 keV level. The intensity ratio of the transition 1199 to 1285 keV was deduced to be 0.78. Assuming that this intensity ratio is also true in the case of β^- decay of ^{160}Tb. From the relative intensity of 0.013 for the 1285 keV γ-ray then the intensity of the 1199 keV transition resulting from the deexcitation of the 1285 keV level sould be 0.011 %. Thus most of the 1199 keV peak observed in the β^- decay of ^{160}Tb arise from the deexcitation of the 1286 keV level.

The transition at 1005 keV as suggested by Ludington et al. [78] has not been seen in the present single measurement. The reason for this is that there exists an intense peak at 1003 keV which would mask the presence of a weaker peak like the 1005 keV.

The present coincidence work were able to confirm the suggested levels at 1285 [80] and 1288 keV [78]. The former level was confirmed by the presence of a γ-ray transition at 1285 keV, which connects this level with the ground state level. The log ft value of 11.40 obtained for this level is consistent with a spin/parity assignment of 1^-. A strong coincidence of the 246 keV transition with the 197 keV gate supports and confirms the level at 1288 keV. Furthermore it supports the presence of an energy transition at 1005 keV which connects this 1288 keV level with the level at 283 keV. As was mentioned above, this weak 1005 keV transition was not seen in singles. The upper limit for the relative intensity of this transition could be deduced by assuming a zero B.R. to the 1288 keV level. This assumption is important in order to be consistent with the 5^+ spin/parity assignment to this level. The only observed transition which populates this level is the transition at 246 keV with a relative intensity 0.019. Apart from the 1005

keV there are no other γ-rays seen to depopulate this level. Hence for the required populating total intensity to be greater or equal to the depopulating intensity of the 1288 keV level, the maximum intensity that the transition 1005 keV can have is 0.019. This value of relative intensity is considered to be weak compared to 0.94 of the 1003 keV transition.

There are three energy levels, which were observed in the EC/β^+ decay of ^{160}Ho (Ref: [114]), considered to be populated for the first time in the β^- decay of ^{160}Tb. These levels are 1670, 1694 and 1824 keV

The 1670 keV level is established from the coincidence of 704 keV transition with two gates; 879 and (962 + 966) keV. These two coincidences suggested that the 704 keV transition is in direct cascade with transitions 879 and 966 keV. The coincidence of the 621 keV transition with gate (962 + 966) keV but not with 879 keV gate clearly shows that 621 keV transition is in direct cascade with 962 keV transition. Since 962 keV transition depopulates the 1049 keV level therefore summing up 621 and 1049 keV results in 1670 keV. This confirms the presence of 1670 keV level. From the fact that this level populates the 2^+ (966 keV) and 3^+ (1049 keV) levels, the possible spin would be 2, 3 or 4. The log ft value of 9.46 obtained for this level suggests a spin/parity of 2^+. This assignment confirms the suggestion by Tuli [102].

The level at 1694 keV is established from the coincidence of the 728 keV line with two gates, one at 879 keV and the other at (962 + 966) keV. The log ft value of 9.25 obtained for this level suggested the possibility of spin/parity 4^+.

The level at 1804 keV is suggested from the energy sum relation of a new transition at 518 keV with the level at 1285 keV. Since the level at 1285 keV has a spin/parity of 1^-, thus the most probable spin parity assignment to the 1804 keV level would be 2^+. Two other transitions which were seen to depopulate this level are 454 and 574 keV. The former populates the 2^+ level at 1349 keV while the latter transition populates the 0^+ level at 1230 keV. These two observations

further support the 2^+ spin/parity assignment to the 1804 keV level.

Another level which is observed to be populated for the first time in ^{160}Tb decay is the 1349 keV level. This level was weakly observed in the Coulomb excitation work of McGowan and Milner [115] who assigned a spin parity of 2^+. From the singles measurement a weak energy transition at 1349 keV was observed. Thus it is suggested that this transition is the result of the depopulation of the 1349 keV level to the ground state. The presence of this level is further supported by the observation of another new transition at 454 keV which could be energetically placed between this 1349 keV level and the level at 1804 keV. The zero B.R. obtained for this level suggest the possibility of spin/parity of either 0^+ or 5^+. The observed direct decay to the ground state exclude these two possibilities since there is no γ-transition from 0^+ state to another 0^+ state and the transition from 5^+ state to a 0^+ state is highly forbidden. The latter transition results in a change of 5 angular momentum which is not very likely to occur. Hence the most possible spin/parity assignments are either 1^- or 2^+. The assignment of 2^+ is consistent with the work of McGowan and Milner [115].

The transition at 320 keV was observed to be in coincidence with the 879 and (962 + 966) keV gates. From an energy sum relation, this transition is suggested to connect the levels at 1286 and 966 keV. The transition observed at 1448 keV is too weak to be seen in the coincidence spectrum of 87 keV gate. The results of energy sum relations, suggest that this energy transition could be placed between the levels at 1535 and 87 keV. The placements of these transitions, 320 and 1448 keV, are consistent with the suggestion of Gunther et al. [75]. Another new transition at 112 keV is suggested to depopulate the level at 1398 keV to the level at 1285 keV. This is based on the energy sum relation and a weak coincidence of the 112 keV transition with the 197 keV gate.

The present work has resulted in three new levels being suggested. The levels are 1230, 1338 and 1507 keV.

The level at 1230 is suggested as a consequence of observing two new γ-ray transitions with energies 1143 and 574 keV. The weak coincidence of the 1143 keV transition with the 87 keV gate supports the suggestion of this new level. The transition 574 keV is suggested to be the result from the decay of 1804 keV level to this new level. The zero B.R. suggests that a 0^+ spin/parity assignment is most reasonable since this will conform with β^- decay selection rule. This is further supported by the non-observation of a direct γ-ray to the ground state, which is highly forbidden.

The level at 1338 keV was suggested due to an observation of a gamma ray at 1338 keV. This transition is neither in coincidence with 86 keV gate nor with the 197 keV gate. Thus, since the Q_{β^-} for ^{160}Tb is 1.838 MeV, therefore it is reasonable to assume that this transition resulted from the depopulation of a level at 1338 keV to the ground state. The log ft value for this level was calculated to be 11.82 which is consistent with spin/parity assignment of 1^-.

Another new level at 1507 keV has been observed. A strong coincidence of a new transition at 148 keV with the 309 keV gate has led for its establishment. This is further supported by the observation of two new γ-ray transitions at 1420 and 1507 keV. The energy at 1420 keV could be placed between this new level and the 87 keV first excited state level while the transition 1507 keV arises from the depopulation of this level to the ground state. The direct decay to the ground state and the existence of a transition from this level to a 1^- state level at 1358 keV suggests that the most reasonable spin/parity assignment would be 2^+. The log ft value of 10.71 supports this assignment.

4.6 Discussion.

This section will be divided into two subsections in which the positive and negative parity states will be separately treated. At the beginning of each subsection nuclear models suitable for a description of the nuclear properties of the energy level states are discussed. The states are grouped into various bands specified by a K-quantum number. In each of these

bands, the predictions of energy levels and transition probabilities are compared with experimental values. The results obtained by different models are highlighted in order to emphasize the importance of alternative approaches in describing these states.

4.6.1 Positive parity states.

The ^{160}Dy nucleus having an energy ratio $E_{4_1}^+/E_{2_1}^+$ equal to 3.03 (near the rotational limit of 3.13) is considered to be a deformed nucleus. The low energy properties thus could be described by the collective model of Bohr and Mottelson [28]. Inherent in the model is the approximate decoupling of rotation and vibration, which constitute an adiabatic condition. This implies that the energy spectrum will be that of equation (2.9). The deviations observed for the positive parity states from a simple rotational energy dependence are attributed to non-adiabatic effects such as vibrational coupling or intrinsic motion. The best and the most sensitive indicator to test the validity of the adiabatic condition is the gamma ray branching ratios for transitions from a given state in one band to states in another band. Even a slight mixing of bands, resulting from a partial breakdown of the adiabatic condition, can have an appreciable effect on the transition probabilities [116]. As a result, the reduced transition probability between pure K-bands is multiplied by a correction factor $f(z, I_i, I_f)$. Thus,

$$B(E2; I_i \rightarrow I_f) = B(E2; I_i \rightarrow I_f)_0 f(z, I_i, I_f) \qquad (4.1)$$

The reduced transition probability $B(E2; I_i \rightarrow I_f)_0$ for the adiabatic condition is proportional to the Clebsch-Gordon coefficient [83]. The quantity z is a general mixing parameter. Specifically, if Z_γ represents the mixing parameter between γ and GSB, and $Z_{\beta\gamma}$ refers to the parameter for the mixing between γ and β-bands, then the correction factors for reduced transition probabilities between the states in γ-band to the states in GSB are as given in Table (4.6) for different I_i and I_f.

Table (4.6). The correction factor $f_\gamma(Z_\gamma, Z_{\beta\gamma}; I_i, I_f)$ for the transition probability between the gamma-band and ground state band, with β-γ coupling included.

Initial state K=2 I_i=	Final state K=0 I_f=	$f_\gamma(Z_\gamma, Z_{\beta\gamma}; I_i, I_f)$
I-2	I	$(1+(2I+1)Z_\gamma + I(I+1)Z_{\beta\gamma})^2$
I-1	I	$(1+(I+2)Z_\gamma)^2$
I	I	$(1+2Z_\gamma - 1/3\ I(I+1)Z_{\beta\gamma})^2$
I+1	I	$(1-(I-1)Z_\gamma)^2$
I+2	I	$(1-(2I+1)Z_\gamma + (I+1)(I+2)Z_{\beta\gamma})^2$

Table (4.7). The parameters (MeV) obtained for fits to the positive parity states.

Parameter	ELL	QQ	PAIR
Single shell Z=50-82	0.0205	-0.0223	0.0158
Subshell at Z=64	0.0127	-0.0461	0.0334

In the context of the IBM approach the most suitable limit to describe the deformed nucleus of ^{160}Dy is the SU(3) limit. As mentioned earlier (section 2.3) the Hamiltonian which describes the positive parity states consists of the second and third terms of equation (2.16). The inclusion of the fourth pairing term is important to give the observed non-degeneracy of γ and β-bands. The program PHINT was used to calculate the energy levels. The parameters QQ, and ELL were initialised from the analytical energy equation (2.28). The parameter PAIR was estimated by taking the difference in energy between the γ-bandhead and β-bandhead and equated with the first term of equation (2.46).

The total number of bosons in this nucleus is normally taken to be 14. When considering the possible subshell closure at Z=64 in this nucleus, the situation will be slightly different. The total number of bosons will now be truncated to 7, but the Hamiltonian used is the same as for the normal shell closure at Z=50 or 82, leading to a change in the values of the three parameters. Experimentally, 12 positive parity states have been observed, two of which are newly suggested. These levels are classified into bands and discussed in the context of the geometrical model and the IBM.

Ground State Band ($K^{\pi} = 0^{+}$).

The GSB is formed from the 87(2^{+}) and 283(4^{+}) keV levels, whose spins/parities are well established.

The parameters A and B for the rotational energy spectrum of equation: (2.10) were computed [102] to be 14.04 and -0.0097 keV respectively. The energy levels predicted are shown in the second column of Table (4.8).

In the IBM calculations two cases were considered, and the parameters obtained for either the normal (Z=50-82) or the new proton (Z=64) shell closure are given in Table (4.7). The table shows that the values of QQ and PAIR, which represent the magnitude of quadrupole-quadrupole interactions and pairing forces respectively, are close to one another. For both IBM(Z=50-82) and IBM(Z=64) considerations the PAIR value is

approximately 75% of the QQ value. A result which suggests that there exists an appreciable competition between quadrupole-quadrupole forces and pairing forces in ^{160}Dy. Thus it is thought that this nucleus lies in the transitional region of SU(3) → O(6) but exhibiting more of an SU(3) character. The corresponding energy levels calculated using the appropriate parameters are as given in the fourth and fifth columns of Table (4.8).

Figure (4.10) shows a schematic diagram for comparing the experimental levels with theoretical predictions. The two theoretical approaches are IBM(a) which refers to the calculations performed using the normal Z=50-82 shell closure and IBM(b) which assumes a subshell closure at Z=64. The spins are shown on top of the level. The numbers in the parentheses are the SU(3) quantum numbers, λ and μ.

The predictions of both IBM(a) & (b) clearly show the natural appearance of bands such as a GSB, a γ-band and β-band. The situation is rather different for the rotor model predictions. The position of bands are determined by Eo of equation (2.10) and has to be fixed for each individual band. Furthermore, the parameters A and B vary for different bands. This suggest that the IBM could describe the levels much better than the collective rotational model. Only one set of parameters are needed to describe all the observed states.

Among the three predictions of Table (4.8), the results of IBM(Z=64) give the best estimate of the two GSB levels. The level fitting performed by PHINT using the parameters of Table (4.7) yields a χ^2 value for Z=64 considerations a factor of six lower than that for the normal shell closure at Z=50 or 82. The energy of the 4^+ level estimated on the basis of the rotational model gives a value 7 keV lower than the experimental value, while that predicted by the IBM(Z=64) is 1.5 keV higher than the observed level. Even the IBM(Z=50/82) prediction which is 1.8 keV lower is better than the rotor prediction.

The absolute B(E2) value for the $2_1^+ \rightarrow 0_1^+$ transition was calculated from the results of a lifetime measurement for

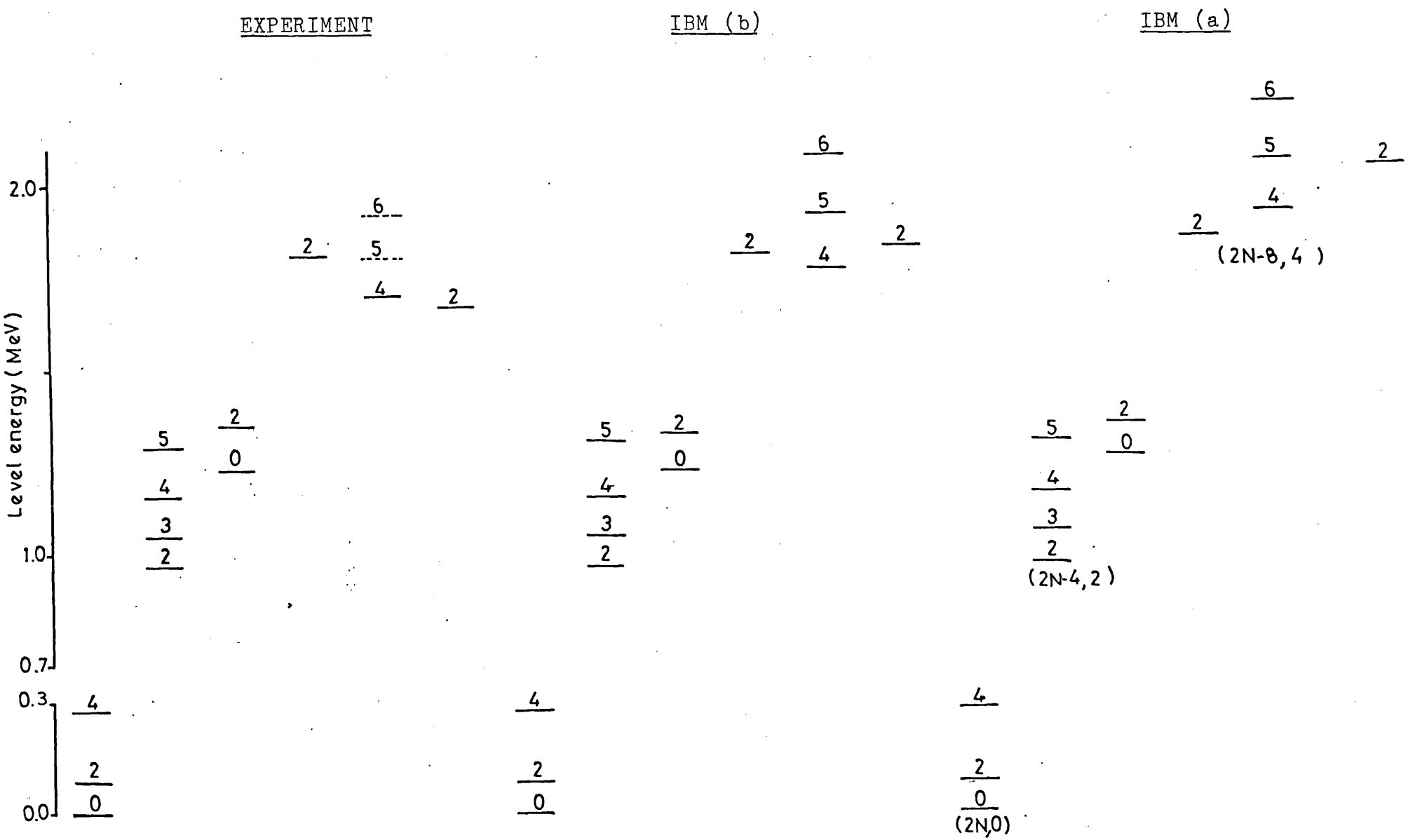

Figure (4.10) The experimentally determined positive parity levels for ^{160}Dy are compared with IBM calculations assuming a) a single Z=50-82 shell and b) a subshell closure at Z=64. The spin is shown on top of the level, (λ,μ) representations are in parentheses.

the first excited state and the intensity of the 87 keV γ-ray. The formulae used in the calculation were discussed previously (section 1.3). The value obtained was 110.33 e^2b^2 and was compared with IBM calculations. The program FBEM was used to calculate the result of the T(E2) operator (equation 2.29) acting on wavefunctions generated by PHINT. The three parameters previously determined are kept unchanged and the two new parameters, E2SD and E2DD are altered to obtain the best fit for the transition probabilities. Again, two cases are considered, the normal Z=50-82 closure and Z=64 subshell closure. The parameters obtained for the two cases are shown in Table: (4.9). The value of 0.142 (IBM Z=50-82) obtained for the E2SD parameter is consistent with predictions made by Warner and Casten [52]. The E2SD values of the T(E2) operator for deformed nuclei were estimated to range between 0.130 - 0.160. From the E2DD value of -0.135, this gives a ratio E2DD/E2SD equals -0.950. For a nucleus near the SU(3) limit this ratio is expected to be -2.958. Since the observed ratio is rather far from the pure SU(3) value, further support is given to the suggestion that ^{160}Dy lies in the SU(3) → O(6) transitional region.

Table: (4.10) show the comparison between experimental and theoretical absolute B(E2) values. The B(E2) value for $2_1^+ \rightarrow 0_1^+$ transition is well predicted by both IBM considerations, with the overall fit somewhat better for the (Z=64) consideration. The χ^2 value obtained is a factor of four lower than that for the Z=50-82 consideration.

Gamma band ($K^\pi = 2^+$).

This band consists of 4 levels at 966(2^+), 1049(3^+), 1155(3^+) and 1288(5^+) keV. The level at 1288 keV was first proposed by Ludington et al. [78] and was confirmed in the coincidence work. The zero B.R. established for this level supports the spin/parity of 5^+.

This band has been a matter of great interest among earlier workers. These workers [75, 77-82] have been concerned with the gamma-ray transition rates connecting the levels in

Table (4.9). The parameters used in program FBEM to calculate absolute B(E2) values (e^2b^2).

Parameter	E2SD	E2DD
Single shell Z=50-82	0.1420	-0.135
Subshell at Z=64	0.2490	-0.385

Table (4.10). Experimental absolute B(E2) values (e^2b^2) compared with IBM calculations assuming
(a) a single Z=50-82 and
(b) a subshell closure at Z=64.

Transition	Exp	IBM (a)	IBM (b)
$2_1^+ \longrightarrow 0_1^+$	110.33 †	110.55	110.39
$2_2^+ \longrightarrow 0_1^+$	1.67 *	2.20	1.95
$2_2^+ \longrightarrow 2_1^+$	3.09 *	3.36	2.93
$2_2^+ \longrightarrow 4_1^+$	0.222*	0.216	0.216

† Lifetime taken from present work.

* Lifetime averaged from Mc Gowan and Milner (1981) and Inamara et al. (1975).

Table (4.11). Band-mixing parameter $Z_\gamma(X10^3)$ from the measured B(E2) ratios and comparison with other works. (Uncertainties in the last significant figures are shown in parentheses).

Level (keV)	Transitions	B(E2) ratios		Z_γ X10^{-3}		
		Exp	Theory†	Present	(Das.)	(Gun.)
966	$\frac{2_2 \rightarrow 0_1}{2_2 \rightarrow 2_1}$	0.53(3)	0.70	47.8 (78)	56.5(67)	43.5(50)
	$\frac{2_2 \rightarrow 0_1}{2_2 \rightarrow 4_1}$	7.18(34)	13.9	37.8 (28)	37.5(41)	40.7(50)
	$\frac{2_2 \rightarrow 2_1}{2_2 \rightarrow 4_1}$	13.56(136)	19.9	32.0 (53)	27.1(48)	39.8(66)
1049	$\frac{3_1 \rightarrow 2_1}{3_1 \rightarrow 4_1}$	1.52(8)	2.5	38.9 (44)	42.3(61)	43.4(35)
1155	$\frac{4_2 \rightarrow 2_1}{4_2 \rightarrow 4_1}$	0.18(4)	0.34	42.76(76)	32.1(62)	

(Das.) Dasmahpatra BK (1976) [75]

(Gun.) Gunther et al. (1968) [81]

† Calculated from adiabatic-symmetric rotor model.

Table (4.12). Band-mixing parameter $Z_{\beta\gamma}(X10^3)$ from the measured B(E2) ratios.
(Uncertainties in the last significant figures are given in parentheses).

Level	Transitions	BE(2) ratios		$Z_{\beta\gamma}$ $X10^{-3}$	
		Exp	Theory†	Present*	Ref:
966	$\frac{2_2 \rightarrow 0_1}{2_2 \rightarrow 2_1}$	0.53(3)	0.70	-6.5(27)	-9.4(66)
	$\frac{2_2 \rightarrow 0_1}{2_2 \rightarrow 4_1}$	7.18(34)	13.19	-1.4(34)	-6.9(82)
	$\frac{2_2 \rightarrow 2_1}{2_2 \rightarrow 4_1}$	13.58(136)	19.9	-3.1(35)	-7.8(36)
1155	$\frac{4_2 \rightarrow 2_1}{4_2 \rightarrow 4_1}$	0.18(4)	0.34	-1.3(18)	+4.4(33)

* The values of $Z_{\beta\gamma}$ is calculated by assuming Z_γ=0.0389(44) obtained from the ratio B(E2; $3_1 \rightarrow 2_1$)/B(E2; $3_1 \rightarrow 4_1$).

† Calculated from adiabatic-symmetric rotor model.

Table (4.13). Experimental ratios of ft values for the β transitions to the γ-band of ^{160}Dy in comparison with theory.

$\frac{I_iK_i \rightarrow I_fK_f}{I_iK_i \rightarrow I_f'K_f}$	Present*	Theory†
$\frac{33 \rightarrow 22}{33 \rightarrow 32}$	0.38	0.35
$\frac{33 \rightarrow 22}{33 \rightarrow 42}$	0.017	0.04
$\frac{33 \rightarrow 32}{33 \rightarrow 42}$	0.046	0.144

* These values are obtained using 26.80, 6.45 and 0.17 as the percentage of β^- feeding to the 2^+, 3^+ and 4^+ levels of the gamma vibrational band.

† Calculated from the relation

$$\frac{ft(I_iK_i \rightarrow I_fK_f)}{ft(I_iK_i \rightarrow I_f'K_f)} = \frac{\langle I_iK_i\lambda\Delta K|I_f'K_f\rangle^2}{\langle I_iK_i\lambda\Delta K|I_fK_f\rangle^2}$$

where $\langle \ldots . | .. \rangle$ are the Clebsch-Gordon coefficients and λ is the multipole order of the β transitions. This has been assumed to be 1.

this band with the levels in the GSB. These rates enabled them to compute the coupling parameter Z_γ between the γ-band and GSB. The results between these workers were inconsistent with one another. The calculations performed by [75, 77] show that the value of Z_γ can be described uniquely and the average value obtained was 0.0419 ± 0.0035. On the other hand, the calculations of [73-82] conclude that such an unique description for the Z_γ value is not possible.

In order to try to resolve this problem, the values of Z_γ have been evaluated from different B(E2) ratios. In doing so all the transitions concerned are assumed to be of pure E2 character. The various transition probability correction factors were taken from Table: (4.6). The parameter $Z_{\beta\gamma}$ of the table was initially set to zero in calculating Z_γ. The values of Z_γ obtained from the calculations are shown in Table (4.11). A comparison with other workers was also made in this table. The deduction is that, within the experimental uncertainties the Z_γ values obtained could not be described uniquely.

These anomalous values of Z_γ obtained, suggest the possibility of the mixing with another low-lying positive parity band. Such a band would be the beta-vibrational band which has been observed in this region.

Assuming there is a coupling of γ and β-bands, the B(E2) ratios could be reanalysed to determine the mixing parameter $Z_{\beta\gamma}$ and see if a unique value or otherwise could be obtained. The correction factors for the transition probability are that of Table: (4.5). The difference now is that the value of Z_γ has to be fixed at a certain value. The most reasonable value of Z_γ is the value obtained from the ratio $\frac{B(E2;\ 3_1^+ \rightarrow 2_1^+)}{B(E2;\ 3_1^+ \rightarrow 4_1^+)}$ of Table (4.11). The reason is that the 3^+ state of the γ-band does not find a similar state in the β-vibrational band to mix with. From the results of Table (4.12) it can be concluded that the values of $Z_{\beta\gamma}$ obtained are unique within the experimental errors. Thus in the geometrical model the B(E2) ratios for transitions connecting γ-band and GSB in

^{160}Dy can be described by the second order mixing theory of Lipas [76]. This conclusion is consistent with the suggestion of Hamilton [82].

The anomalous values observed for Z_γ Table (4.11) suggest that the ^{160}Dy nucleus appears to be different from strongly deformed nuclei, like ^{168}Er [117, 118, 119]. This difference is further supported from the comparison of ft ratios for ^{160}Dy with Alaga's rule. The ft ratios of the transitions populating the gamma vibrational band of strongly deformed nuclei are known to obey the rule [74] closely. It is observed from Table:(4.13) that although the first ratio agrees well with theory the other two differ significantly. It may be argued that in view of the strong mixing of the γ-vibrational band with GSB observed the analysis of the B(E2) data, the ft ratios cannot be expected to agree with the theoretical values unless this mixing is taken into account. The situation is different in the IBM predictions for the B(E2) ratios from γ-band levels to levels in the GSB. Firstly, for transitions between different representations of SU(3) these ratios are independent of the parametrisation chosen for the E2 operator [120]. Secondly, despite the apparent existence of K=0 and K=2 bands in the (2N-4, 2) representation of SU(3), the structure of the IBA wavefunctions do not need the inclusion of bandmixing as has been shown by geometrical model. This is related to the fact that the 'K=2' band contains a small admixture of K=0 resulting from the transformation of Vergados to Elliot basis [121]. The overlap amplitude $\langle K=0|K=2\rangle$ of the $K=0(\beta)$ in the $K=2(\gamma)$ band increases with a decrease in boson number. This explains why the consideration of Z=64 subshell closure gives better predictions since the boson number has been reduced to half the original number (Refer Table: 4.14).

The absolute B(E2) values for transitions $2^+_2 \rightarrow 0^+_1$, $2^+_2 \rightarrow 2^+_1$ and $2^+_2 \rightarrow 4^+_1$ were deduced from the lifetime of the 966 $(2^+_{2^+})$ keV taken to be the average from McGowan and Milner and Inamara et al. [122]. The relative intensities of Table: 4.1 were used in the calculations. Comparison between the predictions of IBM(Z=50/82) and IBM(Z=64) again reveal that latter calculations are in better agreement with experiments. The

predictions for energy levels are shown in Table: (4.8).

β-band ($K^\pi = 0^+$).

This band consisted of two observed levels, one at 1230(0^+) keV and the other at 1349(2^+) keV. The former level is newly suggested while the latter was suggested by Ref.[115] and confirmed in our work. The zero B.R. to the 1230 keV level is consistent with spin/parity 0^+. The IBM(Z=64) prediction for this level gives very accurate result while the prediction for 1349 keV is lower by 27 keV. The observed weak β-g transition compared with (γ-g) transition is consistent with the IBM prediction for deformed nuclei [121].

βγ-band ($K^\pi = 2^+$).

This band is proposed due to an observation of a level at 1670 keV. This level, suggested to have spin/parity 2^+ was observed to decay only 2_2^+ and 3_1^+ states of the γ-vibrational band. Assuming that these transitions are pure E2, the ratio $\frac{B(E2;\ 2^+ \rightarrow 2_2^+)}{B(E2;\ 2^+ \rightarrow 3_1^+)}$ was calculated to be 0.35(25). The high percentage error in this ratio is attributed to the errors in the relative intensities of the transitions. The ratio estimated by IBM(Z=50/82) is 0.024 while that of IBM(Z=64) is 0.042. Neither of these predictions are in agreement with the experimental ratio. But if we were to take into account the experimental error and then assume a minimum ratio of 0.10, the most accurate prediction will be that of IBM(Z=64). This level at 1670 keV is suggested to be the bandhead of this $K^\pi = 2^+$ band. The IBM(Z=50/82) predicted this level at 2042 keV while that of Z=64 consideration estimated it to be at 1826 keV.

ββ-band ($K^\pi = 0^+$).

The level at 1804 keV with spin/parity 2^+ is suggested to be a member of this band. The transitions, 454 and 574 keV, to the β-band strongly support this suggestion. Furthermore the predicted B(E2) ratios in Table (4.14) are in agree-

Table (4.14). Experimental B(E2) ratios compared to the calculation of IBM(Z=50/82) and IBM(Z=64).

		B(E2) ratios		
Initial level	Final level	Experiment	IBM(Z=50/82)	IBM(Z=64)
966	0	1.	1.	1.
	87	1.85 (9)	1.54	1.64
	283	0.136(7)	0.094	0.139
1049	87	1.52 (8)	2.29	1.66
	283	1.	1.	1.
1155	87	0.18 (4)	0.29	0.26
	283	1.	1.	1.
1670	966	0.35 (25)	0.024	0.042
	1049	1.	1.	1.
1805	1230	1.15 (66)	1.91	0.76
	1349	1.	1.	1.

ment with experimental values. The IBM(Z=64) prediction is within the experimental error while that of IBM(Z=50/82) is slightly out of range. The level prediction by the normal IBM(Z=50/82) placed this level at 1845 keV. Although this estimate is in good agreement with the experimental level, the IBM(Z=64) consideration gives better value. The latter predicts the level at 1802 keV, only 2 keV below the experimental level.

<u>$\gamma\gamma$-band ($K^\pi = 4^+$)</u>.

The level at 1964 keV with spin/parity 4^+ is suggested to be the bandhead of this band. The zero branching ratio to GSB supports this assignment. It may be argued that this member could be a 4^+ member of $\beta\gamma$-band ($K^\pi = 2^+$) with its bandhead at 1670 keV. This possibility is overruled by the fact that the difference in energy between this level and the 2^+ state at 1670 keV of $\beta\gamma$-band is only 24 keV. For a 4^+ state level to be in the same band as the 2^+ state level, the energy separation should be approximately 200 keV which is similar to their energy separation in GSB. The assignment of 4^+ to level 1694 keV confirms the suggestion of Avotina et al.[123]. The IBM prediction with Z referred to 50 or 82 placed this level at 1920 keV, too high by 226 keV. Interestingly, a large discrepancy was also observed for the K=4 bandhead in ^{154}Gd by Van Isaacker et al. [124], and was accounted for by the inclusion of g bosons (J=4). The new prediction at 1776 keV reduces the difference to 82 keV and suggests that the consideration of a subshell closure at Z=64 may provide an alternative approach to the introduction of the J=4 degrees of freedom.

An analysis of the B(E2) values for the possible transitions from the 1694 keV(4^+) level on the basis of the IBM shows that the strongest transition would be expected to occur to the 2_2^+ level. Experimentally, only one transition was observed to depopulate this level. The transition is the $4^+ \rightarrow 2_2^+$ transition. This suggests that the s-d boson space alone is sufficient to account for this level.

Level 1507(2^+) keV.

This is the only level which could not be described by s-d boson space. As has been pointed out by Van Isaacker et al. [124], one consequence of a subshell closure at Z=64 would be the formation of a second low-lying $J^\pi = 0^+$ or 2^+ state, which is different from the collective $J^\pi = 0^+$(s boson) and $J^\pi = 2^+$(d boson) states. Thus it is suggested that the level 1507 keV could be such a possible intruder 2^+ state, which could be described as the result of a d′ boson. The intruder states are normally found in the region of excitation energy ≈ 2 MeV.

4.6.2 Negative parity states.

The deviation from the leading order rotational energy equation, for the negative parity states, may be accounted by the Coriolis coupling [28]. This Coriolis force gives rise to a coupling between bands with ΔK=1. This leads to modification in the various matrix elements involving the coupled bands. The wavefunctions of the states can be expanded in terms of pure K states |IK> as; [84]

$$\Psi_I = \sum_{K=0}^{I} \alpha_K |IK> \qquad (4.2)$$

where the (normalised) expansion coefficients α_K depend on the intrinsic Coriolis element and the energy separation of the intrinsic states [125]. The reduced transition probability for the decay of the negative parity states to positive parity states is given by the expression[85] :

$$\frac{B(E1;\ I_iK_i \rightarrow I_fK_f)}{B(E1;\ I_iK_i \rightarrow I'_fK_f)} = \left[\frac{\sum_{K_i} \alpha_{K_i} <I_iK_i 1\Delta K|I_fK_f><K_f|M'(E1)|K_i>}{\sum_{K_i} \alpha_{K_i} <I_iK_i 1\Delta K|I'_fK_f><K_f|M'(E1)|K_i>}\right]^2 \qquad (4.3)$$

where $<K_f|M'(E1)|K_i>$ is the electric dipole matrix element in the intrinsic coordinate system. The bracket <....|..> is

the Clebsch-Gordon coefficient. Subscripts i and f refer to the initial and final states respectively. For example I_i indicates initial spin and K_i refers to the K-quantum number of the initial spin. The notation ΔK is the difference between K_i and K_f.

In the context of IBM approach, to generate the negative parity states an $f(L^\pi = 3^-)$ boson is coupled to the s-d boson space. The total number of boson (N) now comprises of the sum of all the three types of bosons, s, d and f, i.e. $N = n_s+n_d+n_f$. The Hamiltonian used to describe the coupling of these bosons, is the sum of three separate Hamiltonians, H_{sd}, H_f and H_{df}, as given by equation (2.21). The Hamiltonian, H_{sd} describes the coupling of s and d boson which gives rise to the positive parity states. The parameters used in this Hamiltonian are the same as the ones used previously to describe the positive parity states, namely the QQ, ELL and PAIR. H_f is the Hamiltonian of an f-boson given by equation (2.22) and H_{df} refers to equation (2.23) which describes the coupling between d and f bosons.

In the present work a total of eight negative parity states were observed, one of which is newly suggested. These states occur in pairs with spin/parity 1^-, 2^-, 3^- and 4^-. They are grouped into three separate bands specified by K-quantum numbers $K^\pi = 0^-$, 1^- and 2^-. Each of these bands are separately treated whereby the level properties are discussed in terms of Coriolis coupling theory and the IBM descriptions.

<u>$K^\pi = 0^-$ band</u>.

The new level at 1338 keV is suggested to be the bandhead of this band. The log ft value of 11.82 obtained for this level is consistent with spin/parity 1^- assignment. The observed direct decay to ground state 0^+ further supports this spin/parity suggestion.

The calculation of Soloviev [126] predicts this band to start approximately at 1170 keV. This prediction is lower by 168 keV than the observed experimental level. On the other

hand, the Coriolis coupling calculation of Ref: [84] placed this 1^- level at 1600 keV, too high by 262 keV.

In the IBM(Z=64) calculations, program PHINT diagonalised equation 2.21 to obtain the negative parity states. The parameters obtained for the Hamiltonians, H_f and H_{df}, are shown in Table:(4.15). The parameters for the Hamiltonian H_{sd} are the same as that obtained for the positive parity states in the case of IBM(Z=64) [Refer Table:(4.7)].

Table (4.15). The parameters (MeV) obtained for fits to the negative parity states in the IBM(Z=64) consideration.

Parameter	HBAR3	FELL	FQQ
Subshell at Z=64	0.75	0.0177	0.0015

A positive value of FQQ indicate that the bandheads of the bands with high value of K-quantum number are placed at lower excitation energy compared to bandheads for bands with small values of K. Specifically, the bandhead of $K^\pi = 2^-$ band is lower than the bandhead of $K^\pi = 1^-$. The parameter FELL determines the level spacings within each band. The effect of the parameter HBAR3 on the energy spectrum is to adjust the bandhead of each band either up or down in response to a change in its numerical value. It behaves similarly to the Eo parameter for rotor energy spectrum of equation (2.9).

The results of the level predictions are shown in Table: (4.16) together with the Coriolis coupling calculations[84]. The IBM(Z=64) calculations give better predictions to all the negative parity states. The 1^- level ($K^\pi = 0^-$) is predicted at 1335 keV, indeed an excellent agreement with experimental level at 1338 keV.

Table (4.16). Experimental negative parity states compared with Coriolis coupling and IBM(Z=64) calculations.

J	K	Energy (keV)		
		Exp	K–V	IBM(Z=64)
2	2	1264.7	1330	1271.0
1	1	1285.6	1430	1257.9
3	2	1286.7	1360	1322.6
1	0	1338.1	1600	1335.7
			1170†	
2	1	1358.6	1580	1360.3
4	2	1386.3	1470	1364.9
3	1	1398.6	1520	1400.9
4	1	1535.1	1830	1600.1

K–V Kocbach L and Vogel P (1970)[84]

† Soloviev et al. (1964)[126]

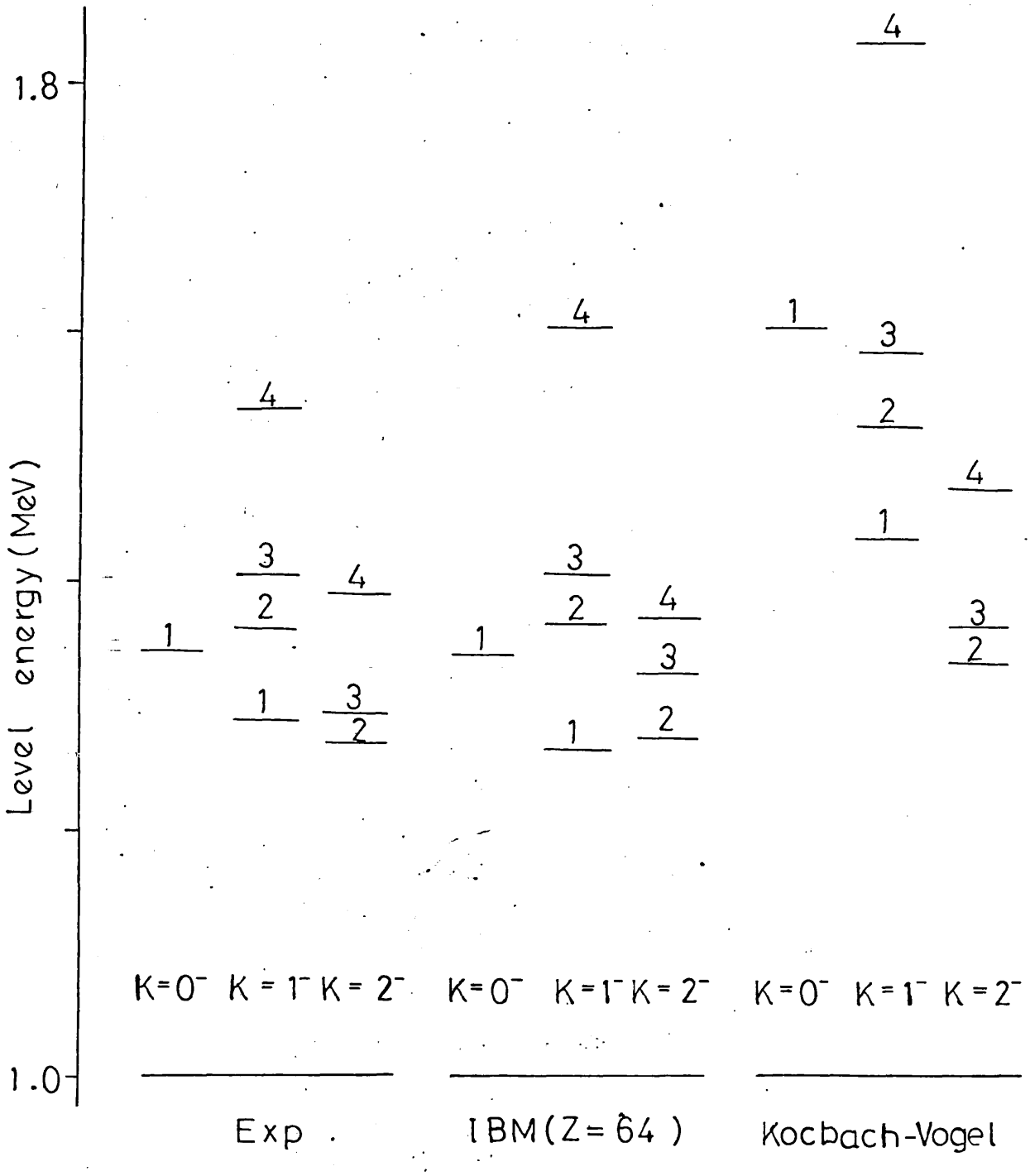

Figure (4.11) The experimentally determined negative parity levels for ^{160}Dy are compared with IBM calculations (Z=64) and Coriolis coupling predictions of Kocbach and Vogel.

Figure (4.11) shows the comparison between experimental values and the theoretical predictions for the negative parity states. The two predictions are of IBM(Z=64) and Coriolis coupling of Kochbach and Vogel [84].

$K^{\pi} = 1^-$ band.

This band comprised of the levels at 1285(1^-), 1359 (2^-), 1398(3^-) and 1535(4^-) keV. The level at 1285 keV was first suggested by McAdams and Otteson [80] and was confirmed in the present work. The log ft value of 11.40 supports spin/parity 1^-.

The K-quantum number assignment to all these levels are consistent with the B(E1) ratios of Table (4.17).

From the result of Table (4.16) and Figure (4.11) the Z=64 subshell consideration in the IBM gives better predictions. Particularly for the 1359 keV level, the prediction gives a value of 1360 keV which is considered to be in excellent agreement. A slightly large difference is observed for 1535 keV level. The estimated level at 1600 keV is approximately 65 keV above the experimental value. This is still considered to be good since the prediction of Kochback and Vogel[84] placed this level at 1830 keV, too high by 295 keV.

In predicting the B(E1) ratios for transition from this band to levels in γ-band and GSB, the present work adopts the method of Coriolis coupling. The reason for this is to check the validity of the claim made by Krane [85] who conclude that Coriolis coupling method could only explain the high energy transitions. Furthermore, the observation of more transitions in the present work provides an extended test of this method. The evidence for such a Coriolis mixing can be clearly seen from the experimental E1 branching ratios of the negative parity states to the γ-band and GSB. The levels with spin/parity 2^- and 4^- deexcites predominantly to the γ-band, while the levels with 1^- and 3^- populate mainly the GSB.

The method of Coriolis coupling assumes the mixing

Table (4.17). Experimental B(El) branching ratios for transitions from negative parity states in ^{160}Dy compared with the adiabatic-symmetric rotor model.

Transitions E/E' (keV)	Energy level (keV)	Exp	B(El) ratios Theory for different K_i			Deduced K_i
			0	1	2	
215/298	1264	0.38(3)	2.0*	2.0	0.5	2
1002/1199	1286	0.72(5)	1.33	0.75	0.75*	2
309/392	1357	1.34(8)	2.0*	2.0	0.5	1
1115/1310	1397	0.97(5)	1.33	0.75	0.75*	1
230/337	1385	0.72(4)	5.3*	5.3	0.60	2
379/486	1535	0.59(13)	5.3*	5.3	0.60	1
1285/1199	1285	1.04(25)	0.5	2.0	2.0*	1

* Calculated from the forbidden transition

of bands with $\Delta K=1$. Hence the wavefunction of a particular level will be the sum of all the wavefunctions of the levels with same spin from other bands. The magnitude of these wavefunctions is proportional to the expansion coefficients α_K as given in equation (4.2). Since these α_K depend on the energy separation and the intrinsic Coriolis element therefore a precise determination of energy levels do not change the values of α_K considerably. Thus, the present work have taken the values of Gunther et al. [75] as given in Table (4.18).

The next important step is to calculate the various matrix element ratios. Defining;

$$R = \frac{< 0^+|M'(E1)|1^- >}{< 2^+|M'(E1)|1^- >} \qquad (4.4)$$

$$R' = \frac{< 2^+|M'(E1)|2^- >}{< 2^+|M'(E1)|1^- >} \qquad (4.5)$$

and

$$R'' = \frac{< 0^+|M'(E1)|1^- >}{< 0^+|M'(E1)|0^- >} \qquad (4.6)$$

These ratios can be estimated by equating few experimental B(E1) ratios with the theory of equation (4.3). From this equation the B(E1) ratios for the deexcitation of 2^- states to members of γ-band and GSB are given by:

$$\frac{B(E1;\ 2^- \rightarrow 3_1^+)}{B(E1;\ 2^- \rightarrow 2_2^+)} = 2\left[\frac{1 + 0.5\sqrt{2}\ \varepsilon_2}{1 - \sqrt{2}\ \varepsilon_2}\right]^2 \qquad (4.7)$$

and

$$\frac{B(E1;\ 2^- \rightarrow 0_1^+)}{B(E1;\ 2^- \rightarrow 2_2^+)} = \frac{3R^2}{(1 - \sqrt{2}\ \varepsilon_2)^2} \qquad (4.8)$$

where

$$\varepsilon_2 = \left(\frac{\alpha_2}{\alpha_1}\right) R' \qquad (4.9)$$

For the 1265(2^-) keV [$K^\pi = 2^-$] level the experimental B(E1) ratio to the 2^+ and 3^+ states of γ-band is 0.38. Equating this with equation (4.7) yields the value of

$$\varepsilon_2 = -15.95$$

Substituting this value of ε_2 into the second equation, Equation (4.8); and using the experimental ratio of 0.009 will result in the value of R = 1.29.

The identical calculations performed for the level 1359(2^-) keV [$K^\pi = 1^-$] give values of

$$\varepsilon_2 = 4.04$$

and

$$R = 1.08$$

The average value of R is then 1.18(09). From equation it follows that

$$R' = \left|-(\varepsilon_2)_{1265\ \text{keV}}\ (\varepsilon_2)_{1359\ \text{keV}}\right|^{\frac{1}{2}}$$

Hence by substituting the various ε_2 values, R′ was calculated to be 8.08(80).

Again using equation (4.3) the analytical formula for the B(E1) ratios for transitions can be deduced by de-exciting the 3^- states to members of GSB. This reduces to:

$$\frac{B(E1;\ 3^- \rightarrow 4_1^+)}{B(E1;\ 3^- \rightarrow 2_1^+)} = \frac{4}{3}\left[\frac{1 + \frac{1}{2}\sqrt{3}\ \varepsilon_3}{1 - \frac{2}{3}\sqrt{3}\ \varepsilon_3}\right]^2 \qquad (4.10)$$

where

$$\varepsilon_3 = \frac{\alpha_1}{\alpha_0} R'' \qquad (4.11)$$

For the 1287(3^-) keV level the experimental B(E1) ratio of 0.72 to the 4^+ and 2^+ GSB yields a value of

$$\varepsilon_3 = 0.1539$$

Substituting the appropriate values of α_1 and α_0 (Table: 4.18) into equation (4.11) results in the value of

$$R'' = 0.041$$

Similar type of calculation performed for level 1398(3^-) keV, of the K = 2^- band, results in the values of:

$$\varepsilon_3 = -0.08$$

and

$$R'' = 0.025$$

The average value taken for R'' is 0.033(1).

The values of R, R' and R'' are summarised in Table: (4.19). From these values of R, R' and R'' and the Coriolis coefficients of Table (4.18), the B(E1) ratios for all transitions deexciting every negative parity states were then calculated. The expression used is that of equation (4.3). The results are shown in Table (4.20). The Coriolis coupling method gives good agreement with experimental results.

The only discrepancy observed for transitions deexciting this $K^\pi = 1^-$ band is that of the 1398(3^-) keV level. The relative B(E1) predicted for the transition from this level to 4^+ level of γ-band is 0.29, while the experimental value is 1.72(40). The latter value is almost six times greater than the prediction. The energy of the transition involved is 242 keV. From the table of relative intensities (Table: 4.1) there is a disagreement between the present relative intensity for this transition with that of Ref: [78]. Suppose the calculation was based on the relative intensity of Ludington et al. then the experimental B(E1) ratio would be 0.28 which is in fact in excellent agreement with the prediction. Energetically, this transition can also fit the levels at 1507(2^+) keV which is a newly suggested level, and the level at 1264 keV.

Hence it is postulated that a 242 keV transition decays from two branches; one from the well established 1398 (3^-) keV level to 1155(4^+) keV level, and the other from

Table (4.18). The expansion coefficient of Coriolis mixed wavefunction for negative parity states.

Level (keV)	I	K	α_0	α_1	α_2
1265	2	2		+0.39	-0.92
1359	2	1		+0.92	+0.39
1287	3	2	+0.18	-0.68	+0.70
1399	3	1	-0.21	+0.67	+0.71
1386	4	2		+0.54	-0.84
1535	4	1		+0.84	+0.54
1285	1	1	-0.12	+0.99	

Table (4.19). The deduced ratios of the matrix elements. (Uncertainties in the last significant figures are given in parentheses).

$\frac{\langle K_f=0^+\|M'(E1)\|K_i=1^-\rangle}{\langle K_f=2^+\|M'(E1)\|K_i=1^-\rangle}$	$\frac{\langle K_f=2^+\|M'(E1)\|K_i=2^-\rangle}{\langle K_f=2^+\|M'(E1)\|K_i=1^-\rangle}$	$\frac{\langle K_f=0^+\|M'(E1)\|K_i=1^-\rangle}{\langle K_f=0^+\|M'(E1)\|K_i=0^-\rangle}$
1.18(9)	8.04(80)	0.033(2)

Table (4.20). Experimental B(El) ratios for transitions from negative parity states in ^{160}Dy compared with the calculations using Coriolis coupling.

Level (keV)	I_i	I_f	B(El) ratios Exp	B(El) ratios Theory
1264	2^-	2_2^+	1.0	1.0
		3_1^+	0.38 (3)	0.39
		2_1^+	0.009(1)	0.0027
1286	3^-	2_1^+	1.0	1.0
		4_1^+	0.72 (5)	0.93
		2_2^+	0.21 (9)	0.36
		3_1^+	0.57 (4)	0.59
1385	4^-	3_1^+	1.0	1.0
		4_2^+	0.72 (4)	0.62
		4_1^+	0.039(2)	0.012
1358	2^-	2_2^+	1.0	1.0
		3_1^+	1.34 (8)	1.59
		2_1^+	0.154(8)	0.143
1398	3^-	2_1^+	1.0	1.0
		4_1^+	0.96 (5)	0.99
		2_2^+	0.25 (9)	0.23
		3_1^+	0.41 (4)	0.27
		4_2^+	1.72 (40)	0.29

—— continued ——

Level (keV)	I_i	I_f	B(E1) ratios	
			Exp	Theory
1535	4^-	3_1^+	1.0	1.0
		4_2^+	0.59 (13)	0.37
		5_1^+	1.43 (43)	2.46
		4_1^+	0.055(12)	0.096
1285	1^-	0_1^+	1.04 (25)	1.08
		2_1^+	1.0	1.0

1507(2^+) keV level to 1264(2^-) keV level. The relative intensity of the former is 0.004 while the latter is 0.022. Hence the bulk of the 242 keV peak comes from the new level at 1507 keV.

$K^\pi = 2^-$ band.

This band consists of three energy levels at 1265(2^-), 1287(3^-) and 1386(4^-) keV.

The E1 character of transitions 298 and 215 keV from level 1265 keV to the levels at 966(2^+) and 1049(3^+) keV respectively suggest that this level has spin/parity of either 2^- or 3^-. The log ft value of 8.18 suggest the spin/parity 2^-.

The spin/parity of the level at 1286 keV was determined from the conversion coefficient (α_K) values of the transitions 1199 and 1003 keV which depopulate this level to 2^+ and 4^+ states of GSB. The log ft value 9.23 confirms the spin/parity 3^-.

The 1386 keV level was assigned 4^- in view of the log ft value and from the α_K coefficient of the 337 keV which depopulates this level to 1049(3^+) level of the γ-band.

The K-quantum number assignment for all these three levels were consistent with the B(E1) ratios of Table:(4.17). The energy levels are well predicted by the IBM(Z=64) as shown in Table (4.16).

The relative B(E1) ratios for transitions depopulating these levels to states in GSB and γ-band were calculated similar to that of $K^\pi = 1^-$ band. The results of Table (4.20) shows good agreement with experimental values.

It is also of interest to examine the β^--decay branching ratios in the context of Coriolis coupling calculations. If the β-transitions from the $K = 3^-$ ^{160}Tb ground state are assumed to be of the allowed Gamov-Teller type, only the K=2 part of the final-statewave function should contribute, and

Table (4.21). Relative β^-—intensities $(ft)^{-1}$ from ^{160}Tb decay to negative parity states in ^{160}Dy.

Final state (keV)	I	K	Relative $(ft)^{-1}$	
			Exp	Theory*
1338	1	0	0.0002	0.00†
1535	4	1	0.06	0.02
1398	3	1	0.30	0.21
1358	2	1	0.55	0.18
1285	1	1	0.0006	0.00†
1264	2	2	1.00	1.00
1287	3	2	0.089	0.20
1386	4	2	0.06	0.04

* Krane KS (1982) [85]

† Present calculation.

the β-branching ratios $(ft)^{-1}$ should be proportional to the quantity [127]

$$\alpha_2^2 < 331 - 1|I_f 2 > ^2$$

Table (4.21) shows a comparison between the measured values and those expected on the basis of the model. The agreement is satisfactory, particularly in view of the simplifying assumptions made. To account for the difference, the K=1 part of the wavefunction should be included in the calculation. The results contained in this table provide more supportive evidence for the K-quantum number assignments to the negative parity levels, and is particularly satisfactory for the newly observed 1^- level at 1338 keV.

CHAPTER V

THE NUCLEUS OF ^{188}Os

5.1 Introduction.

The ^{188}Os nucleus is situated in a transition region between those nuclei 150 < A < 180, possessing large equilibrium deformations, and the spherical nuclei near the doubly magic ^{208}Pb. Knowledge of the properties of the excited states in ^{188}Os would thus, provide insight into the details of their structure, and would form a basis for the evaluation of different microscopic and phenomenological nuclear models.

Yamazaki et al. [128], has discussed the properties of ^{188}Os both in terms of Bohr and Mottelson [29] [BM] and Davydov and Fillipov [129] [DF] models. As far as the ground state ($K^\pi = 0^+$) and gamma ($K^\pi = 2^+$) bands are concerned, the predictions of both models appear to parallel one another. The only difference is that the DF model, which assumes asymmetric equilibrium, was able to fit the experimental values for the ratios $B(E2; 2_2^+ \rightarrow 0_1^+)/B(E2; 2_2^+ \rightarrow 0_1^+)$ and $E_{4_1}+/E_{2_1}+$ while the hydrodynamical BM model could not. The experimental values for B(E2) ratio between transitions from the $K^\pi = 2^+$ band to the $K^\pi = 0^+$ band cannot be fitted by the DF predictions, which means that the band coupling is overestimated. Furthermore, the experimental value for the E0 matrix element in the $2_2^+ \rightarrow 2_1^+$ transition seems to favour the BM model.

The failure of the phenomenological models to provide a satisfactory account of the structure has prompted a detailed investigation of nuclear deformation on a microscopic level. The theoretical calculations of Kumar and Baranger [57] have involved detailed predictions concerning the structure of nuclei in the mass region near A=180. The calculations involve the residual pairing and quadrupole interactions applied to spherically symmetric independent-particle wavefunctions. The predictions for the ^{188}Os nucleus show good agreement for the energy levels, but only for the $B(E2; 2_1^+ \rightarrow 0_1^+)$ and

$B(E2; 4_1^+ \rightarrow 2_1^+)$ values. Agreement for other B(E2) values were not as good. The directional correlation work of Krane and Steffen [111] show that the PPQM gives good estimates to the E2/M1 mixing amplitudes for the 478 and 635 keV transitions. However, the theory seems to encounter difficulty, notably concerning the decay of the 0_3^+ state.

A somewhat extended approach to PPQM was taken by Sahu et al. [130]. The intrinsic calculation was performed in the framework of Hartree-BCS theory employing the pairing and Q.Q. interaction. The level energies up to I=10 in GSB and up to I=4 in the γ-band show good agreement with experiment. On the other hand, a discrepancy was observed in the prediction of the K=4 band. The position of this bandhead was estimated to be at 3394 keV, more than twice the observed level at 1278 keV [131]. The prediction for the ratio $B(E2; 2_2^+ \rightarrow 2_1^+)/B(E2; 2_2^+ \rightarrow 0_1^+)$ is consistent with the experimental value.

In explaining a rather large quadrupole moment ($Q_{2_1^+}$), for the first excited 2_1^+ state, Weeksand Tamura [132] employ a boson expansion technique [133] (section 2 - 3). Astonishingly, the predicted $K^\pi = 4^+$ bandhead was only 185 keV higher than the experimental value, much better than the prediction of Sahu et al. [130]. Although this technique has quite accurately predicted the decay of the 0_2^+ state, the energy level was somewhat too low.

This low prediction of the 0_2^+ state was later improved by Hess et al. [134]. He employs the General Collective Model [section 2.2.3] and the calculations, which were based on the Potential Energy Surface (PES), gave accurate prediction of the 0_2^+ state but not the 0_3^+ state. The prediction at 2030 keV for the latter state was too high by 552 keV compared to the experimental value at 1478 keV. Furthermore, PES predicted the $B(E2; 2_2^+ \rightarrow 0_1^+)$ value 15 times lower than the experimentally observed value. Thus, there still existed many discrepancies between the nuclear models and the experimental data available for ^{188}Os.

Almost all the models which have been discussed only explained certain properties of nuclear structure, but

failed for others. The more unified IBM might be expected to give a better description of the nuclear structure of ^{188}Os. In terms of IBM limits, Casten and Cizewski [135] have classified this medium mass A=188 nucleus to lie in the transitional region between the O(6) and SU(3) limits. Although the basic trend of the nuclear properties within this transitional region has been discussed before, detailed calculations, coupled with the most recent experimental data has never been previously carried out for ^{188}Os. Since the γ-unstable model of Wilets and Jeans [136] is the closest geometrical analogue of the O(6) limit of IBA [135,137], the success of this model in reproducing the experimental data may be interpreted as supportive evidence for the γ-soft cores in nuclei. More refined parametrizations which make a distinction between proton and neutron bosons were presented by Bijker et al. [138] and Scholten [139].

The present study seeks to understand the nucleus of ^{188}Os in detail, within the context of IBA-1. Especially sc for the relative decay modes of 0^+ states and the predictions of possible M1 transitions, both of which form basic tests in understanding the O(6) character of a nucleus [53].

The nucleus of ^{188}Os can be populated either β^- decay of ^{188}Re, or by EC/β^+ decay of ^{188}Ir. The former mode of decay is preferable due to its relatively longer half-life.

Among the earliest coincidence and directional correlation studies from ^{188}Re β^- decay was that of Arns et al.[140]. Gamma rays were detected using 2"×2" NaI(Tl) crystals mounted on 6342A phototubes. A total of 17 energy transitions were obtained whereby the relative intensities for stronger transitions were found to have an error of 10 %. In establishing the energy level scheme, 4 gates at 155, 478, 633 and 829 keV were taken, resulting in 9 energy levels to be proposed. A new level at 1730 keV with spin 2 and unknown parity was suggested. The result of directional correlation measurements indicated an M1 character for the 829 keV transition.

Much more extensive studies involving e-e, e-γ and γ-γ coincidences from both ^{188}Re and ^{188}Ir were later performed by Warner and Sheline [141]. The detectors used were two

7.62 cm X 7.62 cm NaI(Tl) scintillation counters. Two more transitions were observed from the ^{188}Re decay, and from ^{188}Ir decay γ-γ coincidences established 3 new levels at 789, 1732 and 1846 keV.

The works of Wyly et al. [142] and Yamazaki [143], based on β-γ directional correlation in ^{188}Re and ^{188}Ir decay respectively, mainly confirmed previous data without providing new results.

The studies by Harmatz and Handley [144], using both modes of decay, established a spin/parity of 2^- for the 1305 keV level. This was in contradiction with the measurement made later by Bashandy and Hanna[145] where a high resolution, double focussing beta-ray spectrometer was used. The spin/parity of this level was suggested to have 3^-.

Yamazaki and Sato [146] employed Ge(Li) spectrometer in their β-γ and γ-γ coincidence studies. Three Ge(Li) γ-ray spectrometers; 2 cm^2 X 5 mm thick, 6 cm^2 X 10 mm thick and 30 cm^3 coaxial, were used for the determination of γ-ray intensities. A total of 35 gamma rays were observed from the β^- decay of ^{188}Re. In the coincidence study, the 30 cm^3 coaxial Ge(Li) was used in conjunction with a 5 cm X 5 cm NaI(Tl) spectrometer. A total of three energy gates at 155, 478 and (633 + 635) keV were taken to construct the decay scheme of ^{188}Os nucleus. The level proposed by [144] at 1705 keV was not seen. The level at 1305 keV was suggested to have spin parity of 2^+ in contradictions with 2^- [144] and 3^- [145] suggested earlier. Two levels at 789 (3^+) and 1808 keV were observed for the first time to be populated in the decay of ^{188}Re (1^-). These levels were well established levels from the EC/β^+ decay of ^{188}Ir (2^-). Two new levels at 1457 (1^+, 2^+), and 2021 (2^+) were proposed.

The most recent work on the β^- decay of ^{188}Re was that of Svoren et al. [147]. The gamma rays were detected with a large volume high resolution Ge(Li) detector. A total of forty-one γ-rays were observed. Eleven transitions at 312, 515, 558, 624, 634, 811,1071, 1302, 1305, 1549 and 1808 keV

were considered to be new. Energies at 794, 963, 967 and 1170 keV observed by Yamazaki [146] were also seen but were attributed to the radiative background of the laboratory. None of the others at 641, 880 and 1230 keV were observed. There was no coincidence measurement being made. The level scheme was constructed based on the energy sum relations. This resulted in 18 energy levels of which 5 levels were suggested to be populated for the first time by β^- decay of ^{188}Re. These levels were; 478 and 1843 keV observed in ^{188}Ir EC/β^+ decay, 1480 and 1705 keV observed by Sharma and Hintz [148] from (p,t) reaction studies, and 1414 keV observed from the reaction (α,2nγ) by Yates et.al. [131].

The transition observed at 487, 558 and 811 keV could not be placed in the decay scheme. Transitions at 487 and 811 keV were observed in the decay of ^{188}Ir, Ref [146], and were associated with the deexcitation of the $K^\pi = 2^+$, 4^+ level at 965 keV. However, there is no way that this level could be found to be populated other than the β^- decay, which would not be expected from 1^- ^{188}Re.

The level at 2021 keV seen by Yamazaki and Sato [146] was suggested to have an energy of 2023 keV. The energy level determination using 1865 and 2023 keV transitions differ by 1.6 keV.

In studying the nuclear properties of ^{188}Os the methods of β^- and EC/β^+ decay were not the only means of probing this nucleus. There were several reaction studies performed earlier.

A high spin ground state was studied by Newton et al. [149] by Coulomb excitation ^{186}W(^{4}He, 2nγ). Ge(Li) detectors were used and a maximum spin of 10^+ was observed.

Casten et al. [150] measured the γ-γ coincidence from ^{188}Os(O^{16}, $O^{16}\gamma$) reaction. The detectors used were NaI(Tl). Milner et al. [151] used two reaction modes ^{188}Os(α, $\alpha'\gamma$) and ^{188}Os(O^{16}, $O^{16}\gamma$) while Lane and Saladin [152] employ He, O^{16} and sulphur ions in their Coulomb excitation studies. In search of 0^+ states Sharma and Hintz [148] employ a (p,t) reaction.

In the $^{186}W(\alpha, 2n)\ ^{188}Os$ study, Warner et al. [153] were able to identify up to spin 12^+ in the GSB: Yamazaki et al. [128] using the same reaction technique, would only identify up to 10^+ of the GSB and 5^+ of the γ-band. A γ-γ coincidence studies the same reaction, using 19 gates, led Yates et al. [131] to propose a 6^+ state in a γ-band at 1424, and a 4^+ state of $K^\pi = 4^+$ at 1279 keV. A level at 1414 keV with spin/parity 3^- was also established.

Other reaction studies pertaining to this nucleus were; ^{188}Os (α, α') by Burke et al. [154], ^{189}Os (d,t) by Thompson et al. [155] and ^{190}Os (p,t) by Sharma and Hintz [156] and also by Thompson et al. [157]. The last named assign the level at 1823 keV, a 0^+ spin/parity, in contradiction with other workers.

In searching for 0^+ states Macphail et al. [158] employed (n,γ) reactions. A total of 5 0^+ states, energies below 2 MeV, were identified with the level at 1966 keV being a new suggestion.

The present work on ^{188}Os populated by the β^- decay of ^{188}Re was undertaken to remove discrepancies observed earlier, especially as regards to the level scheme.

5.2 Single spectra.

The single spectra were measured using the 12 % Ge(Li) efficient detector and also an intrinsic Germanium detector.

The radioactive source used was ^{188}W, produced by double neutron capture at Reactor PLUTO in Harwell. The reaction is of the form ^{186}W (2n, γ) ^{188}W. The ^{188}W decays with a half-life of 70 days to ^{188}Re which further decays ($T_{\frac{1}{2}}$ = 17 hrs.) to ^{188}Os. The final product, resulting from the double neutron capture in natural ^{186}W (95 % pure), contains 10 µCi of ^{188}W and 10 mCi of ^{187}W as an impurities. The half-life of ^{187}W which decays to ^{187}Re, which is stable, is approximately 24 hrs.

The radioactive source was left for three weeks for

Table (5.1) Energies (keV) and relative intensities I_γ in the decay of ^{188}W.

Energy (keV)	Intensities normalised I_γ(478 keV) = 100		
	Present	Ref:[147]	Ref:[146]
	^{188}Re		
63.26(13)	7.51 (150)		
85.29(13)	3.58 (45)		
141.78(25)	0.38 (4)		
205.61(14)	0.55 (13)		
207.62(17)	0.85 (22)		
227.15(14)	21.14 (76)		
290.49(12)	32.15 (91)		
	^{188}Os		
154.99(04)	1450 (114)	1432 (35)	1545 (150)
312.22(25)	0.38 (9)	0.31 (7)	-
322.72(31)	1.62 (11)	1.51 (10)	1.62(2)
453.34(12)	7.5 (5)	6.78 (18)	7.2 (4)
477.95(11)	100	100	100
485.97(28)	8.0 (4)	7.50 (31)	8.1 (3)
514.87(25)	0.54 (5)	0.49 (5)	-
633.01(10)	119.97 (98)	119.57 (108)	} 141 (14)
635.22(15)	13.73 (98)	14.18 (46)	}
650.13(18)	0.047(7)	-	-
672.59(10)	10.81 (43)	10.63 (31)	10.3 (1)
785.42(28)	0.58 (18)	-	-
825.44(25)	2.23 (35)	4.89 (49)	3.8 (10)
829.51(12)	39.75 (107)	39.29 (108)	39.8 (40)
845.20(12)	0.62 (9)	0.69 (5)	0.6 (2)
931.31(6)	54.23 (16)	54.04 (14)	58.3 (60)
1017.57(12)	1.25 (18)	1.43 (12)	1.60(4)
1027.24(28)	0.21 (5)	-	-
1070.98(25)	0.057(13)	0.077(15)	-

— continued —

Energy (keV)	Intensities normalised I_γ(478 keV) = 100		
	Present	Ref:[147]	Ref:[146]
1132.23(11)	8.31 (30)	8.46 (37)	9.4 (9)
1149.62(16)	1.51 (36)	1.65 (39)	} 3.6 (4)
1150.76(16)	1.51 (36)	1.65 (39)	}
1174.35(25)	1.73 (9)	1.94 (15)	2.1 (3)
1191.83(14)	1.07 (5)	1.33 (9)	1.2 (3)
1209.72(25)	0.30 (3)	0.28 (3)	-
1238.51(25)	0.20 (3)	-	-
1302.42(32)	0.58 (8)	0.62 (9)	-
1304.96(31)	0.44 (9)	0.52 (8)	-
1307.99(14)	6.60 (39)	6.47 (3)	6.6 (7)
1323.16(12)	1.01 (15)	0.83 (6)	1.3 (4)
1354.71(15)	0.046(10)	-	-
1457.55(8)	1.86 (18)	1.91 (12)	1.8 (4)
1505.34(25)	0.38 (11)	-	-
1549.36(25)	0.19 (5)	0.25 (5)	-
1610.32(10)	8.22 (47)	9.41 (40)	10.5 (18)
1652.81(15)	0.27 (6)	0.32 (5)	-
1660.28(24)	0.64 (12)	-	-
1669.84(21)	0.78 (10)	1.02 (8)	0.6 (2)
1711.19(20)	0.25 (7)	-	-
1785.19(13)	1.23 (15)	1.99 (11)	2.6 (3)
1793.23(14)	0.057(13)	-	-
1802.13(11)	3.59 (22)	3.61 (17)	4.1 (5)
1807.61(28)	0.19 (3)	0.11 (2)	-
1846.46(12)	0.052(13)	-	-
1865.20(16)	0.46 (9)	0.54 (5)	0.6 (2)
1871.21(21)	0.16 (5)	-	-
1888.74(22)	0.26 (9)	-	-
1940.68(15)	0.29 (6)	0.20 (2)	-
1957.29(15)	1.04 (8)	1.51 (11)	1.6 (3)
1975.91(12)	0.24 (16)	-	-
2022.76(10)	0.21 (5)	0.17 (2)	-
2043.86(10)	0.17 (5)	-	-

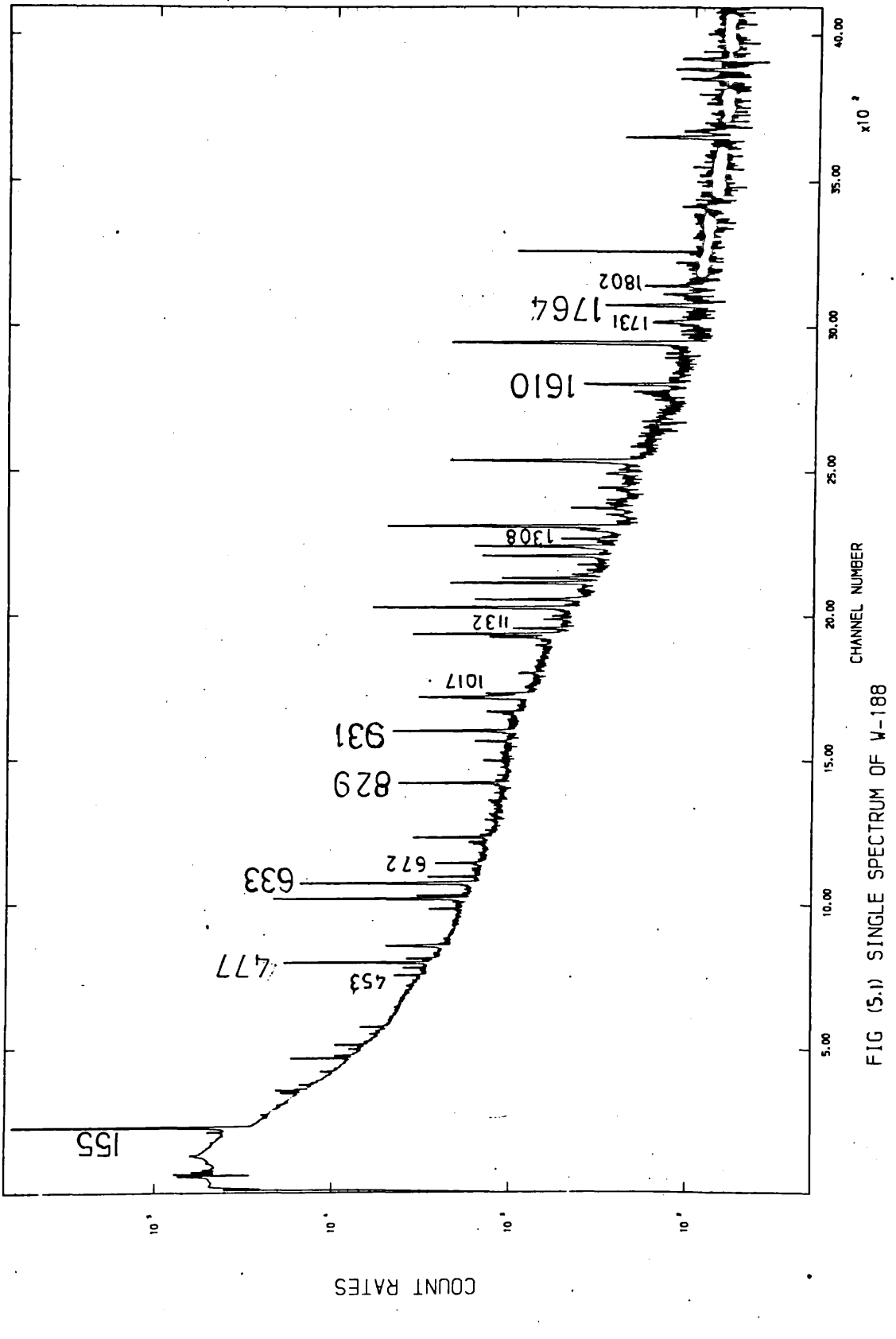

FIG (5.1) SINGLE SPECTRUM OF W-188

radioactivity from the impurity ^{187}W to die away before any singles measurement were taken. Two singles measurement were made within a time interval of two weeks. This step was taken to ensure that the observed γ-rays were the result of ^{188}W decay and not a mixture with ^{187}W decay.

Figure (5.1) shows the single spectrum obtained from the 12 % Ge(Li) detector. It comprises of γ-rays of ^{188}Re and ^{188}Os.

The analyses of singles spectra enabled a total of 59 γ-rays to be identified. Such γ-rays arise from the decay of levels in both the ^{188}Re and ^{188}Os nuclei. The Q_{β^-} value for the decay of ^{188}W to ^{188}Re is 0.349 MeV while Q_{β^-} for ^{188}Re decay to ^{188}Os is 2.119 MeV. Thus γ-rays with energies < 349 keV can either arise from ^{188}Re or ^{188}Os. Ten γ-rays were observed to be within this range. From the coincidence results (see later), three γ-rays were identified as belonging to ^{188}Os and seven to ^{188}Re. The seven energies are 63, 85, 141, 205, 207, 227 and 290 keV. The γ-ray at 205 keV is a newly suggested transition.

The number of γ-rays belonging to the ^{188}Os nucleus is 52. Eleven transitions suggested by Svoren et al. were confirmed at 312, 515, 1070, 1209, 1302, 1305, 1549, 1652, 1807, 1940 and 2023 keV. A total of fourteen γ-rays were identified for the first time in the decay of ^{188}Re to ^{188}Os. The energies are: 650, 785, 1027, 1238, 1355, 1505, 1660, 1711, 1793, 1846, 1871, 1888, 1975 and 2043 keV.

Table (5.1) shows the relative intensities of γ-rays resulting from the β^- decay of ^{188}W. The first seven energies belong to the ^{188}Re nucleus and the remainder belong to the ^{188}Os nucleus. This is the first time that the intensities of γ-rays from both nuclei are combined together with the same normalisation. The intensities are normalised to 100; the intensity of 478 keV in ^{188}Os.

The intensities of the γ-rays are compared with the works of Svoren et al. [147] and Yamazaki and Sato [146]. The

present results are consistent with the results of Svoren et al. [147] for most parts. The only discrepancy observed is for the 825 γ-ray. The present result obtained an intensity of 2.2(4) while Svoren et al. quoted a value of 4.9(5). Although the present value is almost 50 % that of Svoren et al., it is consistent with an intensity of 1.7(6) obtained in the (n,γ) reaction [158]. Furthermore, a value of 3.8(10) obtained by Yamazaki and Sato [146] is only slightly higher.

5.3 Coincidence measurement

The coincidence data were collected on three magnetic tapes using the DPDCS. The analyses were performed offline, as discussed in sections 3.6.2 and 4.3.

In constructing the decay scheme of ^{188}Os, eight energy gates were taken. The energies were 155, 322, 478, (633 + 635), 829, 931, 1132 and (1149 + 1150) keV. Selected in this manner these energy gates are well defined and clear of neighbouring peaks, they form good reasons for their choices.

The gate at 155 keV is important since such a transition depopulates the first excited state of ^{188}Os and most transitions will be in cascade with it, therefore showing up in the coincidence spectra. Furthermore, the 155 keV gate is needed to confirm the existence of a 478 keV level with spin/parity 4^+. This level was suggested for the first time by Ref: [147] to be populated in the β^- decay of ^{188}Re (spin/parity 1^-). The suggestion was based entirely on energy sum considerations.

The 322 keV gate was chosen to confirm the presence of a 790 keV 3^+ member of the γ-band.

The two gates, one at 478 keV and a doublet at (633 + 635) keV, were chosen due to their special interrelationship in the decay scheme. The gate at 478 keV allowed a distinction to be made between transitions which were in coincidence either with the 633 or 635 keV lines, since the standard gate width of about 2 keV would encompass both the 633 and 635 keV peaks.

The 478 keV transition depopulates the same level as that at 633 keV, whereas the 635 keV line is involved in a different cascade. Thus, the coincidence spectra resulting from the 478 keV gate is expected to be similar to the coincidence spectra from the 633 keV gate. By comparing the coincidence results of these two gates the transitions which were in coincidence with either the 633 or 635 keV lines could be identified.

The selection of the 829 keV line as a gate helped to confirm a new level at 1948 keV. A strong coincidence was expected with a transition at 486 keV, previously observed (Ref: [146, 147]) but not placed in the decay scheme.

The gate at 931 keV was needed to confirm a level at 1871 keV. The last two gates, 1132 keV and a doublet (1149 + 1150) keV, were taken to check for the existence of higher energy levels.

The summary of the coincidence results are shown in Table (5.2). The energy gates are shown on the upper row while the entries VS, S and W refer to the degree of coincidence, Very Strong, Strong and Weak respectively as explained in section 3.6.2. The coincidence spectra for all the energy gates are shown in Figures (5.2 - 5.9).

Of the 52 γ-rays observed in the singles spectrum, 38 were seen in the coincidence spectra. The three at 650, 1354 and 1846 keV with intensities 0.047, 0.046 and 0.052 were too weak to show up in the coincidence spectra. The remaining 11 higher energy transitions go directly to the ground state.

5.4 Decay scheme and level properties.

The decay scheme (Figure 5.10) was established on the basis of the coincidence results of eight gates (Table 5.2) and the energy sum relations (Table 5.3). On the left of the Figure 5.10, the energy levels (keV), percentage β^- feeding, log ft values spins and parities are shown. The number at the top of the arrow indicates the energy of the transition.

Table (5.2). Summary of gamma-gamma coincidence results in ^{188}Os.

Transitions Energy (keV)	Gates(keV)							
	155	322	477	633(5)	829	931	1132	1149(50)
154.99	-	VS	VS	S	S	S	S	S
312.22	W	S	-	-	-	-	-	-
322.72	S	-	-	-	-	-	-	-
453.34	-	W	VS	S	-	-	-	-
477.95	VS	-	-	-	VS	-	S	-
485.97	W	W	S	S	S	-	-	-
514.87	-	W	-	W	-	-	-	-
633.01	-	-	-	-	S	-	W	-
635.22	S	-	-	-	-	-	-	S
672.49	S	S	-	VS	-	-	-	-
785.42	-	-	-	-	-	W	-	-
825.44	-	-	W	W	-	-	-	-
829.51	S	S	VS	VS	-	-	-	-
845.20	-	-	W	-	-	-	-	-
868.58	-	-	-	S	-	-	-	-
931.31	VS	-	-	-	-	-	-	-
1017.57	W	-	-	S	-	-	-	-
1027.24	-	-	W	-	-	-	-	-
1070.98	-	-	W	-	-	-	-	-
1132.23	-	-	S	VS	-	-	-	-
1149.62	S	-	-	-	-	-	-	-
1150.76	-	-	-	S	-	-	-	-
1174.35	-	-	S	W	-	-	-	-
1191.83	-	-	S	S	-	-	-	-
1209.72	-	-	S	S	-	-	-	-
1238.51	-	-	W	W	-	-	-	-
1302.42	W	-	-	-	-	-	-	-
1307.99	-	-	VS	VS	-	-	-	-
1323.16	W	-	-	-	-	-	-	-
1505.34	W	-	-	-	-	-	-	-
1549.36	W	-	-	-	-	-	-	-
1610.32	VS	-	-	-	-	-	-	-

— continued —

Transitions Energy (keV)	Gates(keV)							
	155	322	477	633(5)	829	931	1132	1149(50)
1652.81	W	-	-	-	-	-	-	-
1669.84	VS	-	-	-	-	-	-	-
1785.19	VS	-	-	-	-	-	-	-
1793.23	W	-	-	-	-	-	-	-
1802.13	VS	-	-	-	-	-	-	-
1711.19	W	-	-	-	-	-	-	-
1888.74	W	-	-	-	-	-	-	-

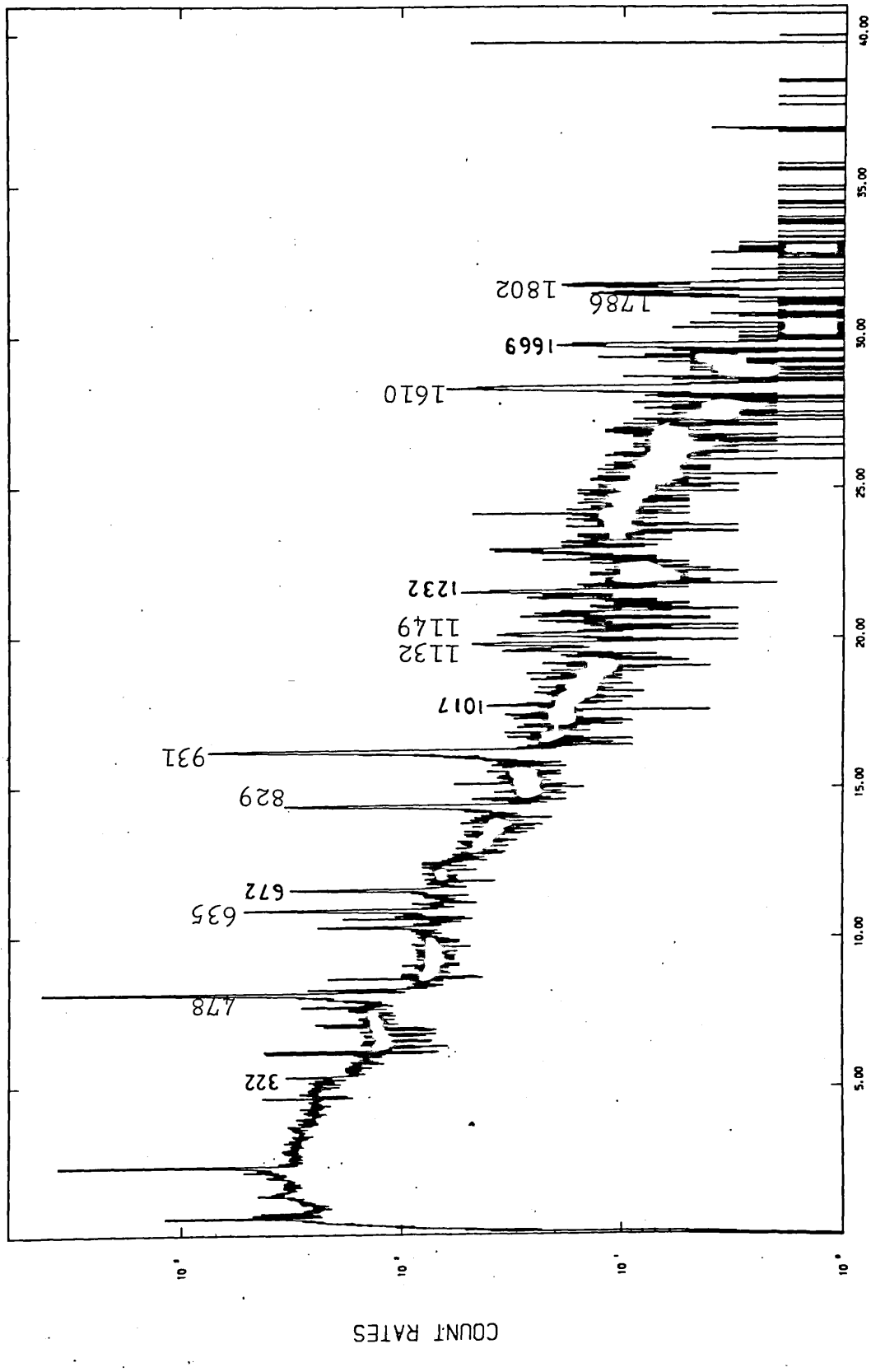

FIG (5.2) 155 KEV IN COINCIDENCE WITH W-188

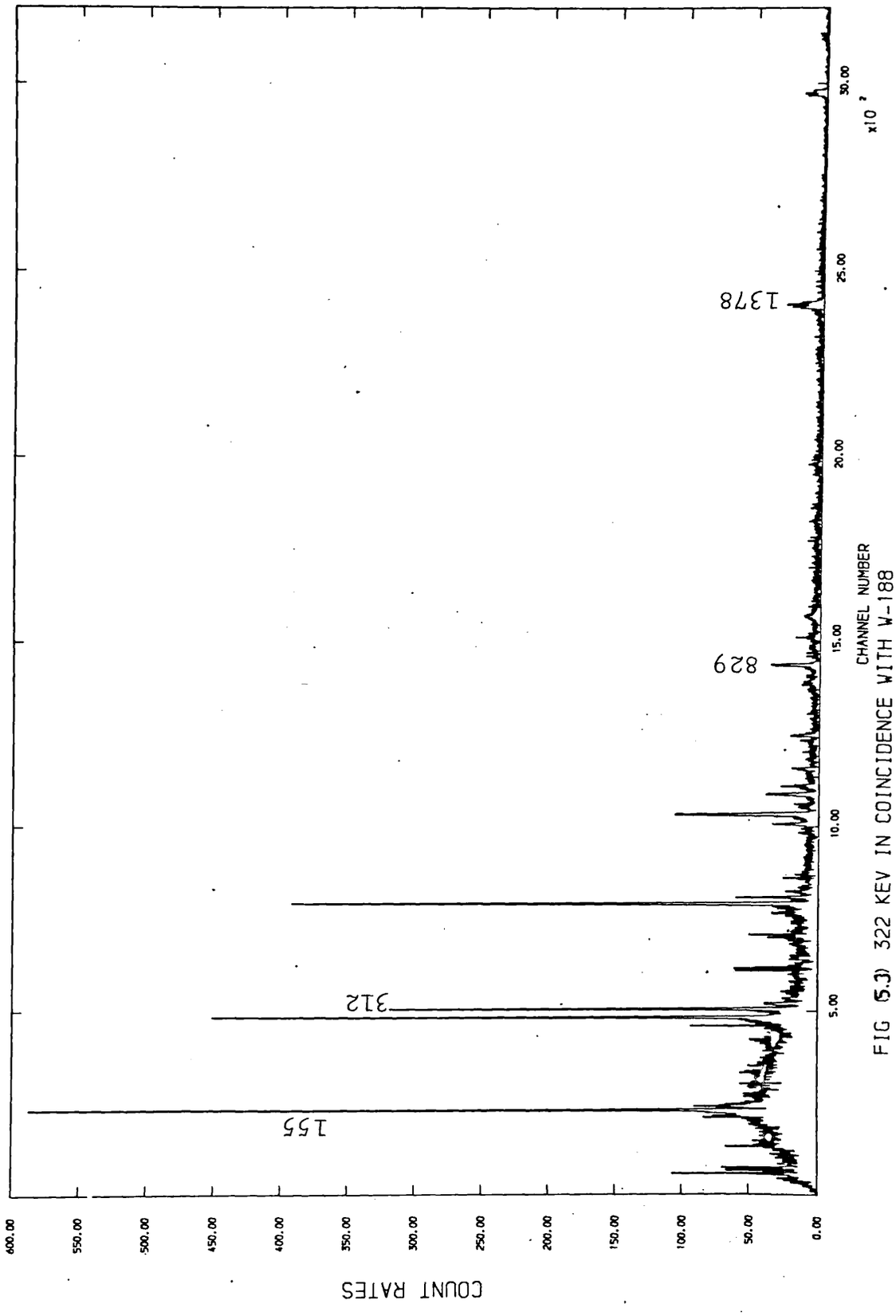

FIG (5.3) 322 KEV IN COINCIDENCE WITH W-188

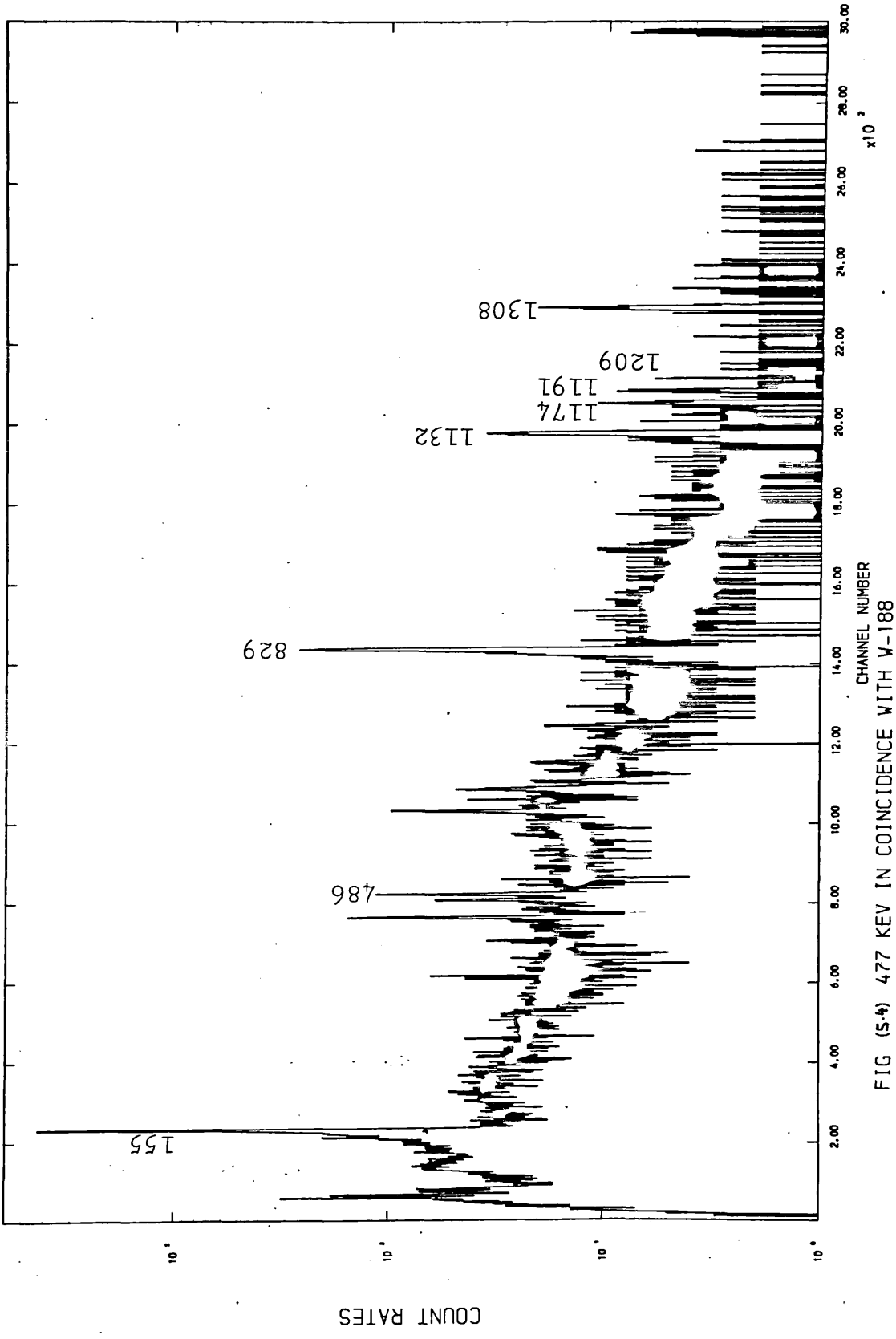

FIG (5.4) 477 KEV IN COINCIDENCE WITH W-188

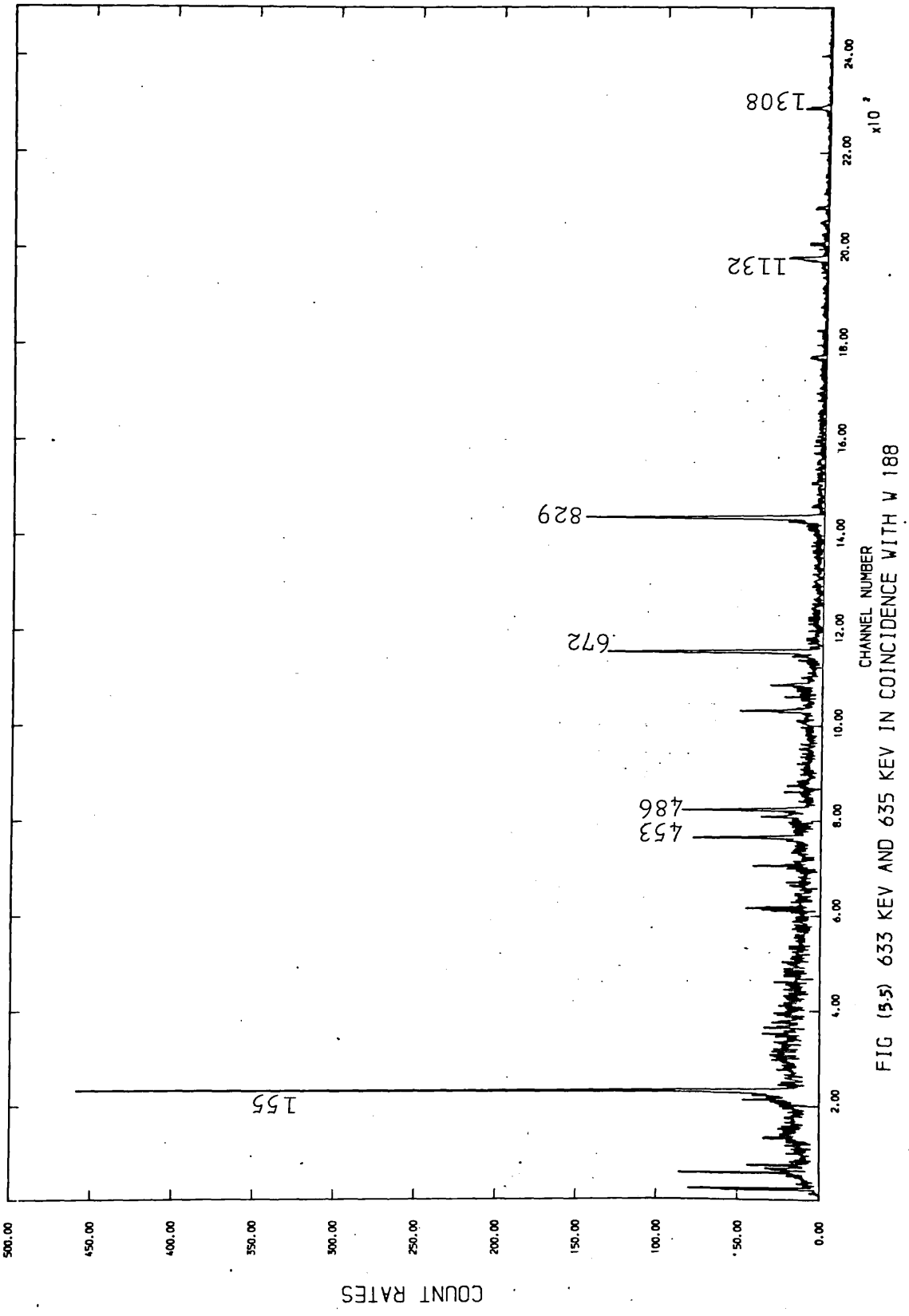

FIG (5.5) 633 KEV AND 635 KEV IN COINCIDENCE WITH W 188

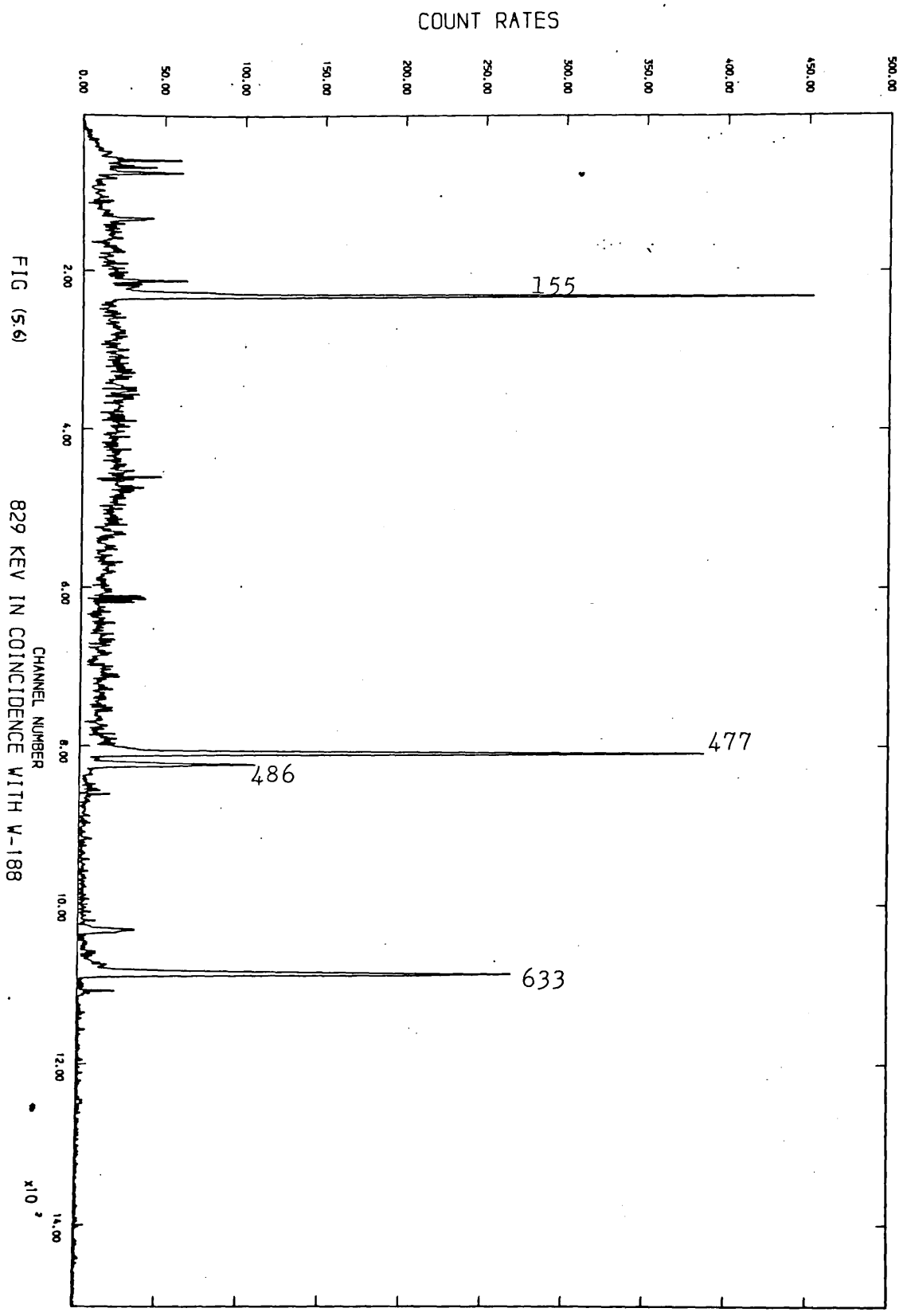

FIG (5.6) 829 KEV IN COINCIDENCE WITH W-188

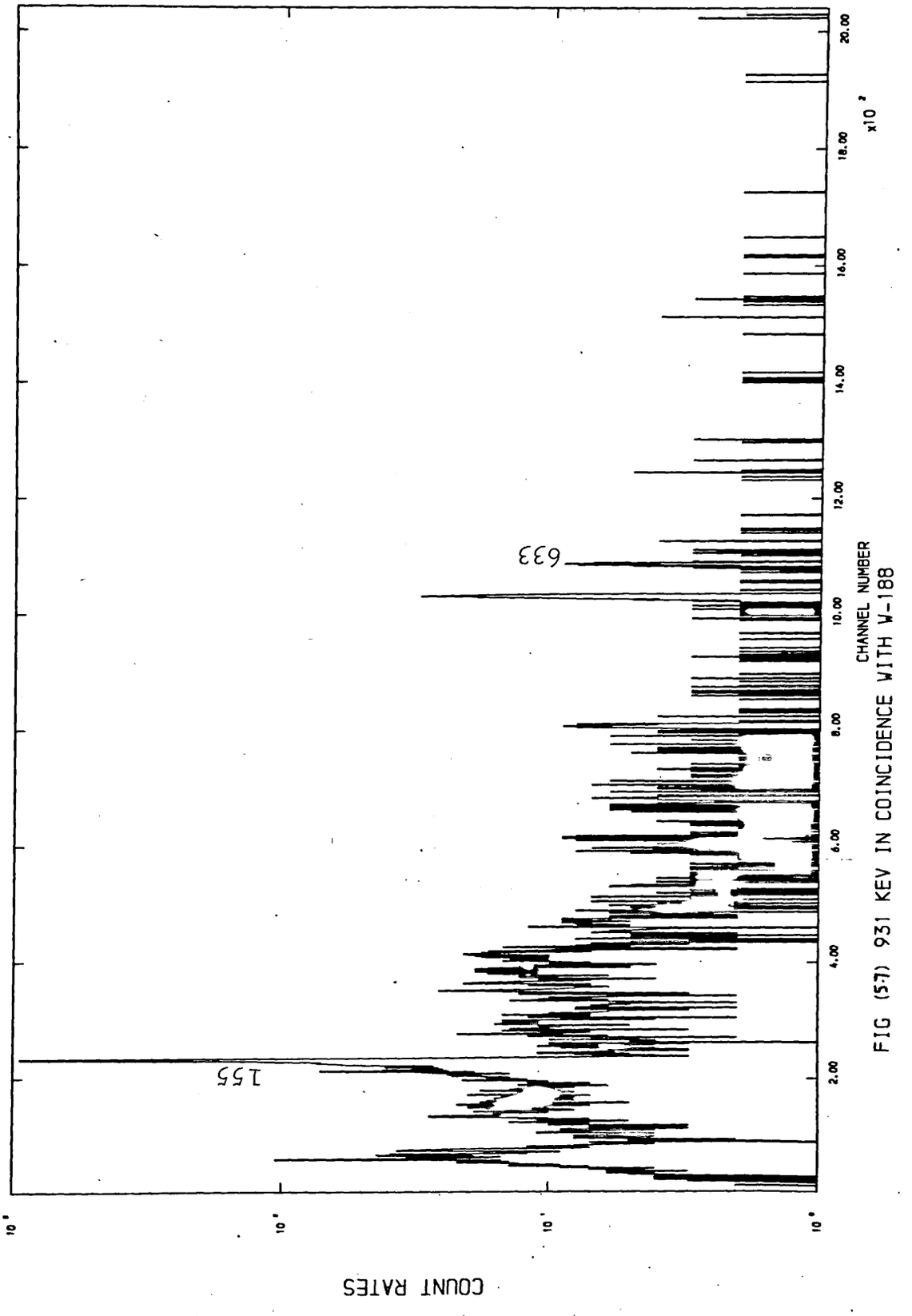

FIG (57) 931 KEV IN COINCIDENCE WITH W-188

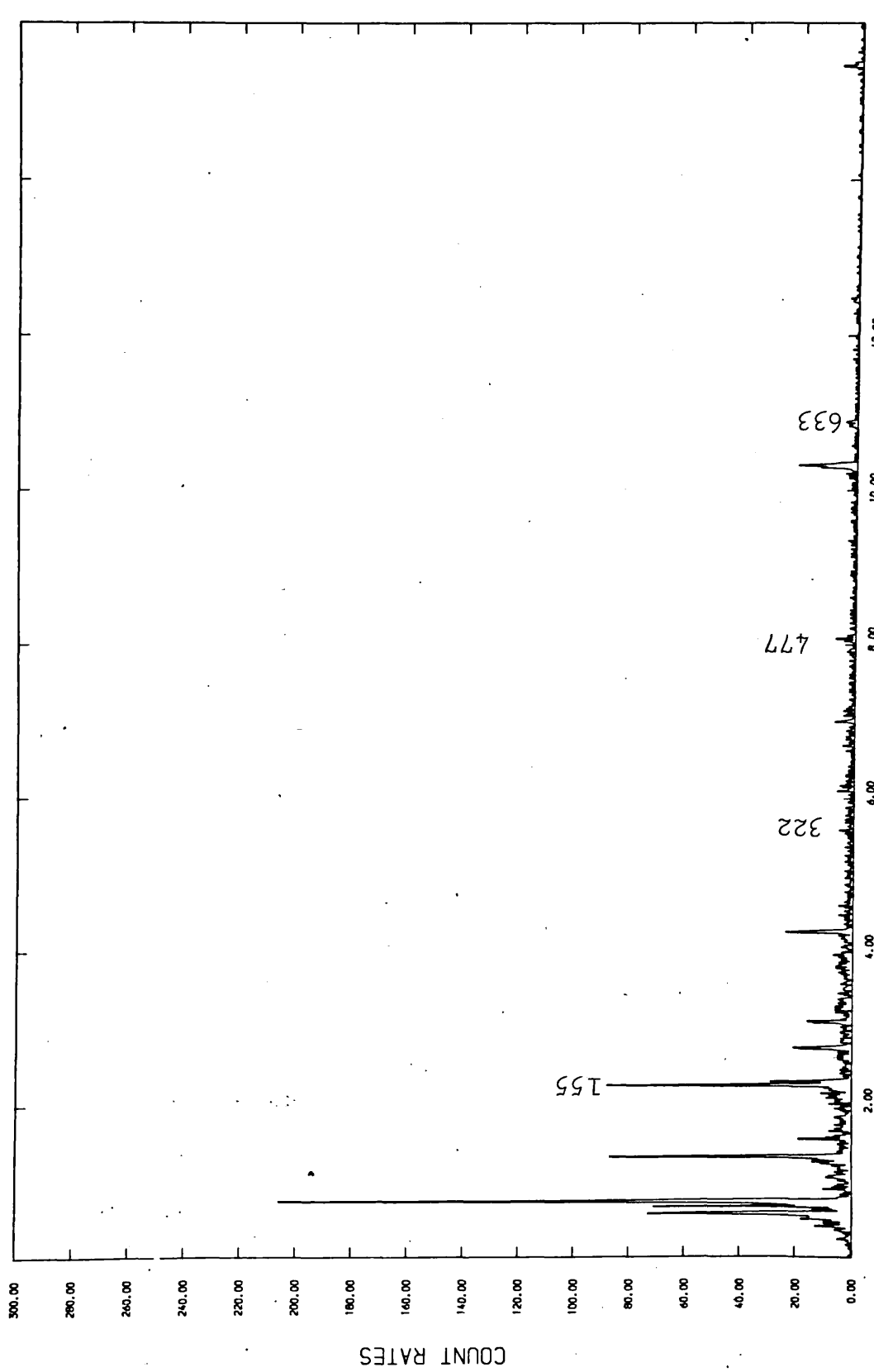

FIG (5-8) 1132 KEV IN COINCIDENCE WITH W-188

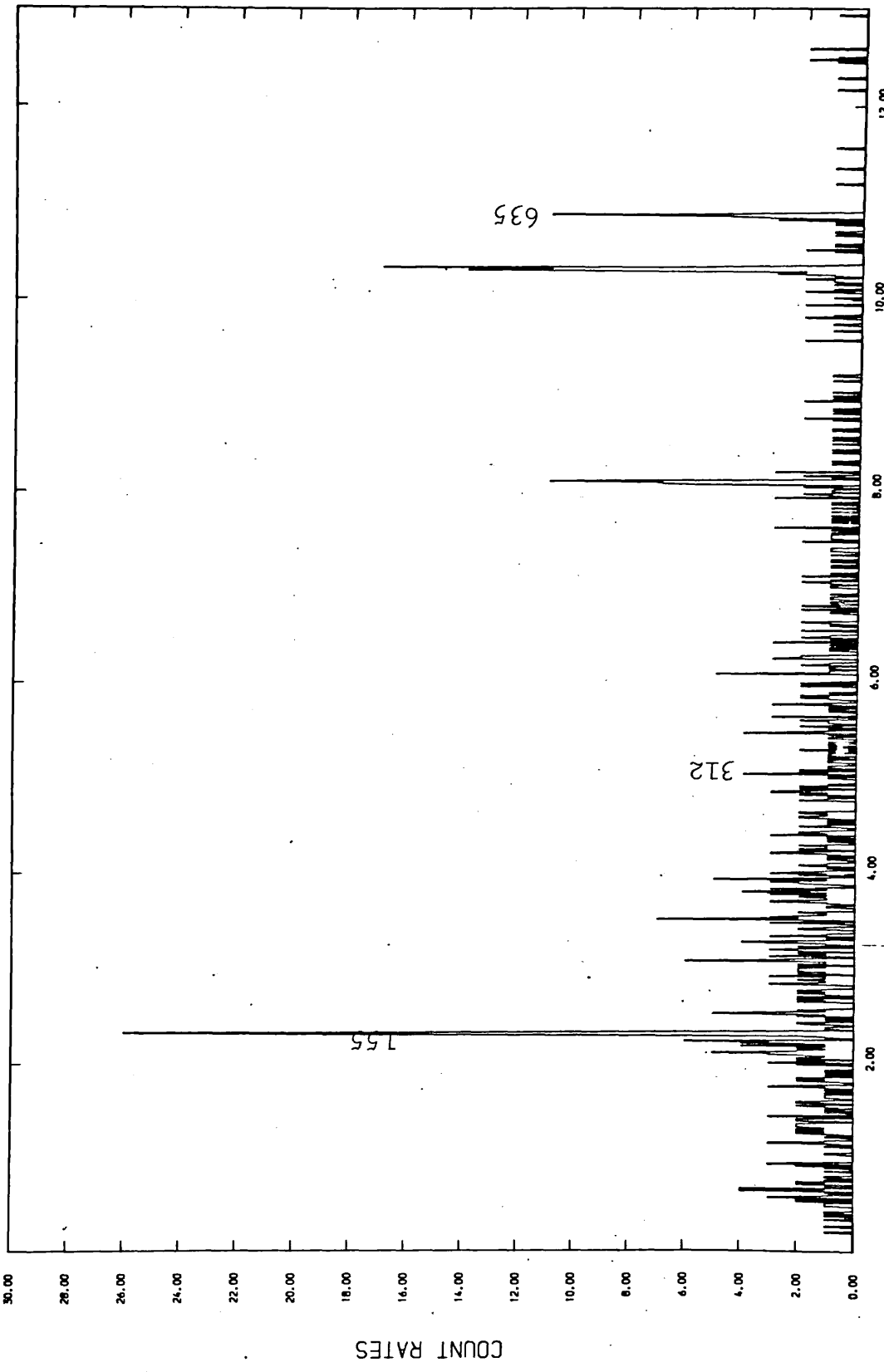

FIG (5·9) 1·149 KEV AND 1150 KEV IN COINCIDENCE WITH W-188

Table (5.3). Summary of energy (keV) sum relations in ^{188}Os nucleus.

Energy of transition (keV)	Sum(keV)	Energy level(keV)
154.99	154.99	154.99
322.72 + 154.99	477.71	477.71
477.95 + 154.99	632.94	632.98
633.01	633.01	
312.22 + 322.72 + 154.99	789.93	790.07
635.22 + 154.99	790.21	
453.34 + 477.95 + 154.99	1086.28	1086.29
931.31 + 154.99	1086.30	
514.87 + 312.22 + 322.72 + 154.99	1304.80	
1149.62 + 154.99	1304.61	1304.79
1304.96	1304.96	
825.44 + 477.95 + 154.99	1458.38	
1302.42 + 154.99	1457.41	1457.78
1457.55	1457.55	
672.59 + 312.22 + 322.72 + 154.99	1462.52	1462.49
829.51 + 477.95 + 154.99	1462.45	
845.20 + 477.95 + 154.99	1478.14	1478.15
1323.16 + 154.99	1478.15	
1027.24 + 477.95 + 154.99	1660.18	
1505.34 + 154.99	1660.33	1660.26
1660.28	1660.28	
1070.98 + 477.95 + 154.99	1765.17	1765.24
1610.32 + 154.99	1765.31	
1017.57 + 312.22 + 322.72 + 154.99	1807.50	
1174.35 + 477.95 + 154.99	1807.29	1807.55
1652.81 + 154.99	1807.80	
1807.61	1807.61	

—— continued ——

Energy of transition (keV)	Sum(keV)	Energy level(keV)
1191.83 + 477.95 + 154.99	1824.77	1824.80
1669.84 + 154.99	1824.33	
1209.72 + 477.95 + 154.99	1842.66	1842.66
1865.20	1865.20	1865.69
1711.19 + 154.99	1866.18	
785.42 + 453.34 + 477.95 + 154.99	1871.70	
1238.51 + 477.95 + 154.99	1871.45	1871.45
1871.21	1871.21	
1150.76 + 312.22 + 322.72 + 154.99	1940.69	
1307.99 + 477.95 + 154.99	1940.93	1940.62
1785.19 + 154.99	1940.18	
1940.68	1940.68	
485.97 + 672.59 + 312.22 + 322.72 + 154.99	1948.49	1948.36
1793.23 + 154.99	1948.22	
1802.13 + 154.99	1957.12	1957.21
1957.29	1957.21	
1975.91	1975.91	1975.91
2022.76	2022.76	2022.76
1888.74 + 154.99	2043.73	2043.79
2043.86	2043.86	

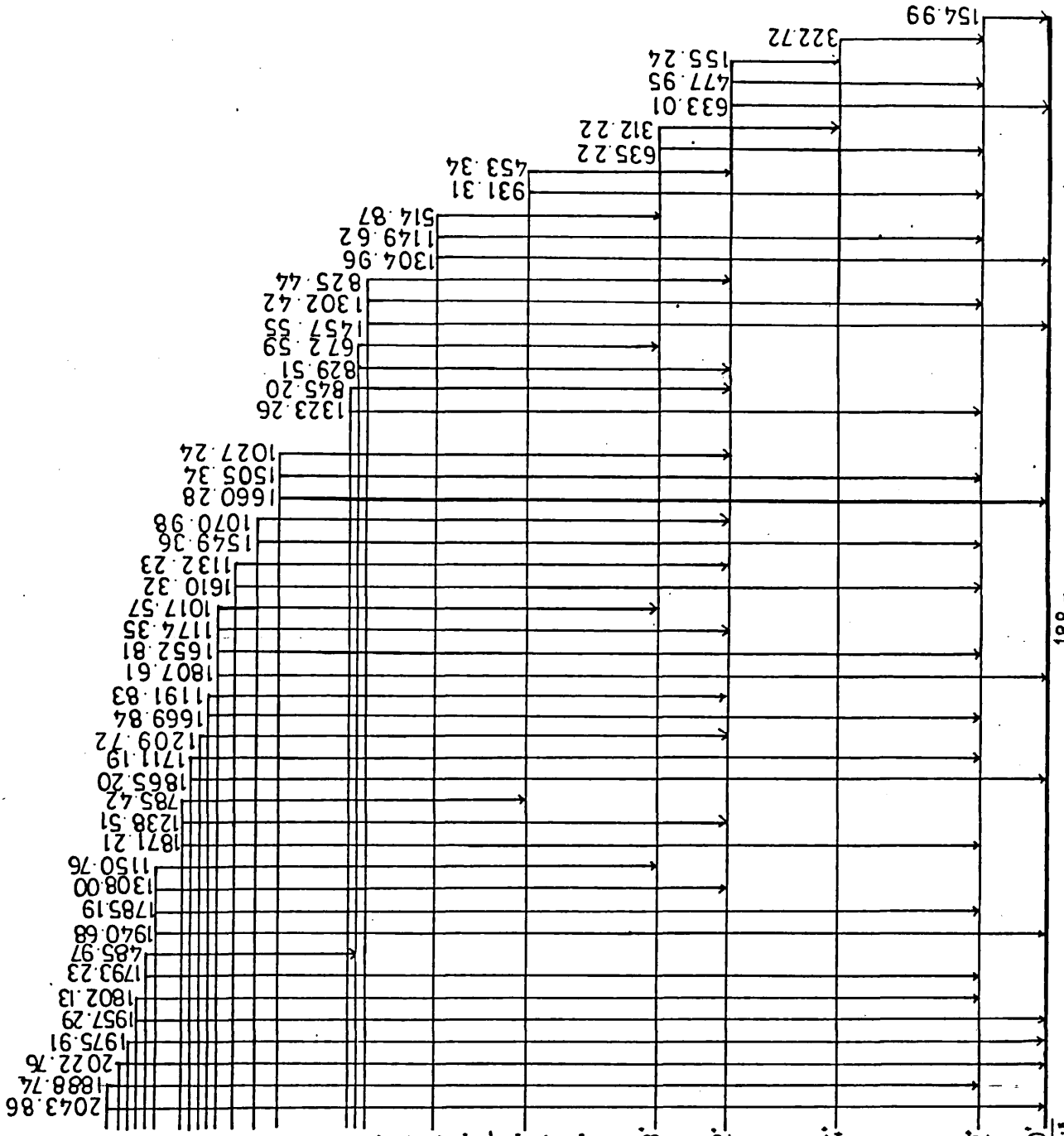

Figure (5.10) Decay scheme of ^{188}Os.

Table 5.4 shows the Branching ratios (B.R's), the log ft values for the β^- decay of ^{188}Re and the deduced spins and parities. The B.R's were calculated from the total intensity balance between the intensity of the decay and feeding γ-rays for each level. The B.R. to the ground state was taken to be (70.8 ± 0.2) %, an average between the values of Svoren et al. [147] and Singh and Viggar [158].

The log ft values were calculated according to the relations given in Ref: [106], the end point energies of the β^- decay were calculated using the Q_{β^-} (max.) of 2.119 MeV [159,160]. The deduced spins/parities were worked out according to the β^- decay selection rules (Table 1.1).

It is reasonable to assume that there is no β^- feeding to the 478 keV level, with spin/parity 4^+, from 1^- ^{188}Re parent. In order to establish a zero B.R. it is implied that the total γ-intensity populating the level is at least equal to the depopulating γ-intensity. The only γ-transition observed in this level is that at 312 keV, with a relative intensity of 0.41. However, the depopulating transition at 322 keV has a relative intensity of 1.74, greater than the populating intensity. To be consistent with no β^- feeding of the 478 (4^+) keV level, an additional transition with a relative intensity of at least 1.33 should populate this level. One possibility is that a transition at 155.24 keV occurs between the 633 keV level and that at 478 keV. Such a transition would be a doublet with the intense 154.99 keV line (energy difference only 0.25 keV). The present work suggests that 0.73 % of the total γ-intensity of a doublet 155 keV transition would populate the 478 keV level.

Table (5.5) shows experimental and theoretical K-shell conversion coefficients (α_K) for β^- decay of ^{188}Re. The β^- electron intensities were taken from Ref: [158] and the relative intensities of the γ-transitions were taken from singles measurements reported in the present work (Table 5.1). The experimental α_K were deduced using equation (1.16). The theoretical α_K were taken from Ref: [110]. The multipolarity of the energy transitions, given in the last column of Table

Table (5.4). Summary of the level properties in ^{188}Os.

Energy Level (keV)	E_{β^-} (keV)	ΣI_γ feed	ΣI_γ decay	B.R.* %	log ft	deduced J
154.99	1964.71	189.26	2638.66	25.82	8.43	2
477.71	1641.99	1.75	1.74	-	-	4
632.94	1486.76	69.22	223.72	1.63	9.17	2
790.07	1329.63	14.12	14.11	-	-	3
1086.29	1033.41	0.58	62.26	0.65	9.00	0
1304.79	814.91	-	2.65	0.0279	10.01	2
1457.78	661.92	-	4.70	0.0495	9.47	2
1462.49	657.21	8.00	50.72	0.45	8.51	2
1478.15	641.55	-	1.63	0.017	9.88	0
1660.26	459.44	-	1.23	0.013	9.53	2
1704.24	415.46	-	0.25	0.0026	10.09	0
1765.24	354.46	-	16.56	0.17	8.07	0
1807.55	312.15	-	6.86	0.072	8.26	2
1824.80	294.90	-	1.85	0.019	8.70	0
1842.66	277.04	-	0.30	0.0032	9.44	2
1871.45	248.25	-	0.94	0.0099	8.25	2
1940.62	179.08	-	9.82	0.10	7.25	2
1948.36	171.34	-	8.06	0.08	7.27	2
1957.21	162.49	-	4.63	0.048	7.45	2
1975.91	143.79	-	0.24	0.0025	8.55	2
2022.76	96.94	-	0.21	0.0022	7.95	2
2043.79	75.91	-	0.44	0.0046	7.16	2
1865.69	254.00	-	0.71	0.0075	9.06	2

* B.R. of Ground state assumed 70.8% an average between the works of Svoren et al. (1975) and Singh et al. (1981).

Table (5.5). Comparison between experimental and theoretical α_k conversion coefficients. (Uncertainties are given in parentheses). The deduced multipolarities are shown in the last column.

Energy (keV)	α_k X 10^{-3} Theory E1	Theory E2	Theory M1	Exp	Mult.
155	100	290	1310	323 (29)	E2
312	17.80	54	190	43 (10)	E2
322	16.70	49	175	46 (4)	E2
453	7.60	22	74	19.4(14)	E2
477	6.90	19	64	23 (6)	E2/M1
515	5.90	16.7	53	14.5(10)	E2
633	3.90	10.5	31	12.8(2)	E2
635	3.90	10.5	31	13.2(8)	E2
672	3.50	9.1	27	3.4(2)	E1
825	2.36	5.9	16	23.7(38)	E0/M1/E2
829	2.35	5.9	16	2.2(1)	E1(+M2)
845	2.27	5.7	15	6.8(10)	E2
931	1.90	4.9	11.8	4.6(1)	E2
1017	1.58	3.9	9.0	9.4(14)	M1
1070	1.44	3.6	8.2	4.8(12)	E2
1132	1.30	3.0	7.1	3.2(2)	E2
1149	1.28	3.1	6.8	5.4(13)	M1/E2
1150	1.28	3.1	6.3	5.4(13)	M1/E2
1174	1.24	3.0	6.8	6.5(4)	M1(+E2)
1191	1.20	2.9	6.3	3.8(2)	E2
1209	1.17	2.8	6.0	5.0(6)	M1/E2
1305	1.04	2.5	4.9	2.8(6)	E2
1308	1.03	2.5	4.9	4.8(4)	M1
1323	1.00	2.4	4.8	1.9(3)	E2
1457	0.85	1.9	3.9	2.1(3)	E2(+M1)

(5.5), were deduced from the comparison of experimental and theoretical α_K values.

Yamazaki and Sato [146], from studies of the ^{188}Re decay, included energies at 641, 795, 880, 965, 1170 and 1230 keV in their decay scheme. Two of these were not observed in the present work and four were identified as background: 641 from ^{80}Br, 795 from ^{134}Cs, 880 from ^{185}Os and 1230 from ^{182}Ta. From the eleven new transitions suggested by Svoren et al. [147] only nine were observed. The gamma ray at 810 keV was observed but was attributed to the radiative background from ^{58}Co. The non observance of the 624 keV transition in the present work eliminates the possibility of a level at 1414 keV being populated by β^- feeding. Such a level was observed in the $(\alpha, 2n\gamma)$ reaction studies [131] and was even suggested for the first time to be populated in the ^{188}Re decay [147]. To be consistent Yates et al. [131] assigned to that 1414 keV level a spin/parity of 3^-, which is however, unlikely to be populated in the β^- decay of 1^- ^{188}Re.

A strong coincidence of the 322 keV transition with the 155 keV gate supports the suggestion of a level at 478 keV. Furthermore, a strong coincidence of the 312 keV transition with the 322 keV gate confirms the presence of a 790 keV level.

Present results pertaining to previously reported levels at 1458, 1463, 1808, 1825, 1941, 1957 and 2023 keV agree for the most part with those in Ref: [158].

The level at 1458 keV is established from a strong coincidence of the 825 keV transition with two gates; 478 and (633 + 635) keV. Further support for this level is given from the coincidence of 1302 keV transition with the first excited state (155 keV gate). The E0 + M1 + E2 admixtures of the 825 keV transition, which populates the 2^+ state at 633 keV, suggests spin/parity 2^+ for the 1458 keV level. The log ft value of 9.47 obtained from the B.R. supports this spin/parity assignment.

A very strong coincidence of the 829 keV transition

with both gates at 478 and (633 + 635) keV has led to the establishment of a level at 1462 keV. The results of both coincidences suggest that the transition 829 keV feeds the 633 keV level directly. From an energy sum relation this gives a value of 1462 keV. The E1(+M2) character of the 829 keV transition indicates that the parity of this level is negative with spin of either 1, 2 or 3. The observed transition from this level to 3^+ state at 790 keV excludes the possible spin/parity 1^- and 3^-, thus leaving 2^- as the only candidate. The low log ft value of 8.51 supports 2^- assignment to this level.

The presence of the 1808 keV level is strongly supported by the coincidence results of γ-transitions at 1652, 1174 and 1017 keV. These transitions are observed in coincidence with the energy gates at 155, 478 and (633 + 635) keV respectively. The M1(+E2) multipolarity of the 1174 keV, which populates the 2^+ state, suggests the possible spin/parity of 1^+, 2^+ or 3^+ for the 1808 keV level. The direct decay to the ground state rules out the possibility of 3^+ spin/parity. The log ft value of 8.26 obtained for the level prefer a 2^+ assignment.

The 1825 keV level is established from a strong coincidence of 1669 keV transition with the 155 keV gate. This is further supported by the coincidence of 1191 keV with two gates, one at 478 keV and the other is a doublet gate at (633 + 635) keV. The E2 character of the 1191 keV suggests the possible spin/parity of $0^+ \rightarrow 4^+$. Transitions 1191 and 1669 keV are the only two transitions observed to depopulate the 1825 keV level. These transitions feed the states 2_2^+ and 2_1^+ respectively. The decay mode of 0^+ states in transitional nuclei favour the population of 2_2^+ and 2_1^+ states. This led to the suggestion that 1825 keV has a spin/parity of 0^+.

The level at 1941 keV is established from the strong coincidence of 1308 keV transition with the gates at 478 and (633 + 635) keV. Further evidence is given by the observed coincidence of 1150 keV with only the doublet gate (633 + 635) keV and not with the 478 keV. This means that the transition is in direct cascade with the 635 keV gate and not with the

633 keV. Since 635 keV depopulates the level at 790 keV therefore the sum of 1150 and 790 keV results in a level at 1941 keV. The M1 multipolarity of the 1308 keV suggests the level to have spin/parity of 2^+.

The observed strong coincidence of 1802 keV transition with the 155 keV gate results in the establishment of the 1957 keV level. The presence of 1957 keV γ-ray in the singles gives a further support for the existence of this level. The suggested spin/parity is 2^+.

The present experimental evidence relating to the 2023 keV level is now conclusive. The transition at 1865 keV was observed in the ^{188}Re decay by both Yamazaki and Sato [146] and Svoren et al. [147]. They suggested that this transition depopulates the level at 2123 keV, although energetically the sum of 1865 keV and 155 keV differ by 1.6 keV from 2023 keV. The present accurate energy measurements indicate that energetically the 1865 keV transition does not fit between the 2023 and 155 keV levels. The difference is ~2.6 keV. Since the Q_{β^-} (max.) of ^{188}Re is 2119 keV, the 2023 keV transition can only be associated with the depopulation of a 2023 keV level.

Similarly, as no coincidences were observed with the 1865 keV transition it can only be associated with the depopulation of a 1865 keV level. In the present work, evidence has been collected to suggest a level at 1865 keV. The observation of a transition at 1711 keV, which energetically fits the levels at 1865 and 155 keV, constitutes further evidence for the presence of a level at 1865 keV. Furthermore, from the coincidence work, a weak coincidence of the 1711 keV line with the 155 keV gate supports this suggestion.

The present work has confirmed the presence of two 0^+ states and one 2^+ states populated in ^{188}Re decay, as was firstly suggested by Svoren et al. [147] based on energy sum relation only. The two 0^+ states are 1478 and 1705 keV, while the 2^+ state is at 1842 keV. The strong coincidence of 845, 1071 and 1209 keV transitions with both gates at 478 keV and (633 + 635) keV support the evidence of the levels at 1478,

1705 and 1842 keV respectively. The log ft value of 9.4 for the 1842 level supports the assignment of spin/parity 2^+.

A total of four new levels are suggested in the present work.

A new level at 1660 keV is suggested due to the observation of three transitions at 1660, 1505 and 1027 keV. A weak coincidence of the 1027 keV transition with the 478 keV gate supports the suggestion for the level at 1660 keV. The direct decay to the ground state favours a 2^+ spin/parity assignment to this level. This is in agreement with the log ft value of 9.53.

A new level at 1948 keV is proposed due to the strong coincidence of the 486 keV transition with the 931 keV gate. This transition at 486 keV was observed both by Yamazaki and Sato [146] and Svoren et al. [147], but could not be placed in the decay scheme. The present coincidence work has for the first time been able to place the transition in the decay scheme. The observation of a new transition at 1793 keV further supports the evidence for a level at 1948 keV. It connects the new level with the first excited state.

The level at 1871 keV is suggested as a consequence of observing three transitions at energies 785, 1238 and 1871 keV. The coincidence results of the transitions 785 and 1238 keV with the 931 and 478 keV gates respectively support this suggestion. The direct decay to the ground state favours a spin/parity of 2^+. This is consistent with the log ft value of 8.3.

The level at 2043 keV is suggested due to the observation of two transitions at 2043 and 1888 keV. Since the Q_β-(max.) of ^{188}Re is 2119 keV, the 2043 keV line can only be associated with the depopulation of a 2043 keV level. The transition at 1888 keV fits energetically between this 2043 keV level and the first excited state at 155 keV. The coincidence result of the 155 keV gate reveal a weak coincidence with the 1888 keV transition. From these facts it is believed

that the 1888 keV transition depopulates the level at 2043 keV. The direct ground state decay favours a 2^+ spin/parity assignment.

5.5 Discussion.

In the framework of the interacting boson model, ^{188}Os has been suggested to lie within the region of the pure O(6) limit, exhibited by ^{194}Pt, and the SU(3) limit of ^{186}Os The presence of five 0^+ states and thirteen 2^+ states with energies less than 2 MeV indicate predominant O(6) characteristics, and therefore the appropriate Hamiltonian would be that of an O(6) limit.

$$H[O(6)] = PAIR(\underset{\sim}{P}.\underset{\sim}{P}) + \frac{ELL}{2}(\underset{\sim}{L}.\underset{\sim}{L}) - 10\sqrt{7}\,\frac{OCT}{2}(\underset{\sim}{T}_3.\underset{\sim}{T}_3) \qquad (5.1)$$

where the analytical solution was given by equation (2.50). From the eigensolution of the H[O(6)], each level can be identified by three quantum numbers (σ, τ, ν_Δ) as defined previously by equations (2.45 - 2.47). The levels fall into groups characterised by a σ value. Energy spacings and level spins are repeated for each group but with different cut-offs given by $\tau=\sigma$. The quantum number ν_Δ further subdivides levels of the same σ.

The boson number in ^{188}Os is 10 which allows the values of σ to be 10, 8 .... and 0. Within the group $\sigma=10$, the values of τ ranges from 0, 1, 2 .... to 10 and ν_Δ=0, 1, 2 and 3. Similarly in the group $\sigma=8$ the cut-off value of τ is 8 and ν_Δ can only have values 0, 1 and 2.

Figure (5.11) shows the theoretical O(6) levels for $\sigma=10$ and $\sigma=8$ groups. For the purpose of simplicity only the lower levels with spins 0^+, 2^+, 3^+, 4^+ and 6^+ are included. The energy unit is arbitrary. A characteristic feature of the levels is therefore a recurring 0^+-2^+-2^+ pattern.

The symmetry of the O(6) limit may be broken by the

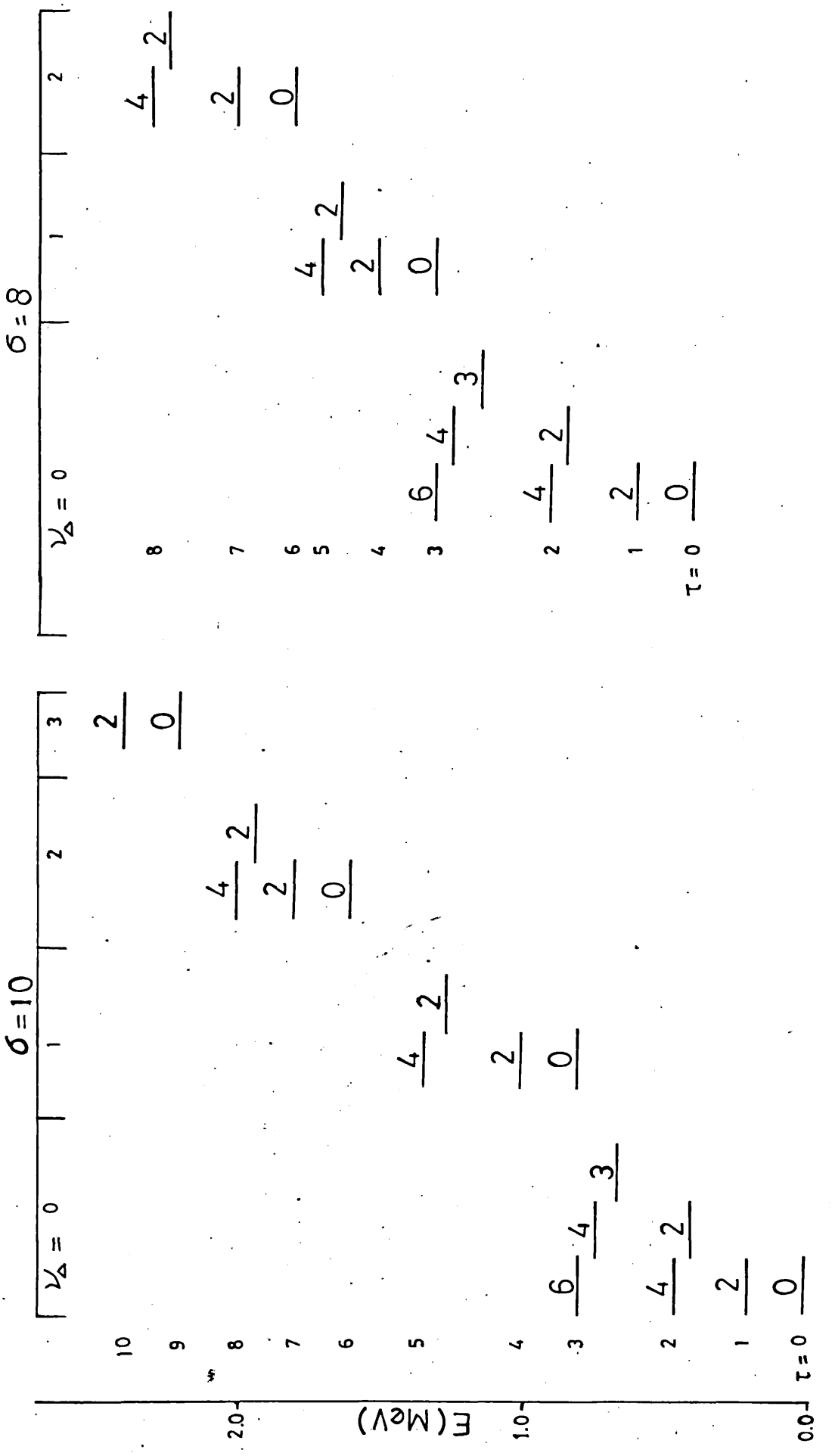

Figure (5.11) Theoretical O(6) level spectrum for N=10.

inclusion of the $\underset{\sim}{Q}.\underset{\sim}{Q}$ interaction term. This quadrupole-quadrupole force is responsible for the occurrence of spectra with SU(3) symmetry and therefore by increasing its strength one can study the transition from O(6) towards the SU(3) limit. The effect of this $\underset{\sim}{Q}.\underset{\sim}{Q}$ perturbation on the O(6) spectrum is that 2_2^+ states will be pushed towards the 4_1^+ states and will come closer to the 3_1^+ state to start to form a rotational gamma band.

The symmetry of the O(6) limit can also be perturbed by the $\underset{\sim}{T}_4.\underset{\sim}{T}_4$ term which describes the coupling of two d-bosons to have total angular momentum of 4. This term affects the position of the 0^+ states. In the unbroken O(6) symmetry the position of these 0^+ states are governed by the pairing term $\underset{\sim}{P}.\underset{\sim}{P}$.

In the present IBA calculations the terms $\underset{\sim}{Q}.\underset{\sim}{Q}$ and $T_4.T_4$ were included in the Hamiltonian 5.1. The program PHINT was used to diagonalise the Hamiltonian to obtain the energies of the positive parity states. Table (5.6) shows the values of the parameters giving the best estimates of the energy level values. The high pairing term expressed by PAIR designates the dominant O(6) characteristic while a relatively high QQ value ($\simeq$ 40 % of PAIR) suggests that the quadrupole-quadrupole interaction in ^{188}Os is considerable. The hexadecupole interaction is small approximately 25 % of the pairing force while the octupole force is even smaller ($\sim$ 2 % of the pairing term). The latter force only affects the higher energy levels where the values of τ are higher.

The energy levels obtained from the best fits are shown in Figure (5.12). The spins are labelled on top of the level while in the parentheses are the O(6) quantum numbers $(\sigma, \tau, \nu_\Delta)$.

The remainder of this section will be used to discuss the positive parity states which are grouped according to 0^+ 2^+ 2^+ sequences in order to exhibit their peculiar O(6) characteristics. This grouping does not include the GSB and γ-band, which will also be discussed. There is only one

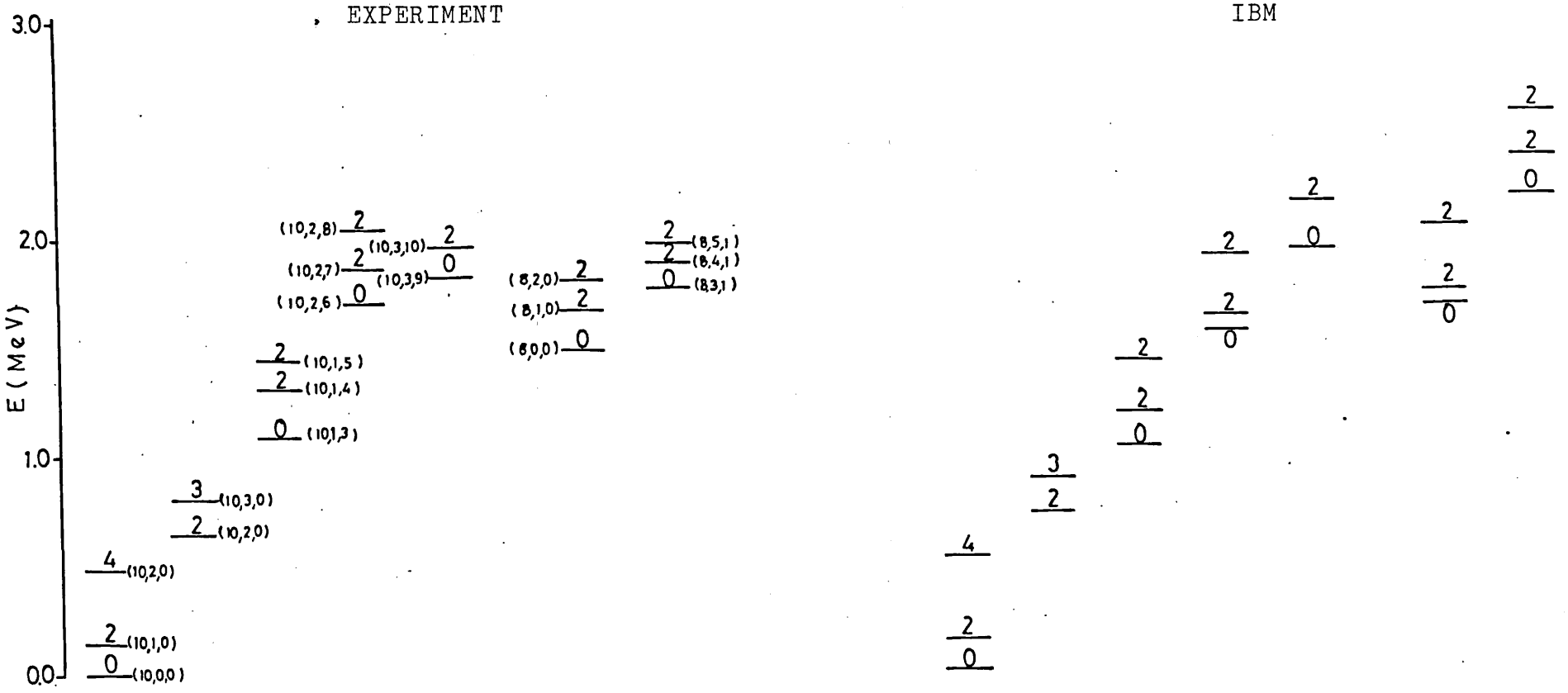

Figure (5.12) The experimentally determined positive parity levels for ^{188}Os compared with IBM calculations. The spin is shown on top of the level and the quantum numbers (σ, τ, ν_Δ) are given in parentheses.

Table (5.6). Parameters(MeV) used in program PHINT to calculate positive parity levels.

Parameters	PAIR	ELL	QQ	OCT	HEX
	0.058	0.035	-0.0225	0.001	-0.015

Table (5.7). Parameters obtained for T(E2) operator in program FBEM to calculate absolute B(E2) values and ratios.

Parameters	E2SD	E2DD
	0.3133	-0.008

Table (5.8). Experimental absolute B(E2) values (e^2b^2 units) in comparison with IBM predictions.

$I_i \rightarrow I_f$	Experimental*	IBM
$2_1 \rightarrow 0_1$	2.75 (10)	1.79
$2_2 \rightarrow 0_1$	0.261(022)	0.100
$2_2 \rightarrow 2_1$	0.157(010)	0.159
$4_1 \rightarrow 2_1$	1.45 (09)	2.49

* Kumar and Baranger (1968)[57]

negative parity state which has been observed from the β^- decay of ^{188}Re.

Ground State Band (GSB).

This band consists of two levels observed at 155(2^+) and 478(4^+) keV. The occurrence of the 4^+ level in the β^- decay of ^{188}Re was first suggested by Svoren et al. [147] and is confirmed in the present coincidence measurement. The IBM predicts the 2^+ level at 154.9 keV and the 4^+ level at 514.9 keV.

The absolute B(E2) values for $2_1^+ \rightarrow 0_1^+$ and $4_1^+ \rightarrow 2_1^+$ transitions were calculated from FBEM. For a pure O(6) nucleus, the parameter E2DD of equation (2.21) is zero [162]. The value of the E2SD parameter was initialised from equation (2.48) by normalising to the experimental absolute B(E2) value for the $2_1^+ - 0_1^+$ transition. Table (5.7) shows the values of the parameters E2SD and E2DD, obtained in the present calculation. The near-zero value of -0.008 for E2DD suggests that the ^{188}Os nucleus is more of an O(6) type than SU(3). The absolute B(E2) values calculated are shown in Table (5.8). The values for the $2_1^+ \rightarrow 0_1^+$ and the $4_1^+ \rightarrow 2_1^+$ transitions are 1.79 and

Table (5.9). Experimental positive parity levels(keV) compared with theoretical predictions.

J	Energy (keV)			
	Exp	IBM *	BET	PPQM
2	155.0	154.9	156.0	178.0
4	477.7	514.9	468.0	474.0
2	632.9	734.0	666.0	600.0
3	790.1	884.8	853.0	874.0
0	1086.3	1019.6	734.0	836.0
2	1304.8	1162.6	1011.0	1131.0
2	1457.8	1413.4	1243.0	-
0	1478.2	1675.9	1215.0	-
2	1660.3	1680.2	-	-
0	1704.2	1527.6	1825.0	-
0	1765.2	2166.2	2497.0	-
2	1807.6	2020.6	1429.0	-
0	1824.8	1917.0	-	-
2	1865.2	1592.4	-	-
2	1871.5	2336.8	-	-
2	1940.6	2561.1	-	-
2	1957.2	2167.2	-	-
2	2021.5	2783.7	-	-
2	2043.8	1888.0	-	-

BET Weeks and Tamura (1980)[133]

PPQM Kumar and Baranger (1968)[57]

* Present calculation.

2.49 e^2b^2 respectively, far from the experimental values of 2.75 ± 0.10 and 1.45 ± 0.09.

Gamma band ($K^\pi = 2^+$).

The 2^+ and 3^+ levels at 633 and 790 keV are bandhead and first excited member of the $K^\pi = 2^+$ band. In terms of the O(6) quantum numbers the 2^+ and 3^+ states can be classified as (10, 2, 0) and (10, 3, 0) respectively. The IBM predictions for these levels are higher than that of BET and PPQM.

From the E2 selection rules of the O(6) limit [162] the 2^+ level is expected to decay predominantly to the first excited 2^+ (10, 1, 0) rather than to the 0^+ (10, 0, 0) ground state as is clearly found experimentally (fifth column of Table: 5.10) and confirmed by the theories of columns six and seven. Similarly, the 3^+ (10, 3, 0) state should decay mostly to the 4^+ (10, 2, 0) state rather than to 2^+ (10, 1, 0) state, which however is not clear experimentally, and predicted to be opposite by IBM, although substantiated by the PPQM. The absolute B(E2) value for the $2_2^+ \rightarrow 2_1^+$ transition predicted by the IBM is 0.159 e^2b^2, in good agreement with the experimental value of 0.157 (090). The PPQM predicted the value to be 0.403, a factor of 2.6 higher. For the $2_2^+ \rightarrow 0_1^+$ transition the experimental value of 0.261 ± 0.022 is nearer to the 0.184 predicted by the PPQM than the IBM at 0.100.

The collective $K^\pi = 2^+$ states are interpreted as the γ-vibrational states of the Bohr-Mottelson model, while the asymmetric rotor model (ARM) [163] regards this band as an anomalous rotational band which is generated by rotational motion along the near-symmetrical axis of an asymmetric model.

The Bohr-Mottelson (BM) calculations [164] predict the ratio $R_1 = B(E2; 3_1^+ \rightarrow 4_1^+)/B(E2; 3_1^+ \rightarrow 2_1^+)$ to be equal to 1.45 and the ratio $R_2 = B(E2; 2_2^+ \rightarrow 0_1^+)/B(E2; 2_2^+ \rightarrow 2_1^+)$ to equal 2.8. The calculation of Davydov and Rostovsky [165] based on ARM predicts the ratios to be 2.8 and 4.5 respectively. The IBM predictions give the values of 0.54 and 1.61 respectively. The experimental ratios of 0.94 ± 0.18 and 3.4 ± 0.2 are closed to the BM calculations although the best individual

Table (5.10). Experimental B(E2) ratios for transitions from positive parity states in ^{188}Os compared with theoretical predictions

E(level)	I_i	I_f	Energy	B(E2) ratio Exp	IBM	PPQM*
633	2	0	633	0.29 (2)	0.62	0.45
		2	477	1.0	1.0	1.0
790	3	2	635	1.06 (26)	1.89	0.47
		4	312	1.0	1.0	1.0
1304	2	0	1304	0.007(2)	0.0035	0.094
		2	1149	0.05 (2)	0.05	0.01
		3	514	1.0	1.0	1.0
1457	2	0	1457	1.0	1.0	-
		2	1302	0.55 (9)	5.25	-
		2	825	20.6 (34)	35.25	-
1660	2	0	1660	1.0	1.0	-
		2	1505	0.97 (33)	1.64	-
		3	1027	3.4 (11)	0.031	-
1871	2	0	1871	0.003(1)	0.00	-
		2	1238	0.035(12)	0.020	-
		0	785	1.0	1.0	-
1957	2	0	1957	1.0	1.0	-
		2	1802	5.21 (51)	0.3	-
1865	2	0	1865	1.0	1.0	-
		2	1711	0.84 (8)	0.67	-
2043	2	0	2043	0.44 (9)	0.5	-
		2	1888	1.0	1.0	-

* Kumar and Baranger (1968)[57]

Table (5.11). The experimental 0^+ decay modes in ^{188}Os. The ratio R is defined as $B(E2; 0_i \rightarrow 2_2)/B(E2; 0_i \rightarrow 2_1)$. The O(6) quantum numbers, σ and τ , are given in square brackets.

Level (keV)	0_i^+	[σ,τ]	R ratio	
			Exp	IBM
1086	0_2^+	[N,3]	5.1 (5)	9.9
1704	0_3^+	[N,6]	1.90(23)	0.01
1478	0_4^+	[N-2,0]	4.84(25)	5.0
1825	0_5^+	[N,9]	7.4 (10)	8.5
1765	0_6^+	[N-2,3]	5.88(34)	3.5

agreement is for the IBM value for R_1. The IBM predictions are regarded as equally good since the BM calculations needed to use first order perturbation methods. The predictions of Kumar and Baranger [58] were far from the experimental ratios, particularly for R_1 where the ratio was 2.2.

Levels: 1086 (0^+) – 1305 (2^+) – 1457 (2^+) keV.

The O(6) quantum numbers specifying these levels are shown in the parentheses of Figure (5.12).

The 1086 keV level is the first excited 0^+ state and therefore there is no problem in assigning the quantum numbers. The nature of this level has been subjected to discussion as either belonging to β-vibrational bandhead or two phonon-gamma vibrational bandhead. Yamazaki [43] considered this level as a two phonon-gamma vibrational state from the fact that the energy is approximately twice the gamma vibrational energy. However, the present ratio $B(E2; 0^+ \rightarrow 2_2^+)/B(E2; 0^+ \rightarrow 2_1^+)$ of 5.1 (5),

is neither consistent with the two phonon-gamma vibrational ratio (=0.2) [166], nor with the pure β-vibrational ratio of 200. The IBM prediction for the ratio gives a value of 9.9, almost twice the experimental ratio. The predicted level at 1019 keV by the IBM is better than the predictions of BET and PPQM at 734 and 836 keV.

The levels 1305 (2^+) and 1457 (2^+) keV are suggested to be the members of this [0^+ 2^+ 2^+] group. From Table (5.10) it can be seen that the B(E2) ratios of the transitions depopulating the 1305 keV level are in good agreement with IBM predictions. For the 1457 keV level, the only appreciable disagreement is for the ratio B(E2; $2^+ \rightarrow 2_1^+$)/B(E2; $2^+ \rightarrow 0_1^+$) where the IBM prediction is a factor of ten higher. The observed 2^+ level at 1305 keV is predicted by the IBM at 1162 keV, better than the BET at 1011 keV and PPQM at 1131 keV. The second 2^+ member of this [0^+ 2^+ 2^+] group is predicted at 1413 keV, in good agreement with the experimental value at 1457 keV. The BET prediction at 1243 keV is lower by 214 keV than the observed value.

Levels: 1478 (0^+) – 1660 (2^+) – 1807 (2^+) keV.

The 0^+ state at 1478 keV is the second excited state observed in ^{188}Os. In the context of the O(6) limit, it has been identified as the bandhead of the states in the σ=N-2 group, having the quantum numbers (8, 0, 0). This assignment is consistent with the B(E2) ratios for transitions depopulating the 1478 keV level. There exists another neighbouring 0^+ state at 1704 keV which could be mistaken as having the same quantum numbers. Suppose R defines the ratio B(E2; $0^+ \rightarrow 2_2^+$)/ B(E2; $0^+ \rightarrow 2_1^+$), then the values of R for both 0^+ states can be evaluated experimentally and compared with the IBM predictions. The experimental values of R obtained for the levels 1478 keV and 1704 keV are 4.84 (25) and 1.90 (23) respectively.

Suppose the 1478 keV level is assigned with the quantum numbers (10, 6, 2), which designated the second 0^+ excited state in the group σ=N, and the 1704 keV level with the quantum numbers (8, 0, 0) which is the first 0^+ state in the group

σ=N-2. The IBM predictions based on these quantum numbers assignment give the values of R to be 0.01 and 5.0 respectively. These ratios do not correspond with the experimental values. If on the other hand, the quantum numbers are interchanged, (8, 0, 0) is assigned to the 1478 keV level while (10, 6, 2) is assigned to the 1704 keV level, then the predicted values of R will be 5.0 and 0.01 respectively. The first ratio is consistent with the experimental value of 4.84 ± 0.25 and therefore the 1478 keV level can be considered as the first 0^+ state in the group σ=N-2. Although the second ratio (0.01) is far from the experimental of value 1.90 ± 0.23, it is still reasonable to assign the level 1704 keV with the quantum numbers (10, 6, 2). Table (5.11) shows that the experimental R value of the 1704 keV level is the smallest compared to that obtained for the other levels. From the IBM predictions, the smallest R value obtained is for the level with the quantum numbers (10, 6, 2) and therefore suggests that the assignment of the (10, 6, 2) quantum numbers to the 1704 keV is appropriate.

The new level at 1660 keV, with spin/parity 2^+ is suggested to be a member of the present $[0^+\ 2^+\ 2^+]$ group. This suggestion is borne out by the fact that the energy difference of 182 keV is close to that (155 keV) between the first excited state to the ground state of ^{188}Os. The IBM calculations give a 2^+ level at 1680 keV, which is only 20 keV above the experimental value. The experimental B(E2) ratios for transitions depopulating this state are shown in Table (5.10) together with the IBM predictions. The B(E2; $2^+ \rightarrow 2_2^+$)/B(E2; $2^+ \rightarrow 0_1^+$) is predicted too low while the B(E2; $2^+ \rightarrow 2_1^+$)/B(E2; $2^+ \rightarrow 0_1^+$) ratio prediction is two standard deviation higher than the experimental value.

Another level which is considered to be a member of the $[0^+\ 2^+\ 2^+]$ group is the 1807 keV level. The selection rules of the T(M1) operator in the O(6) limit (Equation: 2.22) favour the presence of M1 transitions to depopulate this level to the states in the group σ=N. Three transitions at 1017, 1174 and 1652 keV were observed to depopulate this level. These transitions populate the states at 3^+ (10, 3, 0), 2^+ (10, 2, 0) and 2^+ (10, 1, 0) respectively. The two available conversion coefficients (α_K) for transitions 1017 and

Table (5.12). Parameters obtained for T(M1) operator in program FBEM to calculate B(M1) ratios.

Parameters	E2SD	E2DD	M1E2	M1ND
	0.3133	-0.008	-0.9	0.157

Table (5.13). Calculated B(M1) ratios compared with IBM predictions.

				B(M1) ratio	
E(level)	I_i	I_f	Energy	Exp	IBM
1807	2	2_1	1652*	1.0	1.0
		2_2	1174	17.9 (41)	13.5
		3_1	1017	19.8 (53)	66.8
1941	2	2_1	1786*	0.22(6)	13.1
		2_2	1308	2.97(72)	4.7
		3_1	1150	1.0	1.0

* Transition assumed of M1 character.

1174 keV indicate that these transitions are of M1 and M1/E2 characters respectively (Table: 5.5). These experimental observations are consistent with the predictions of the O(6) limit for M1 transitions from a σ=N-2 (2^+) 1807 keV level.

Assuming that the transition at 1652 keV to the 155 (2^+) keV level is also of an M1 multipolarity, the B(M1) ratios for the three transitions can be calculated. The theoretical B(M1) ratios were calculated by FBEM as a result of the T(M1) operator, equation (2.22), acting on the wavefunctions of the energy levels generated by PHINT. The parameters, E2SD and E2DD, of the T(E2) operator in equation (2.50) are the same as those obtained previously in calculating the B(E2) values. The values of the M1E2 and M1ND parameters obtained for the T(M1) operator are shown in Table (5.12). The absolute value of the M1E2 parameter is higher than the value of M1ND suggesting that the competing E2 character in the M1 transition $I \pm 1 \longrightarrow I$ is expected to be small. The suggestion is observed experimentally, the transition 1017 keV which connects the 2^+ 1807 keV level to the 790 keV level has an M1 multipolarity.

The B(M1) ratios computed using FBEM are shown in Table (5.13) together with the experimental ratios. The results for the 1807 keV level indicate that the IBM predictions could satisfactorily account for the B(M1; $2^+ \longrightarrow 2_2^+$)/B(M1; $2^+ \longrightarrow 2_1^+$) ratio. The ratio of B(M1; $2^+ \longrightarrow 3_1^+$)/B(M1; $2^+ \longrightarrow 2_1^+$) is overestimated by a factor of 3.4.

Levels: 1704 (0^+) – 1865 (2^+) – 2043 (2^+) keV.

The 0^+ state at 1704 keV is considered to be a second 0^+ excited state in the group σ=N. As has been previously discussed, the assignment of the quantum numbers (10, 6, 2) is appropriate, even though the R value obtained experimentally is far from the prediction of the IBM.

Two new levels at 1865 (2^+) and 2043 (2^+) keV are suggested to be members of the σ=N [0^+ 2^+ 2^+] group. The suggestion of the 1865 keV level as a member is borne out by the fact that the energy difference of 161 keV is close to that (155 keV) between the first excited state and the ground

state of ^{188}Os. The IBM prediction for the B(E2; $2^+ \rightarrow 2_1^+$)/ B(E2; $2^+ \rightarrow 0_1^+$) ratio gives a value of 0.67, which is near to the experimental ratio of 0.84 ± 0.08. In the case of the 2043 keV level, the IBM prediction of 0.5 for the B(E2) ratio gives a good agreement with the experimental value of 0.44 ± 0.09.

The predicted levels for both states are approximately 300 keV lower than the observed values. Although these differences in the values are exceptionally high, the IBM considerations are valuable as neither the BET nor PPQM could predict the levels in this energy region (≃ 2 MeV).

Levels: 1765 (0^+) – 1871 (2^+) – 1941 (2^+) keV.

The state at 1765 keV is the second 0^+ state in the group designated by σ=N-2. The IBM prediction of such a level at 2166 keV is better than the estimation of the BET at 2497 keV. The calculated value of R on the basis of the IBM equals 3.5, near to the experimental value of 5.9 supports the assignment of (8, 3, 3) as the quantum numbers to the 1765 keV level.

A new level at 1871 keV, of spin/parity 2^+, is assigned as a member of this σ=N-2 [0^+ 2^+ 2^+] group. The B(E2) ratios predictions by the IBM for the depopulating transitions are in reasonable agreement with the experimental ratios. The theoretical 0.02 value for the B(E2; $2^+ \rightarrow 2_1^+$)/B(E2; $2^+ \rightarrow 0_2^+$) ratio is slightly off the experimental ratio of 0.035 ± 0.012. Since the 1871 keV level belongs to the σ=N-2 group, the direct transition to the ground state (σ=N) is highly forbidden. This is observed experimentally where the B(E2; $2^+ \rightarrow 0_1^+$)/ B(E2; $2^+ \rightarrow 0_2^+$) ratio is 0.003, near to the zero value predicted by IBM.

The last member of the σ=N-2 0^+ 2^+ 2^+ sequence at 1941 keV is expected to decay through M1 transitions. Four transitions at 1150, 1308, 1786 and 1941 keV were observed to depopulate this level. The two available conversion coefficients (α_K) for transitions 1150 and 1308 keV indicate that these transitions are of M1/E2 and M1 multipolarities respectively. The 1786 keV to the first excited state is assumed to

be of M1 multipolarity, consistent with the O(6) selection rule $\Delta\tau=-1$. The full energy transition at 1941 keV to the ground state suggests an E2 multipolarity rather than M1 character. Thus only three transitions at 1150, 1308 and 1786 keV are available for the calculations of the B(M1) ratios. The experimental results, compared with the IBM estimates, are shown in Table (5.13). The $B(M1; 2^+ \rightarrow 2_2^+)/B(M1; 2^+ \rightarrow 3_1^+)$ prediction at 4.7 is near to the experimental value of 3.0 ± 0.7 but there is a large difference for the $B(M1; 2^+ \rightarrow 2_1^+)/B(M1; 2^+ \rightarrow 3_1^+)$ ratio.

Levels: 1824 (0^+) – 1957 (2^+) keV.

The 0^+ level at 1824 keV is the last of the 0^+ states in the group $\sigma=N$. Due to the truncation of $\tau=\sigma$ (Figure: 5.11), only 2^+ is associated with this 0^+ state. The present work suggests that such a 2^+ state is the level observed at 1957 keV. The predicted value of R for the 0^+ state is 8.5 which agrees with the experimental value of 7.4 ± 1.0. Considering the fact that BET and PPQM could not predict the 0^+ state, the 1917 keV prediction by the IBM, although 93 keV higher than experiment, is considered to be the best estimate. The assignment of the level at 1957 (2^+) keV to this group is supported by the energy difference of 133 keV, not far from the corresponding GSB difference of 155 keV. The 2^+ level is predicted at 2167 keV, 210 keV higher than experimentally observed. Although the prediction of the level is exceptionally high, again it is regarded as the best since neither BET nor PPQM could give estimates.

Levels: 1842 (2^+), 1948 (2^+), 1975 (2^+) and 2022 (2^+) keV.

There remain four positive parity levels the nature of which is not certain. All of these states have spin/parity 2^+.

The level at 1842 keV is confirmed by the coincidence work. It was suggested by Svoren et al. [147] through the energy sum relations. The 1948 keV level is confirmed from the coincidence results of the 486 keV transition. This transition was observed both by Yamazaki and Sato [146] and

Svoren et al. [147], but they could not place it in the level scheme. The present result has, for the first time been able to place the 486 keV transition in the ^{188}Os decay scheme. The 1975 keV level established in this work is suggested as the 1973 ± 3 keV level reported from (d,t), (p,t) and (d,p) reactions [158]. The result pertaining to the 2022 keV is now conclusive. Previously [146, 147] the transition at 1865 keV was suggested to depopulate the 2022 keV state, but now this fact is disputed. Only one transition to the ground state is observed to depopulate the 2022 keV level and the 1865 keV transition is alternatively suggested to be a full energy transition.

In the context of IBM, these four states could not be described by the s-d boson space. Since Van Isaacker et al. [124] suggested that there could be intruder states of spin/parity 2^+ near 2 MeV, such a possible explanation could apply to the four states under consideration here. These intruder states can be regarded as the results of s′-bosons and d′-bosons, outside the normal s-d bosons space.

Level: 1457 (2^-) keV.

This is the only negative parity level observed in ^{188}Os prepared by the β^- decay of ^{188}Re. Two transitions observed to depopulate this level are at 672 and 829 keV. The former populates the 3^+ state of the γ-band while the latter feeds the 2^+ state of the γ-band.

The results of comparing experimental and theoretical conversion coefficients (α_K) indicate that the 672 keV transition has an E1 multipolarity and the 829 keV transition has a small admixture of M2 with E1 multipolarity. Assuming both transitions are of pure E1 multipolarity, the B(E1) ratio can be calculated. From the relative intensities of Table (5.1) the B(E1; $2^- \rightarrow 3_1^+$)/B(E1; $2^- \rightarrow 2_2^+$) ratio is calculated to be 0.51 ± 0.03. The K-quantum number for this level can be deduced by comparing the experimental B(E1) ratio with the prediction of the symmetric rotor model. The predicted value depends on the K-quantum number. When K is assumed

to be 1 the B(E1) ratio is predicted to be 2.0, but when K=2, the ratio is 0.5. The result clearly shows that the 1457 keV level with spin/parity 2^- is in fact a member of a rotational band with $K^\pi = 2^-$. Indeed, it is the bandhead of the rotational band.

CHAPTER VI

CONCLUSION

In the present work, the collective states of ^{160}Dy and ^{188}Os have been studied experimentally and their interpretation by different nuclear models were compared.

Experimentally, the work has succeeded in resolving many of the discrepancies raised by previous workers regarding the transitions and level schemes. In addition, the use of a 70 c.c. 12 % efficient Ge(Li) in singles measurements and with a 10 % Ge(Li) in γ-γ coincidence mode as part of a DPETS allowed a larger number of transitions and levels than before to be included in the decay schemes. The use of an intrinsic Ge detector to measure low energies has given a good check for transitions less than 350 keV.

Theoretically, the properties of both nuclei have been explained in the context of the interacting boson model. Other models such as the collective model, which was applied to ^{160}Dy, and PPQM and BET used in ^{188}Os, were discussed as a matter of comparison and found to give not a good overall agreement with experiment.

^{160}Dy nucleus.

The levels in this even-even nucleus are populated by β^- decay of ^{160}Tb. The long half-life ($T_{\frac{1}{2}} \simeq 70$ days) makes it suitable for extensive studies.

The results of singles measurements revealed the presence of 50 γ-transitions. Two weak transitions at 320 and 1448 keV, suggested earlier were confirmed and the relative intensities are now uniquely determined. Four γ-ray energies at 621, 704, 707 and 728 keV previously observed from ^{160}Ho decay [102], were seen for the first time in the decay of ^{160}Tb. Ten new transitions at 112, 148, 454, 518, 574, 1143, 1338, 1349, 1420 and 1507 keV were suggested. The relative intensities for all other transitions are consistent with those

reported earlier. The only appreciable difference observed is the intensity of the 242 keV transition. The present value of 0.026 (6) is in agreement with 0.021 (8) of McAdam and Otteson [80], but far from the 0.004 (3) of Ludington et al. [78]. The 242 keV peak is suggested to be a doublet; one results from the decay of well established level at 1398 keV and the other component arises from the deexcitation of a new level at 1507 keV. A transition at 1005 keV, not seen in the singles spectra, but inferred to exist from the coincidence results, was suggested to have a maximum intensity of 0.019.

From the γ-γ coincidences, twenty levels were established. Among these, three levels at 1285, 1288 and 1349 keV were confirmed. The level at 1285 keV with spin/parity 1^- was suggested by McAdam and Otteson [80] while the 5^+ state at 1288 keV was observed by Ludington et al. The presence of 1349 keV level was observed by McGowan and Milner [115] and the suggested spin/parity 2^+ is confirmed in this work. Another three levels at 1670, 1694 and 1824 keV were seen for the first time to be populated by β^- decay of ^{160}Tb. These levels were populated by EC/β^+ decay of ^{160}Ho. The present work has established three new levels at 1230, 1338 and 1507 keV. The level at 1230 keV with spin/parity 0^+ is suggested to be the β-vibrational bandhead. The 1^- level at 1338 keV is suggested as the bandhead of the $K^\pi = 0^-$ band, which is consistent with these predictions of Soloviev [126]. The level at 1507 keV with spin/parity 2^+ is considered as an intruder state. With the exception of the 1507 keV level, all the levels observed in the present work could be grouped into specific bands defined by quantum number K. The twelve positive parity states could be classified into six bands, while the eight negative parity states are grouped into three bands with $K^\pi = 0^-$, 1^- and 2^-.

The lifetime measured for the first excited state (87 keV level) is consistent with previous workers.

The energy ratio $E_{4_1^+}/E_{2_1^+}$, equal to 3.03, classifies ^{160}Dy as a rotationally deformed nucleus, and with neutron number equal to 94 has been suggested to lie at the edge of a

deformation region as does the ^{152}Sm nucleus.

Within the context of the geometrical model of Bohr and Mottelson, the most appropriate description of the levels would be as collective rotational, and therefore the states are expected to follow the leading order energy dependence of equation (2.9). The observed deviations, of positive parity states from the leading order dependence were attributed by Tuli [102] to the coupling of rotation-vibration modes, which eventually lead to band-mixing. The best indicators of band-mixing are the values of B(E2) ratios. For transitions connecting the states of different bands, the B(E2) ratios are expected to obey the rule of Alaga[74]. The present work reveals no such consistency for B(E2) ratios for transitions between the γ-band and the GSB.

To account for such deviations from Alaga's rule coupling parameter Z_γ between the γ-band and the GSB was evaluated from the FOP theory of Lipas [76]. This allows Z_γ to be calculated from each B(E2) value, and the results indicate no unique value of Z_γ in contradiction to that claimed by Gunther et al. [75] and Marshalek [77]. The present work proceeds further by assuming a mixing between γ- and β-bands, and the mixing parameter $Z_{\beta\gamma}$ was extracted from each of the B(E2) ratios for transitions connecting states in the γ-band to states in the GSB. A unique value of $Z_{\beta\gamma}$ equal to $-3.72(29) \times 10^{-3}$ was obtained. A result in contradiction with the findings of Dasmahpatra [81], who concluded that $Z_{\beta\gamma}$ values obtained for different B(E2) ratios are non-unique. The mixing of bands are again clearly indicated by the ft ratios of Table (4.13). The inconsistency of the results with those derived on the basis of a symmetric rotor suggests that the states in the γ-band are not pure rotational states, but instead are mixed with states of the neighbouring β-band.

The non-dependence of the negative parity states on the I(I+1) level sequence is clearly shown in Figure (4.11). The deviations are attributed to the Coriolis force which results in the mixing of the bands with $\Delta K=1$. This causes the wavefunction of a state to have components from states

of other bands. Such a mixing of bands with $K^{\pi} = 0^-$, 1^- and 2^- is clearly indicated from the results of the B(E1) ratios. The levels with spin/parity 2^- and 4^- deexcite predominantly to states in the γ-band ($K^{\pi} = 2^+$), while levels with spin/parity 1^- and 3^- deexcite mostly to states in the GSB ($K^{\pi} = 0^+$). The present calculations pertaining to the band-mixing for the B(E1) ratios (Table: 4.20) show good agreement with experimental values, suggesting that Coriolis couplings do occur in ^{160}Dy.

In the context of the Interacting Boson Model, the description of the SU(3) limit with the perturbation by the $\underset{\sim}{P}.\underset{\sim}{P}$ (pairing term) give good results for both the energy levels and B(E2) values. Undoubtedly, the predictions of B(E2) for transitions from γ-band to GSB allowed the significance of the difference between the geometrical model and IBM to be evaluated. While it has been shown that such a ratio can be reproduced in the Bohr-Mottelson description by the explicit introduction of β-γ band-mixing, in the framework of the IBA, the natural appearance of band admixtures represents a fundamental characteristic arising from the underlying SU(3) symmetry of the model. It should also be emphasised that the geometrical model as used here involves a formalism applicable specifically to deformed nuclei which allows the extraction of all parameters necessary to describe a given nucleus. The IBA uses a Hamiltonian which is applicable across a wide range of nuclei, and which for a certain combination of terms provides a prediction for deformed nuclei.

An important result of the IBM calculations is that referring to the new proton subshell at Z=64 which clearly gives better agreement with experiment as compared to the calculations for the normal shell closure at Z=50 or 82.

A good example is the absolute B(E2) values of Table (4.10). Even though the IBM (Z=50 or 82 shell closure) predictions are close to experimental values, those predictions with the Z=64 subshell give values which are in fact in better agreement, particularly for the $2_1^+ \rightarrow 0_1^+$ transition. The B(E2) ratios of Table (4.14) further illustrate the effectiveness of the Z=64 subshell closure in ^{160}Dy. A physical basis

is thus established for the truncation of the boson number from 14 to 7.

In the case of the positive parity levels, the predictions for GSB and γ-band energies using both approaches (i.e. normal and subshell closure) are essentially identical [Table (4.18) and Figure (4.10)]. For the states in the (2N-8, 4) representation, the results of Z=64 consideration are much better. Particularly, for the bandhead of $K^{\pi} = 4^{+}$ band at 1694 (4^{+}) keV: the zero branching ratio to the GSB supports this assignment. The IBM prediction with Z referred to 50 or 82 placed this level at 1920 keV, too high by 226 keV. A large discrepancy was also observed for the $K^{\pi} = 4^{+}$ bandhead in ^{154}Gd by Van Isaacker et al. [124] and was accounted for by the inclusion of g-bosons (J=4). The new prediction at 1776 keV reduces the difference to 82 keV and suggests that the consideration of a subshell closure at Z=64 may provide an alternative approach to the introduction of the J=4 degrees of freedom. This improved agreement with experiment is equally true for the 5^{+} and 6^{+} states ($K^{\pi} = 4^{+}$) observed from EC/β^{+} decay of Ho. The experimental value for the 5^{+} level is 1802 keV and the 6^{+} level is at 1929 keV. Using the normal shell closure at 50 or 82, the former level is predicted at 2061 keV while the latter at 2230 keV. As can be seen the difference between the predictions and the experimental values are indeed large. For the 5^{+} state the difference is 259 keV and for the 6^{+} state it is 301 keV. The new predictions (Z=64) at 1915 and 2089 keV reduce the difference to 113 and 160 keV respectively.

Another level, in the (2N-8, 4) representation, which is well predicted by Z=64 subshell closure is the 2^{+} state at 1804 keV. It is predicted at 1802 keV while the normal IBM (Z=50/82) estimates the level to occur at 1845 keV.

The good predictions of IBM (Z=64) do not apply only to the positive parity states. The calculations for the negative parity states [Table (4.16) and Fig. (4.11)] clearly indicate good agreement with experimental values. The $K^{\pi} = 0^{-}$ bandhead is well predicted at 1338 keV. The observed level

is at 1335 keV.

The good agreement obtained from IBM (Z=64) calculations suggests that there is evidence for a subshell closure at Z=64 in the ^{160}Dy nucleus, even though the neutron number is above 90. This conclusion could admit the presence of a level at 1507 keV, spin/parity 2^+, which cannot be described by s-d boson space. As has been pointed out by Ref: [124], one consequence of a subshell closure at Z=64 would be the formation of second low-lying ($\simeq$ 2 MeV) $J^\pi = 0^+$ (s-boson) and $J^\pi = 2^+$ (d-boson) states. The level at 1507 keV might be an intruder state which could be described as a result of a d'-boson.

<u>^{188}Os nucleus</u>.

The ^{188}Os nucleus is populated sequentially from the β^- decay of ^{188}W which firstly decays to ^{188}Re and then to the stable ^{188}Os nucleus.

From the singles measurements of the decay of ^{188}W, fifty-two energies are identified as belonging to ^{188}Os. Of the eleven transitions previously suggested by Ref: [147] 8 are confirmed and one at 810 keV is attributed to the background radiation of ^{58}Co. Fourteen new γ-energies are suggested. The relative intensities obtained for the remainder are in better agreement with the measurements of Svoren et al.[147] than those of Yamazaki and Sato [146]. The largest difference is observed for the 825 keV transition and even here the present value of 2.2 (4) is comparable with the value of 1.7 (6) from (n,γ) reaction.

The results of γ-γ coincidence measurements and energy sum relations enabled twenty-three excited states to be established. Four levels not previously confirmed are established at 1478, 1704, 1842 and 1976 keV. The previously unplaced energies at 1865 and 486 keV help to establish two levels at 1865 and 1948 keV respectively. The three levels at 1660, 1871 and 2043 keV are new suggestions. The results pertaining to other levels are consistent with previous

workers. The present work improves on that of Svoren et al.[147] who did not make any coincidence measurements, and Yamazaki and Sato [146] who used only three gates at 155, 478 and (633 + 635) keV. The existence of the 2023 keV level is now regarded as conclusive. The previously suggested 1865 keV transition from this level is rejected. Such a transition is suggested as depopulating a level at 1865 keV directly to the ground state. The level proposed from (d,t), (p,t) and (d,p) reactions at 1973 ± 3 keV has been determined for the first time from β^- decay at 1976 keV. Also, the 155 keV peak is suggested to be a doublet with energies at 155.0 and 155.2 keV between the levels at 633 and 478 keV. The latter constitutes 0.7 % of the total intensity.

In comparison with nuclear models, the IBA calculations give predictions for most of the energy levels to about 12 % and many B(E2) values were obtained which could not have been predicted before. The O(6) description, with a small $\underset{\sim}{Q}.\underset{\sim}{Q}$ perturbation [SU(3) characteristic], is able to account for most of the nuclear properties. The O(6) characteristic of the energy levels is well displayed by the recurring [0^+ 2^+ 2^+] sequence shown in Figure (5.12). The value of -0.008 near to zero, obtained for the E2DD parameter of the T(E2) operator further supports the characteristic O(6) feature of ^{188}Os. The B(E2) ratios for all the transitions are therefore independent of the E2SD and E2DD parameters. The situation is different for an SU(3) nucleus whereby only B(E2) ratios for transitions connecting different representations are independent of these two parameters.

Of the twenty-two positive parity levels observed, eighteen are able to be described by the normal s-d boson space. This is better than BET and PPQM where only 11 levels could be predicted by the former and 6 by the latter [refer Table (5.9)].

The main problem encountered in the present work is the assignment of the observed O(6) states with the correct quantum numbers (σ, τ, ν_Δ). The presence of 5 excited 0^+ states and fifteen 2^+ states has led to this difficulty since

theoretically the O(6) level spectrum consists of the repeating patterns 0^+, 2^+, 4^+, 2^+, ... corresponding to the different values of σ=N, N-2, ... [Figure (5.11)]. The task was made easier by first establishing the quantum numbers of the 0^+ states, which form the bandheads of the [0^+ 2^+ 2^+] sequences. The 2^+ states are built upon these 0^+ states, and are therefore easier to identify given the additional information from the B(E2) ratios.

In ^{188}Os (N=10) the present work is able to identify two σ groups of states, σ=10 and σ=8. As was mentioned earlier, the truncation of the quantum numbers σ and τ allows only three excited 0^+ states which are expected to occur in the group σ=10 and also another three for the group σ=8. The three excited 0^+ states which are identified to be in the σ=10 group are 1086, 1704 and 1824 keV, while the 0^+ states at 1478 and 1765 keV belong to the σ=8 group. The third 0^+ state in the σ=8 group was not observed, most probably it occurs at energy greater than Q_{β^-} of ^{188}Re.

Another important test for the applicability of the O(6) description to ^{188}Os is the presence of M1 transitions depopulating the states with σ=N-2 to the states in the group σ=N. Also the allowed change in τ is zero as suggested by Warner [53], but these selection rules could not be substantiated experimentally since no experimental data were available. The present work is the first to test the validity of these rules for an O(6) nucleus. From the quantum number assignments of the ^{188}Os states, the 2^+ levels at 1807 and 1941 keV are expected to deexcite predominantly through M1 transitions. The observed M1 and M1/E2 multipolarities of the 1017 and 1174 keV transitions from the 1807 keV level support the predictions of the IBA. This is further substantiated by the observance of two transitions, 1308 and 1150 keV, from the 1941 keV with multipolarities M1 and M1/E2 respectively.

Summary.

As a summary, the present work tries to establish a link between the ^{160}Dy and ^{188}Os nuclei which can only be

achieved through the IBA description. The Hamiltonian used can be truncated to any limit to describe a particular nucleus. Such a procedure is not available in other nuclear models whereby the description is only applicable to one type of nucleus. In terms of the IBA limits, the two nuclei lie in the transitional region between the SU(3) and the O(6) limits. The nucleus of ^{160}Dy exhibits more SU(3) characteristics and the ^{188}Os nucleus displays marked O(6) features. ^{160}Dy and ^{188}Os are two good examples of what will happen to a nucleus when subjected to high perturbative factors such as $\underset{\sim}{P}.\underset{\sim}{P}$ and $\underset{\sim}{Q}.\underset{\sim}{Q}$. In the ^{160}Dy Hamiltonian there is a small perturbation of $\underset{\sim}{P}.\underset{\sim}{P}$. When this perturbation is increased the nucleus will move towards the O(6) limit. In this case the second 2^+ state moves gradually towards the first excited state (2_1^+). This occurs as A for Dy isotopes increases. For the Os isotopes the increase of $\underset{\sim}{Q}.\underset{\sim}{Q}$ perturbation will shift the characteristics away from O(6) toward the SU(3) limit. This happens for Os isotopes of lower A. The general conclusion derived from these observations is that, for any particular series of isotopes lying between the SU(3) and O(6) limits their characteristic features can be determined from the A values. If A is low then inevitably the SU(3) limit should dominate, while for high A values, an O(6) description is the best.

References:

1. Hamilton A, Radioactivity in Nuclear Spectroscopy, Vol. 1 (1972) Gordon & Breach, London.

2. Bateman H, Proc. Cambridge Phil Soc. 15 423 (1910).

3. Rubinson WJ, Chem. Phys. 17 542 (1949).

4. Lederer CM, Hollander JM, Perlman I, Table of Isotopes, 6th ed. (1967) [John Wiley & Sons N.Y.].

5. Heitler W, The Quantum Theory of Radiation, 3rd. ed. Oxford Univ. Press (Clarendon), London & N.Y. 1954.

6. Harihar P, Ullman JD, Wu CS, Phy. Rev. C2 462 (1970).

7. Siegbahn K, α, β & γ-ray spectroscopy (North Holland Pub. Co., Amsterdam, 1965).

8. Morinaga H, Yamazaki T, In Beam γ-ray Spectroscopy (North Holland Pub. Co., 1976).

9. Lobner KEG, The Electromagnetic interaction in Nuclear Spectroscopy ed. Hamilton WD (North Holland Pub. Co., Amsterdam, 1975).

10. Hahn O, Meitner L, Z. Phy. 29 161 (1924).

11. Green T and Rose ME, Phy. Rev. 110 105 (1958).

12. Sliv L, Band I, Tables of Gamma-ray conversion coefficient part I (K-shell), part II (L-shell), Physico Technical Institute, Academy of Science, Leningrad 1956.

13. Church E, Wenesser J, Nucl. Phy. 28 602 (1961).

14. Hager R, Seltzer E, Nucl. Data A4 1 (1968), Nucl. Data A4 397 (1968), Nucl. Data A6 1 (1969).

15. Pauli HC, Alder K, Z. Phy. 202 255 (1967).

16. Rose ME, α, β & γ-ray spectroscopy ed. Siegbahn K (North Holland Pub. Co., Amsterdam, 1965).

17. Rosel F, Fries HM, Alder K, Pauli HC, Atomic Data & Nucl. Data Tables 21 325, 268, 258 (1978).

18. Blatt JM, Weiskopf VF, Theoretical Nuclear Physics 1963 (John Wiley & Sons N.Y.).

19. Wu CS, Moskowski SA, Beta Decay vol. 16 (Interscience Publisher N.Y.).

20. Konopinski EJ, The Theory of Beta Radioactivity (Oxford Univ. Press 1966).

21. Mayer MG, Phy. Rev. 74 235 (1948).

22. Elasser WM, J. Phy. et. radium 4 549 (1933).

23. Mayer MG, Phy. Rev. 75 1969 (1949).

24. Haxel O, Jensen JHD, Suess HE, Phy. Rev. 75 1766 (1949).

25. Feenberg E, Hammack KC, Phy. Rev. 75 1877 (1949).

26. Weisskopf VF, Phy. Rev. 83 1073 (1951).

27. Nilsson SG, Kgl. Dan. Vid. Selsk. Mat.-Fys. Medd. 29, No.16 (1955).

28. Rainwater J, Phy. Rev. 79 432 (1950).

29. Irvine JM, Nuclear Structure Theory vol. 49 (Pergamon Press, Oxford 1972).

30. Bohr A, Mottelson M, Nucl. Structure vol. II (Benjamin WA, Inc. Amsterdam 1975).

31. Bohr A, Mottelson M, Nucl. Structure vol. I (Benjamin WA, Inc. Amsterdam 1975).

32. Faessler A, Greiner W and Sheline RK, Nucl. Phy. 70 33 (1965).

33. Kumar K, Baranger M, Nucl. Phy. 63 177 (1965).

34. Gneuss G, Mosel U, Greiner W, Phys. Lett. 6B 397 (1969).

35. Gneuss G, Greiner W, Nucl. Phy. 171 449 (1971).

36. Hess PO, Siewert M, Maruhn J, Greiner W, Z. Phy. A296 147 (1980)

37. Brink DM, de Toledo Piza AFR, Kerman AK Phy. Lett. 19 413 (1965).

38. Jansser D, Jolos RV, Dönau F, Nucl. Phy. A224 93 (1974).

39. Kishimoto T, Tamura T, Nucl. Phy. A270 317 (1977).

40. Tamura T, Weeks K, Kishimoto T, Phy. Rev. C20 307 (1979).

41. Kishimoto T, Tamura T, Nucl. Phy. A192 264 (1972).

42. Kishimoto T, Tamura T, Nucl. Phy. A207 317 (1976).

43. Kishimoto T, Tamura T, Nucl. Phy. A163 100 (1971).

44. Scholten O, Iachello F, Arima A, Ann. Phys. (N.Y.) 115 325 (1978).

45. Interacting Bosons in Nucl. Physics ed. F. Iachello (Plenum Press, N.Y. 1979).

46. Arima A, Iachello F, Ann. Phys. N.Y. 111 201 (1978).

47. Arima A, Iachello F, Ann. Phys. N.Y. 123 468 (1979).

48. Arima A, Iachello F, Ann. Phys. N.Y. 99 253 (1976).

49. Otsuka T, Arima A, Iachello F, Talmi I, Phy. Lett. 76B 139 (1978).

50. Scholten O, 'The program package PHINT' Kerntysisch Versneller Institute, Report no. 63.

51. Iachello F, 'Group Theory and Nucl. Spectroscopy' Lecture notes in Physics, vol. 119 Nuclear Spectroscopy (Springer-Verlag, Berlin, 1980) pg. 140.

52. Warner DD, Casten RF, Phy. Rev. Lett. 25 2019 (1982).

53. Warner DD, Inst. Phys. Conf. Ser. No. 62 49 (1982) 4th (n,γ) Int. Symp., Grenoble, 7-11 Sept. 1981.

54. Baranger M, Kumar K, Nucl. Phy. 62 113 (1965).

55. Baranger M, Kumar K, Nucl. Phy. A122 241 (1968).

56. Baranger M, Kumar K, Nucl. Phy. A110 490 (1968).

57. Kumar K, Baranger M, Nucl. Phy. A122 273 (1968).

58. Bohr A, Mat. Fys. Medd. Dan. Vid. Selsk 26 14 (1952).

59. Kumar K, Baranger M, Nucl. Phy. A92 608 (1967).

60. Foutti J, Prussin S, Nucl. Inst. Method 72 125 (1969).

61. T.R.C. set Radiochemical Centre Amersham, Buckinghamshire U.K.

62. Neiler JH, Bell PR, α, β and γ-Spectroscopy ed. K. Siegbahn.

63. Meiling W, Stary F, Nanosecond Pulse Technique (Gordon & Breach N.Y. 1968).

64. Chase RL, Rev. Sci. Inst. 39 1318 (1968).

65. Moszynski M, Bengston B, Nucl. Instr. Method 80 233 (1970).

66. Gedcke DA, McDonald WJ, Nucl. Instr. Method 55 377

(1968), 58 253 (1968).

67. Suliman MY, Thomas RN, Nucl. Instr. Method 166 305 (1979).

68. Kowalski K, Nuclear Electronics (Springer-Verlage N.Y. 1970).

69. Groseclose BC, Loper GD, Phy. Rev. A137 939 (1965).

70. Wilson RK, Johnson PO, Stump R, Phy. Rev. 129 2091 (1963).

71. Nathan O, Nucl. Phy. 4 125 (1957).

72. Ofer S, Nucl. Phy. 5 331 (1958).

73. Kumar K, Phy. Rev. Lett. 26 269 (1971).

74. Alaga G, Alder K, Bohr A and Mottelson BR, K. Danske Vidensk. Selsk. Mat.-Fys. Meddr. 29 No.9 (1955).

75. Gunther C, Ryde H, Krien K, Nucl. Phy. A122 401 (1968).

76. Lipas PO, Nucl. Phy. 39 468 (1962).

77. Marshalek ER, Phy. Rev. 158 993 (1967).

78. Ludington MA, Reidy JJ, Wiedenbeck ML, McMillan DJ, Hamilton JH and Pinajian JJ, Nucl. Phy. A119 398 (1968).

79. Keller GE, Zganjar EF, Nucl. Phy. A147 527 (1970).

80. McAdams RE and Otteson OH, Z. Phy. 250 359 (1972).

81. Dasmahpatra BK, J. Phys. G: Nucl. Phy. 2 233 (1976).

82. Hamilton JH, Bull. Acad. Sc. USSR Phys. Ser. 36 17 (1973).

83. Nathan O and Nilsson SG, α, β, γ-ray Spectroscopy ed. by K. Siegbahn (North Holland Publ. Co., Amsterdam,

1965) Chapter X.

84. Kochbach L and Vogel P, Phy. Lett. 32B 434 (1970).

85. Krane KS, Nucl. Phy. A377 176 (1982).

86. Warner DD, Casten RF and Davidson WF, Phy. Rev. C24 1713 (1981).

87. Ogawa M, Broda R, Zell K, Daly and Kleiheinz P, Phy. Rev. Lett. 41 289 (1978).

88. Casten RF, Warner DD, Brenner DS and Gill RL, Phy. Rev. Lett. 47 1433 (1981).

89. Gill RL, Casten RF, Warner DD, Brenner DS, Walters WD, Phy. Lett. 118B 251 (1982).

90. Ibrahim N, Stewart NM, J. Phys. G: Nucl. Phy. 9 L195 (1983).

91. Grotdal T, Nybo K, Thorsteinsen T, Elbek B, Nucl. Phy. A110 385 (1968).

92. Maher JV, Kolata JJ, Miller RW, Phy. Rev. C6 358 (1972).

93. Burson SB, Blair KW, Saxon-D, Phy. Rev. 77 403 (1950).

94. Burson SB, Jordan WC, Le Blanc JM, Phy. Rev. 94 103 (1954).

95. Cork JM, Branyan CE, Rutledge WC, Stoddard AE, Phy. Rev. 78 304 (1950).

96. Reddy KV, Raju BBV, RamaMohan RV, Jnanananda S, Phy. Rev. 138 B33 (1965).

97. Jaklevic JM, Funk EG and Mihelich JW, Nucl. Phy. A99 83 (1967).

98. Johnson CE, Schooley JF, Shirley DA, Phy. Rev. 120

2108 (1960).

99. Postma H, Eversdijk Smulders MC, Huiskamp WJ, Physica 27 245 (1961).

100. Fowler CM, AECU-3194 (1956).

101. Voinova NA, Dzhelepov BS, Zhukovski NN and Yu. v. Kholinov, Izv. Akad. Nauk SSSR (ser. fiz.) 24 856 (1960).

102. Tuli JK, Nucl. Data Sheet 12 477 (1974).

103. Fossan DB, Herskind B, Nucl. Phy. 40 24 (1963).

104. Abou-Leila H, Abd. El-Haliem A, Darwish SM, Nucl. Phy. A175 663 (1971).

105. Ismail HA, El-Naem A, El-Malek SA, Abou-Leila H, Wali-el-Din N, Rev. Roum. Phys. (Rumania) 26 401 (1981).

106. Mozskowski SA, Phy. Rev. 82 35 (1951).

107. Lederer CM, Hollander JM, Perlman I, Table of Isotopes 6th. ed. N.Y. John Wiley and Sons.

108. Wapstra AH and Gove NP, Nucl. Data Table A9 No.4-5 (1971).

109. Ewan GT, Graham GT, Geiger JS, Nucl. Phy. 22 610 (1961).

110. Hager RS, Seltzer EC, Nucl. Data A4 1 (1968).

111. Krane KS and Steffen RM, Nucl. Phy. A164 439 (1971), Phy. Rev. C3 240 (1971).

112. Boehm F, Rogers J, Nucl. Phy. 41 353 (1963).

113. Grigoriev EP, Gromov KY, Zhelev ZT, Islamov TA, Kalinnikov VG, Nazarov UK, Sabirov SS, Bull. Acad. Sc. USSR (Phys. Ser.) 33 585 (1970).

114. Lederer CM and Shirley V, Table of Isotopes 7th. ed. New York: John Wiley and Sons.

115. McGowan FK, Milner MT, Phy. Rev. C23 1926 (1981).

116. Hanser PG, Nielsen OB, Sheline RK, Nucl. Phy. 12 389 (1959).

117. Gunther C and Parsignault DR, Phy. Rev. 153 1294 (1967).

118. Keller GE, Zganjar EF and Pinajian JJ, Nucl. Phy. A129 481 (1969).

119. Kawade K, Yamamoto H, Tsuchiya K, Katoh T, J. Phy. Soc. Japan 34 859 (1973).

120. Warner DD and Casten RF Proc. 4th. Int. Symp. (n,γ) Spectroscopy Grenoble, 62 38 (1982).

121. Casten RF and Warner DD, Proc. 4th. Int. Symp. (n,γ) Spectroscopy Grenoble, 62 28 (1982).

122. Inamara T, Kearns F and Lisle JC, Nucl. Instr. Meth. 123 529 (1975).

123. Avotina MP, GrigorevEP, Dzhelepov BS, Zolotivan AV, Sergreev VO, Bull. Acad. Sc. USSR (Phys. Ser.) 30 542 (1967).

124. Van Isaacker P, Heyde K, Waroquier M, Wenes G, Nucl. Phy. A380 383 (1982).

125. Neergard K, Vogel P, Nucl. Phy. A145 33 (1970).

126. Soloviev VG, Vogel P, Korneichut AA, Bull. Acad. Sc. USSR (Phy. Ser.) 28 1495 (1964).

127. Allsop AL, Hornung S, Krane KS, Stone N, J. Phys. G: Nucl. Phy. 8 866 (1982).

128. Yamazaki T, Nishiyama K, Hendrie DL, Nucl. Phy. A209

153 (1973).

129. Davydov AS, Fillipov GF, Nucl. Phy. 8 237 (1958).

130. Sahu R, Satpathy M, Ansari A, Satpathy L, Phy. Rev. C19 511 (1979).

131. Yates SW, Cunnane JC, Hochel R, Daly PJ, Nucl. Phy. A222 301 (1974).

132/3. Weeks KJ, Tamura T, Phy. Rev. Lett. 44 533 (1980).

134. Hess PO, Maruhn J, Greiner W, J. Phy. G: Nucl. phy. 7 737 (1981).

135. Casten RF, Cizewski JA, Nucl. Phy. A309 477 (1978).

136. Wilets L, Jean M, Phy. Rev. 102 788 (56).

137. Meyer-ter-Vehn J, Phy. Lett. 84B 10 (1979),

138. Bijker R, Dieperink AEL, Scholten O, Spanhoff R, Nucl. Phy. A344 207 (1980).

139. Iachello F, Puddu G, Scholten O, Arima A, Otsuka T, Phy. Lett. 89B 1 (1979).

140. Arns RG, Riggs RD, Wiedenbeck ML, Nucl. Phy. 15 125 (1960).

141. Warner LB, Sheline RK, Nucl. Phy. 36 207 (1962).

142. Wyly LD, Braden GH, Dulaney H, Phy. Rev. 129 315 (1963).

143. Yamazaki T, Nucl. Phy. 44 353 (1963).

144. Harmatz B, Handley TH, Nucl. Phy. 56 1 (1964).

145. Bashandy E, Hanna SG, Nucl. Phy. 84 577 (1966).

146. Yamazaki T and Sato J, Nucl. Phy. A130 456 (1969).

147. Svoren MD, Zganjar EF, Hawk IL, Z. Phy. A272 213 (1975).

148. Sharma HL, Hintz NM, Phy. Rev. Lett. 31 1517 (1973).

149. Newton JO, Stephens FS, Diamond RM, Nucl. Phy. A95 377 (1967).

150. Casten RF, Greenberg JS, Sie SH, Burginyon GA, Bromley DA, Phy. Rev. 187 1532 (1969).

151. Milner WT, McGowan FK, Robinson RL, Stelson PH, Sayer SO, Nucl. Phy. A177 1 (1971).

152. Lane SA, Saladin JX, Phy. Rev. C6 613 (1972).

153. Warner RA, Bernthal FM, Boyno JS, Khoo TL, Sletten G, Phy. Rev. Lett. 31 835 (1973).

154. Burke DG, Shahabuddin MAM, Boyd RN, Phy. Lett. 78B 48 (1978).

155. Thompson R, Ikeda A, Sheline RK, Cunnane JC, Yates SW, Daly PJ, Nucl. Phy. A245 444 (1975).

156. Sharma HL, Hintz NM, Phy. Rev. C13 2288 (1976).

157. Thompson RC, Boyno JS, Huizenga JR, Burke DJ, Elze TW, Nucl. Phy. A242 1 (1975).

158. Macphail MR, Casten RF, Kane WR, Phy. Lett. 59B 435 (1975).

159. Singh B, Viggar DA, Nucl. Data Sheet 33 275 (1981).

160. Schomarak MR, Nucl. Data Sheet 10 553 (1973).

161. Myers WD, Swiatecki WJ: Lawrence Radiation Lab. Univ. of California, Berkeley, report UCRL - 11980 (1965).

162. Arima A, Iachello F, Phy. Rev. Lett. 40 385 (1978).

163. Davydov AS, Chaban AA, Nucl. Phy. 20 499 (1960).

164. Belyak VI, Zaikin DA, Nucl. Phy. 30 442 (1962).

165. Davydov AS, Rostovsky VS, Nucl. Phy. 12 58 (1959).

166. Davydov AS, Rostovski VS, Chaban AA, Nucl. Phy. 27 134 (1961).

ACKNOWLEDGEMENTS

I would like to express my deepest thanks to Dr. N.M.Stewart for his supervision and advice throughout the course of this work.

It has been a great pleasure working at the University of London Reactor Centre and I gratefully acknowledge the help rendered by the staff and technicians of the Centre. The valuable assistance given by Dr. T.D.MacMahon is greatly appreciated.

The interest of Professor E.R.Dobbs, Head of Physics Department is gratefully acknowledged. Thanks are also due to the staff of the Computer Unit of Bedford College.

I wish to thank Dr. W.Gelletly and Dr. Jo Mo from the University of Manchester who kindly provided me with helpful advice and the programs PHINT and FBEM.

I would also like to mention Dr. M.S.S.El-Daghmah Mr. G.Mardirosian and Mr. Elie Eid for their fruitful discussion.

I am very grateful to the Government of Malaysia and the University of Malaya for granting me the financial support throughout the course of my work.

My profound gratitude to my beloved wife without whom I would have lacked moral support and encouragement.